Die Identifizierung von intrazellulären CFDA-Cisplatin-bindenden Proteinen

Inaugural-Dissertation

zur Erlangung des Doktorgrades
der Mathematisch-Naturwissenschaftlichen Fakultät
der Heinrich-Heine-Universität Düsseldorf

vorgelegt von

Sandra Kotz
aus Gronau (Westfalen)

Düsseldorf, Juli 2019

Aus dem Analytischen Zentrallabor des Biologisch-Medizinischen Forschungszentrums der Heinrich-Heine-Universität Düsseldorf und der MS Plattform des Biozentrums der Universität zu Köln.

Gedruckt mit der Genehmigung der
Mathematisch-Naturwissenschaftlichen Fakultät der
Heinrich-Heine-Universität Düsseldorf

Berichterstatter:

1. Prof. Dr. rer. nat. William F. Martin

2. Prof. Dr. rer. nat. Inge Bauer

Tag der mündlichen Prüfung: 07.01.2020

INHALTSVERZEICHNIS

Inhaltsverzeichnis ..... **I**

Abkürzungen ..... **III**

Zusammenfassung ..... **VII**

Summary ..... **IX**

Eidesstattliche Erklärung ..... **XI**

1 Einleitung **1**

1.1 Krebs **1**

1.1.1 Epidemiologie 1

1.1.2 Ovarialkarzinom 2

1.2 Tumorentstehung **3**

1.3 Cisplatin **4**

1.4 Resistenzmechanismen **7**

1.4.1 Erworbene Resistenz 7

1.4.1.1 *Pre-target* Resistenz 7

1.4.1.2 *On-Target* Resistenz 9

1.4.1.3 *Post-Target* Resistenz 10

1.4.1.4 *Off-Target* Resistenz 10

1.4.2 Intrazelluläre Bindung als Mechanismus der Resistenz 11

1.5 CFDA-Cisplatin - Ein Modellkomplex **12**

1.6 Ziele der Arbeit **13**

2 Publikationen **15**

2.1 Combination of two-dimensional gel electro-phoresis and a fluorescent carboxyfluorescein-diacetate-labeled cisplatin analogue allows the identification of intracellular cisplatin-protein adducts **15**

2.2 Assessing the contribution of the two protein disulfide isomerases PDIA1 and PDIA3 to cisplatin resistance **26**

2.3 GRP78 knockdown does not affect cytotoxicity of cisplatin in ovarian cancer cells.. ..... **33**

2.4 Optimized two-dimensional gel electrophoresis in an alkaline pH range improving the identification of intracellular CFDA-cisplatin-protein adducts in ovarian cancer cells 37

3 Diskussion 49

3.1 Nachweis von Intrazellulären CFDA-Cisplatin-Proteinaddukten 50

3.2 Optimierung der 2D-Gelelektrophorese im pH-Bereich 6-10 51

3.3 Bindung von CFDA-Cisplatin an Proteine 53

3.4 CFDA-Cisplatin-bindende Proteine 54

3.5 Zusammenfassung und Ausblick 58

4 Referenzen 62

5 Anhang 76

5.1 Lebenslauf 76

5.2 Danke! 80

ABKÜRZUNGEN

%	Prozent
2D	zweidimensional
A	Adenin
A2780	humane Ovarialkarzinomzelllinie
A2780*cis*	humane cisplatinresistente Ovarialkarzinomzelllinie
ADP	Adenosindiphosphat
AKT1	*RAC-alpha serine/threonine-protein kinase*
ALDH	*Aldehyde dehydrogenase X*
Arg	Arginin
ASB-14	*amidosulfobetaine*
ATP	Adenosintriphosphat
ATP-α	*ATP synthase subunit alpha*
ATP7B	*Copper-transporting P-type adenosine triphosphatase 7B*
BAK	*Bcl-2 homologous antagonist*
BAX	*Bcl-2-associated X protein*
BCL-2	*B-cell lymphoma 2*
BCL-X_L	*B-cell lymphoma-extra large*
β	Beta
BIRC5	*Baculoviral IAP Repeat Containing 5*
BRCA1	*BReast CAncer 1, early-onset*
BRCA2	*BReast CAncer 2, early-onset*
ca.	circa
CA125	*cancer antigen 125*
CDKN1A	*cyclin-dependent kinase inhibitor 1A*
CFDA	Carboxyfluoresceindiacetat
CFDA-Cisplatin	fluoreszierendes Cisplatin-Analogon
CHAPS	3-[3-Cholamidopropyl)-dimethyl-ammonio]-1-propansulfonat
cis-$[Pt(NH_3)_2Cl_2]$	Cisplatin
Cisplatin	*cis*-Diammindichloridoplatin(II)
Cl	Chlorid

cm	Zentimeter
CTR1	*Copper transport protein 1*
Cys	Cystin
DACH	1,2-Diaminocyclohexyl
DNA	Desoxyribonukleinsäure
DTT	Dithiothreitol
EF1A1	*Elongation factor alpha-1*
EGF-Rezeptor	*Epidermal Growth Factor Receptor*
ENOA	Alpha-Enolase
ER	Endoplasmatisches Retikulum
ERBB2	*human epidermal growth factor receptor 2*
ERCC1	*Excision repair cross-complementing 1*
ERCC4	*Excision repair cross-complementing 4*
ESI	Elektrosprayionisation
et *al.*	und andere
ETF	*Electron transfer flavoprotein subunit alpha*
FIGO	*Fédération Internationale de Gynécologie et d'Obstétrique*
g	Gamma
G	Guanin
GAPDH	*Glyceraldehyd-3-phosphate dehyrogenase*
GRP	*Glucose-related-protein*
GSH	Glutathion
GSTO1-1	*Glutathione-S transferase omega 1*
H_2O	Wasser
HE4	*human Epididymis Protein 4*
HED	Hydroxyethyldisulfid
HER-2	*human epidermal growth factor receptor 2*
hnRNP	*Heterogenous nuclear ribonucleoprotein*
HSP 27	*heat shock 27 kDa protein 1*
IDHc	*Cytosolic NADP+ dependent isocitrate dehydrogenase*
IEF	isoelektrische Fokussierung
IGF-1	*Insulin-like growth factor-1*
IPG	Immobilisierter pH-Gradient

kDa	Kilodalton
KDEL	Signalsequenz im ER, Lys-Asp-Glu-Leu
kVh	Kilovoltstunde
LA-ICP-MS	*laser ablation-inductively coupled plasma-mass spectrometry*
LC	Liquid-Chromatographie
MAPK	*Mitogen-activated protein kinase*
MCL-1	*myeloid cell leukemia sequence 1*
Met	Methionin
mL	Milliliter
MLH1	*MutL homolog 1*
mM	Millimolar
MMR	*Mismatch Repair System*
mRNA	*messenger Ribonucleic Acid*
MRP2	*Multidrug resistance-associated protein 2*
MS	Massenspektrometer
MS/MS	Tandem-Massenspektrometrie
MSH2	*Mismatch Repair Protein 2*
MTT	3-(4,5-Dimethylthiazol-2-yl)-2,5-diphenyltetrazoliumbromid
N	Nucleosid
NADP+	Nicotinsäureamid-Adenin-Dinukleotid-Phosphat
NER	*Nucleotide excision repair*
NH_3	Ammonium
NSCLC	*Non-small cell lung cancer*
OC	Ovarialkarzinom
OCT, OCT2	*Organic cation transporter*
OH	Hydroxid
Oxaliplatin	Trans-l-diaminocyclohexanoxalatoplatin
p53	*Tumor protein p53*
p73	*Tumor protein p73*
PACMA31	N-(2,4-Dimethoxyphenyl)-N-(1-oxo-2-propyn-1-yl)-2-(2-thienyl) glycyl-glycine ethyl ester
PARP	*Poly (ADP-ribose) polymerase*
PDI	Protein-Disulfid-Isomerase

pH	*potentia hydrogenii*
PHB	*Prohibitin*
PHGDH	D-3-phosphoglycerate-dehydrogenase
pI	isoelektrischer Punkt
PI3K	Phosphatidylinositol-3-Kinase
PKM	Pyruvate Kinase
PRDX3	*Peroxiredoxin 3*
Pt	Platin
RAD51	*DNA repair protein RAD51 homolog 1*
RNA	Ribonukleinsäure
SDS-PAGE	Natriumdodecylsulfat-Polyacrylamidgelelektrophorese
siRNA	*small interfering RNA*
tRNA	*tranfer RNA*
TLS	transläsionale DNA-Synthese
TOF	*Time of Flight*
TP53	Tumorsupressor 53
uPAR	Urokinase-Rezeptor
UPR	*Unfolded Protein Response*
V	Volt
VDAC	*voltage-dependent anion channel*

ZUSAMMENFASSUNG

Vor über 50 Jahren entdeckte Barnett Rosenberg die zytostatische Wirkung von Cisplatin. Bereits einige Jahre später wurden die ersten Krebspatienten im Rahmen einer Studie mit Cisplatin behandelt. Seit 40 Jahren ist die Behandlung mit Cisplatin ein fester Bestandteil der Krebstherapie. Gegenwärtig erfolgt eine Behandlung mit Cisplatin bei Plattenepithelkarzinomen an Kopf und Hals sowie beim Lungen-, Harnblasen-, Hoden- und Ovarialkarzinom (OC).

Eine Platin-basierte Chemotherapie scheitert häufig an der Resistenz der Tumorzellen. Die Resistenz der Tumorzellen gegenüber Cisplatin hat vielfache Gründe und ist bis heute nicht vollständig verstanden. Da das reaktive Cisplatin bevorzugt mit schwefelhaltigen Aminosäuren interagiert, ist in den letzten Jahren die intrazelluläre Bindung von Cisplatin an Proteine in den Fokus der Forschung gerückt. In einer Tumorzelle existiert für Cisplatin eine Vielzahl von potentiellen Bindungspartnern. Daher ist das Ziel dieser Studie, einen geeigneten methodischen Ansatz zur Identifizierung von intrazellulären Cisplatin-Proteinaddukten zu etablieren und die funktionelle Bedeutung an ausgewählten Proteinen zu untersuchen.

Für die Analyse wurde die humane OC-zelllinie A2780 und deren cisplatinresistente Tochterzelllinie A2780*cis* verwendet, da das OC derzeit mit der höchsten Sterblichkeitsrate aller gynäkologischen Malignome einhergeht. Da bislang die Identifizierung von Cisplatin-Proteinaddukten aus einer komplexen biologischen Probe erfolglos war, wurde die fluoreszierende Modellsubstanz CFDA-Cisplatin verwendet.

Die Identifizierung von intrazellulären Bindungspartnern von Cisplatin wurde durch die Etablierung einer analytischen Methode, bestehend aus dem fluoreszierenden CFDA-Cisplatin, der 2D-Gelelektrophorese und Massenspektrometrie, ermöglicht. Um möglichst viele zytosolische Cisplatin-bindende Proteine identifizieren zu können, erfolgte die 2D-Gelelektrophorese getrennt für zwei verschiedene pH-Bereiche 4 - 7 und 6 - 10.

Für die Identifizierung war die Optimierung einzelner Schritte der 2D-Gelelektrophorese unerlässlich, besonders für Proteine im alkalischen pH-Bereich (pH 6-10). Dadurch war die Identifizierung von EF1A1 (*Elongation factor alpha-1*)

mit einem theoretischen p*I* von 9,10 als ein intrazellulärer Bindungspartner von Cisplatin möglich. Neben EF1A1 wurden sechs Cisplatin-bindende Proteine im sauren pH-Bereich sowie weitere sieben im alkalischen pH-Bereich identifiziert.
Von den insgesamt 14 identifizierten intrazellulären Bindungspartnern von Cisplatin werden PDIA(Protein-Disulfid-Isomerase)1, PDIA3, GRP(*Glucose-related-protein*)78, EF1A1, ENOA (Alpha-Enolase), GAPDH (Glyceraldehyd-3-phosphate dehyrogenase), PKM (Pyruvatekinase) und PHGDH (D-3-phosphoglycerate-dehydrogenase) mit der Tumorentstehung in Verbindung gebracht. Kullmann *et al.* zeigte, dass ein siRNA-vermittelte *Knockdown* von GRP78 und PDIA3 die Cisplatin-induzierte Zytotoxizität in der Zelllinie *A2780cis* nicht beeinflusst wird und diese daher wahrscheinlich nicht an der erworbenen Cisplatinresistenz beteiligt sind. Zudem konnten wir zeigen, dass die spezifische Inhibierung von PDIA1 durch PACMA 31 einen potentiellen antitumoralen Therapieansatz darstellt. Dies muss in weiterführenden pharmakologischen Studien näher untersucht werden.

SUMMARY

More than fifty years ago, Barnett Rosenberg discovered the cytostatic effect of cisplatin. A couple of years later, the first cancer patients were treated with cisplatin in a study. For the last 40 years, treatment with cisplatin has been an integral part of cancer therapy. Currently, cisplatin is being used for squamous cell carcinoma in head and neck as well as in lung, bladder, testicular and ovarian carcinoma (OC).

A platinum-based chemotherapy often fails because of resistance of tumor cells to the drug. Resistance to cisplatin is a multifactorial problem and is still not fully understood. Reactive cisplatin preferably interacts with sulfur-containing amino acids. Therefore, the intracellular binding of cisplatin to proteins has been the focus of research for several years. In tumor cells, cisplatin has a variety of potential binding partners. Consequently, the aim of this study is to establish a suitable methodological approach for the identification of intracellular cisplatin protein adducts and to investigate the functional importance of these selected proteins.

For the analysis, the human OC cell line A2780 and its cisplatin-resistant subline A2780*cis* were used. The OC is currently associated with the highest mortality rate of all gynecological malignancies. So far the identification of cisplatin protein adducts from a complex biological sample has seen unsuccessful, that the fluorescent model substance CFDA-cisplatin was used.

We established a method to detect and identify intracellular binding partners of cisplatin based on the fluorescent CFDA-cisplatin, 2D gel electrophoresis and mass spectrometry. To identify as many as possible cytosolic cisplatin-binding proteins, 2D gel electrophoresis was performed separately for two different ranges: pH 4-7 and pH 6-10.

The optimization of each step of the 2D gel electrophoresis was essential, especially for proteins in the alkaline pH range (pH 6-10). After optimization the identification of EF1A1 (elongation factor alpha-1) with a theoretical pI of 9.10 as an intracellular binding partner of cisplatin was possible. In addition to EF1A1, six cisplatin-binding proteins in the acidic pH range and seven others in the alkaline pH range were identified.

Of the total of 14 identified intracellular binding partners of cisplatin, PDIA (protein disulfide isomerase) 1, PDIA3, GRP (glucose-related protein) 78, EF1A1, ENOA (alpha-enolase), GAPDH (glyceraldehyd-3-phosphate dehyrogenase), PKM (pyruvate kinase) and PHGDH (D-3-phosphoglycerate dehydrogenase) were associated with tumorigenesis. Kullmann et *al.* demonstrated that siRNA-mediated knockdown of GRP78 and PDIA3 does not affect cisplatin-induced cytotoxicity in the A2780cis cell line, and therefore is unlikely to be involved in acquired cisplatin resistance. In addition, we were able to show that the specific inhibition of PDIA1 by PACMA 31 represents a potential antitumoral therapeutic approach. This must be further investigated in further pharmacological studies.

EIDESSTATTLICHE ERKLÄRUNG

Ich versichere an Eides Statt, dass die Dissertation „Die Identifizierung von intrazellulären CFDA-Cisplatin-bindenden Proteinen“ von mir selbständig und ohne unzulässige fremde Hilfe unter Beachtung der „Grundsätze zur Sicherung guter wissenschaftlicher Praxis“ an der Heinreich-Heine-Universität Düsseldorf und der Universität zu Köln erstellt worden ist.

Die Dissertation wurde in vorgelegter oder ähnlicher Form noch bei keiner anderen Institution eingereicht. Ich habe bisher keine erfolglosen Promotionsversuche unternommen.

Düsseldorf, Juli 2019

_____

Sandra Kotz

1 EINLEITUNG

1.1 KREBS

1.1.1 EPIDEMIOLOGIE

Nach den Herz-Kreislauf-Erkrankungen ist Krebs weltweit die zweithäufigste Todesursache. In Deutschland erkrankten im Jahr 2013 etwa 253.000 Männer und 230.000 Frauen an Krebs (Abbildung 1). Die Zahl der Krebssterbefälle lag im gleichen Jahr bei etwa 223.000 (Abbildung 2) [1].

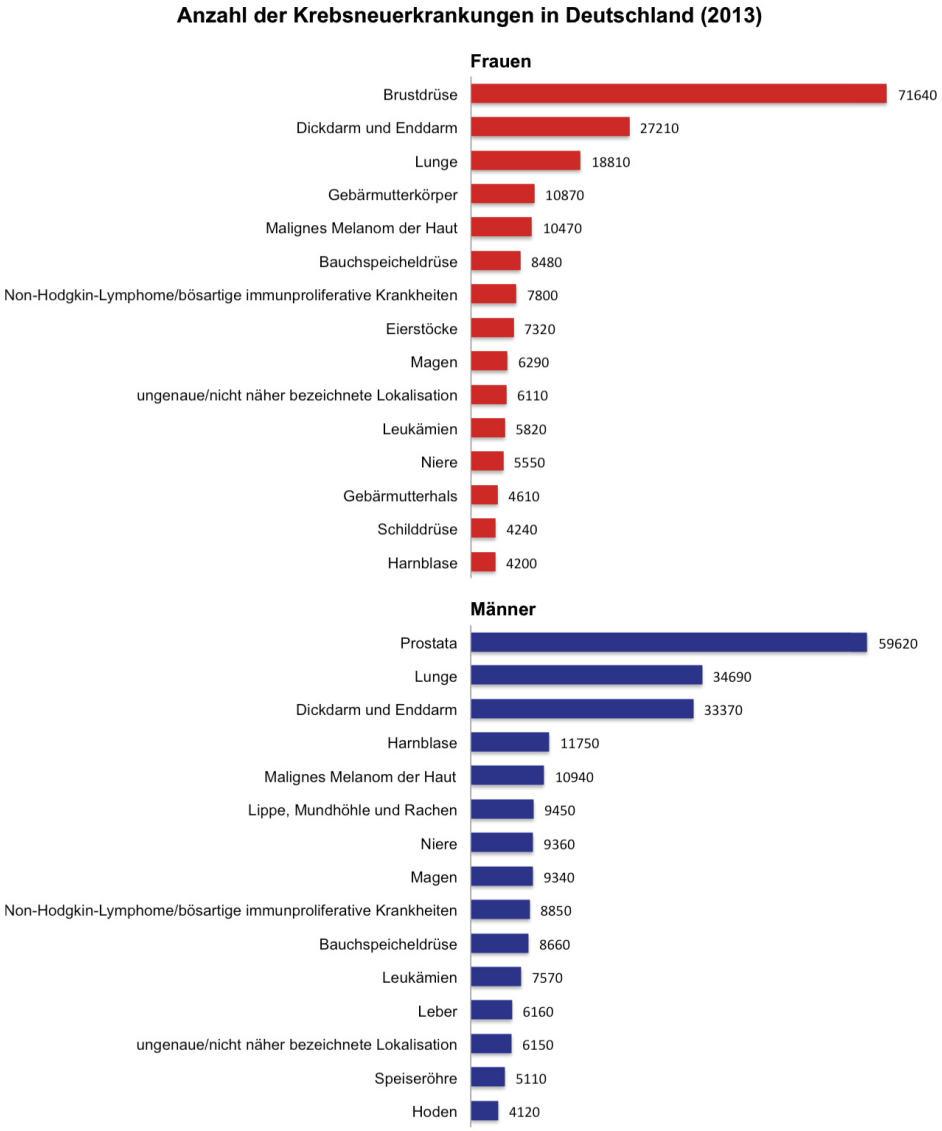

Abbildung 1: Anzahl der Krebsneuerkrankungen in Deutschland (2013) (modifiziert nach [1]).

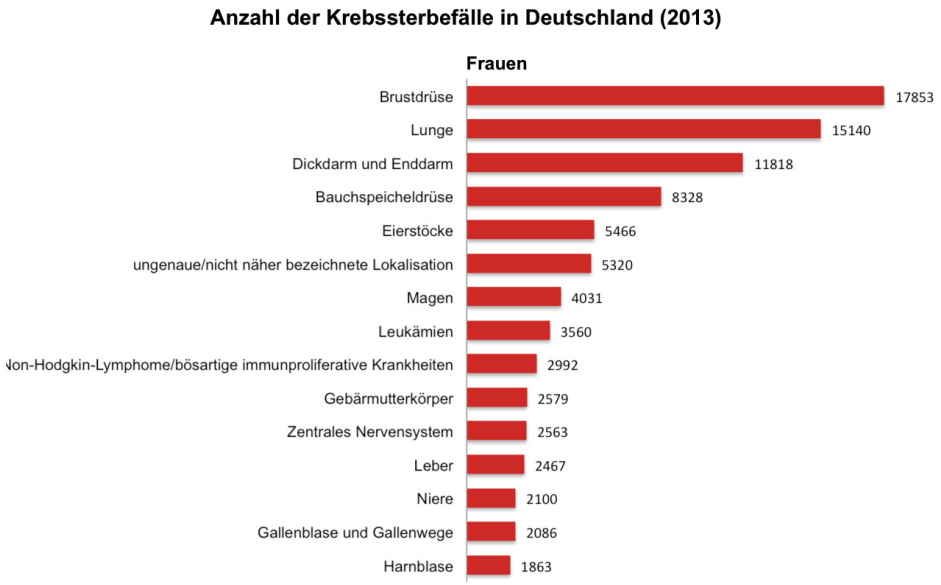

Abbildung 2: Anzahl der Krebssterbefälle in Deutschland (2013) (modifiziert nach [1]).

Im Jahr 2013 war das Ovarialkarzinom (OC) mit 7320 Neuerkrankungen die dritthäufigste gynäkologische Tumorerkrankung und zeigte mit 5466 Sterbefällen die zweithöchste Mortalität (Abbildung 1 & 2). Dadurch kommt zum Ausdruck, dass das OC zu den aggressivsten Tumoren zählt und die schlechteste Prognose aller gynäkologischen Tumorerkrankungen hat [1].

1.1.2 OVARIALKARZINOM

Das OC befällt im Frühstadium ein oder beide Ovarien (*Fédération Internationale de Gynécologie et d'Obstétrique* (FIGO) I), breitet sich danach im Becken (FIGO II), in der Bauchhöhle und über die Lymphknoten (FIGO III) aus und verlässt im Spätstadium die Peritonealhöhle und befällt innere Organe (FIGO IV). Bei etwa 70% der Patientinnen wird das fortgeschrittene OC (FIGO IIIB - IV) diagnostiziert, da zunächst unspezifische Symptome wie z.B. Zunahme des Bauchumfangs ohne Gewichtszunahme, unbestimmte Verdauungsbeschwerden/Völlegefühl, allgemeine Müdigkeit und Erschöpfung auftreten und bislang Strategien für ein effektives Screening fehlen.

Bei etwa 10-15% der OC liegt eine genetische Ursache zugrunde. Mutationen in den Tumorsuppressorgenen *BRCA (Breast Cancer) 1* (44%) und *BRCA2* (17%) erhöhen das kumulative Risiko für ein OC [2]. Zudem erhöht das hereditäre non-polypöse Kolonkarzinom [3], verursacht durch Mutationen in den Genen *hMLH (human mutL homologue) 1*, *hMSH (human mismatch recognition complex) 2*, *hMSH6* und *hPMS2 (human mismatch repair endonuclease)* [8], sowie Mutationen

in den Genen *BRIP (BRCA1-interacting protein) 1* [4] und *RAD51 (DNA repair protein RAD51 homolog 1)* [5] ebenfalls das Risiko für ein OC.

1.2 TUMORENTSTEHUNG

Der Ausgangspunkt eines Tumors ist das Erbgut der Zellen. Onkogene fördern Zellwachstum, während Tumorsuppressorgene Zellwachstum unterdrücken und Reparaturgene Mutationen im Erbgut der Zellen beheben. Ein Tumor entsteht durch Genveränderungen im Erbgut. Versagt das Reparatursystem der Zellen, entstehen die zu einem Tumor führenden Mutationen im Erbgut. Es kommt zu einem Ungleichgewicht zwischen Onko- und Tumorsuppressorgenen und zum unkontrollierten Wachstum von Zellen. Bei der Tumorentstehung handelt es sich um einen mehrstufigen Prozess und dazu gehören nach Hanahan und Weinberg (Abbildung 3) [6, 7]:

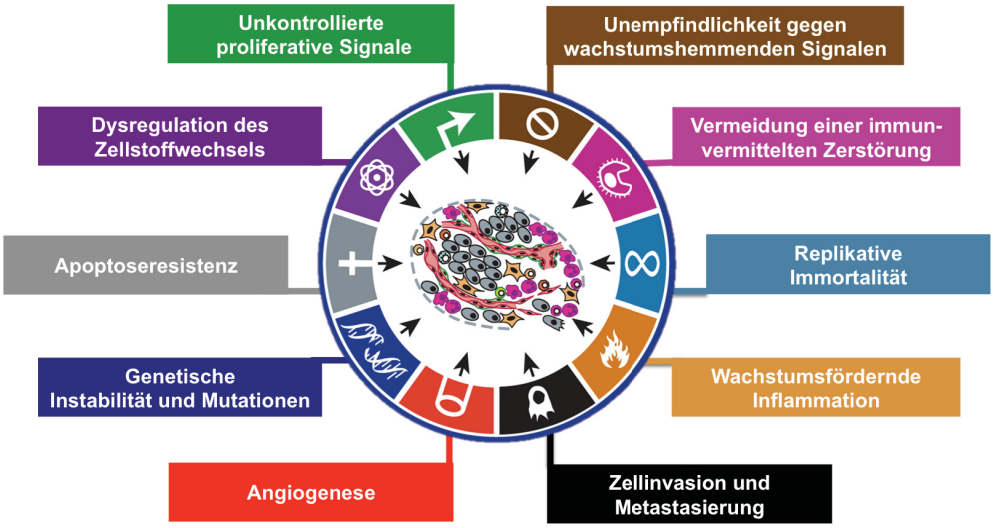

Abbildung 3: Die Tumorentstehung basiert auf der genomischen Instabilität bösartiger Zellen sowie der tumorpromovierenden Inflammation. Dadurch besitzen Tumorzellen die Fähigkeit, Immunzellen aktiv auszuweichen, proliferative Signalwege aufrechtzuerhalten, unempfindlich gegenüber wachstumshemmenden Signalen und resistent gegenüber dem Zelltod zu sein. Sie erlangen replikative Immortalität, induzieren Angiogenese und aktivieren Zellinvasion und Metastasierung. Des Weiteren erfolgt eine Dysregulation des Zellstoffwechsels (modifiziert nach [7]).

Die diversen Fähigkeiten von Tumorzellen verdeutlichen, dass viele komplexe zelluläre Veränderungen bei der Tumorentstehung miteinander interagieren, die für die Entwicklung neuer Therapieoptionen genutzt werden können. In den letzten Jahren war die Einführung einer zielgerichteten Therapie ein wichtiger Fortschritt

in der medikamentösen Krebstherapie. Diese Therapeutika umfassen niedermolekulare Inhibitoren (z.B. Olaparib – ein niedermolekularer PARP (Poly (ADP-ribose) polymerase) – Inhibitor) und monoklonale Antikörper (z.B. Bevacizumab – ein Angiogenesehemmer), die gestörte Signalwege einer Tumorzelle (Zellwachstum, Angiogenese, Metastasierung) als therapeutischen Ansatz nutzen und weiterhin nach einer bzw. in Kombination mit einer platin- und taxanhaltigen Chemotherapie beim OC eingesetzt werden können [8].

1.3 CISPLATIN

In den 1960er Jahren entdeckte Barnett Rosenberg als Nebenbefund die zytostatische Wirkung von Platin-Komplexen, indem er die Wirkung von Wechselstrom auf das Wachstum von Bakterien untersuchte und hierzu Platin-Elektroden verwendete. Dabei stellte er fest, dass das Zellwachstum durch die Komplexverbindung cis-[$Pt(NH_3)_2Cl_2$] (Cisplatin) gehemmt wurde [9].

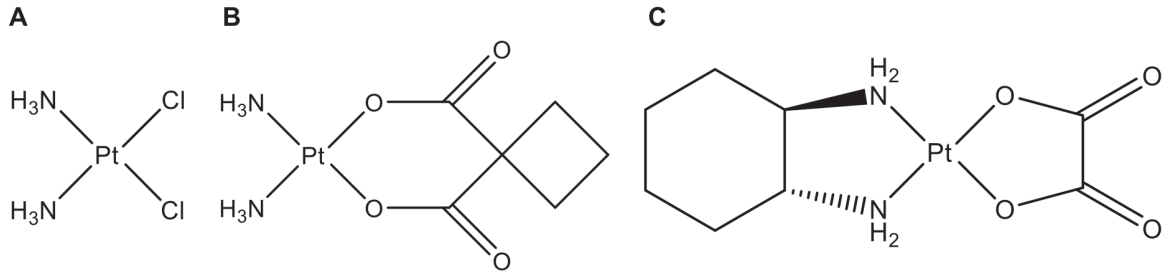

Abbildung 4: Die für die Chemotherapie zugelassenen Platinkomplexe: Cisplatin (A), Carboplatin (B), Oxaliplatin (C)

Cisplatin (*cis*-Diammindichloridoplatin(II)) (Abbildung 4 A) ist ein neutraler, anorganischer, quadratisch planarer Komplex mit Platin in der Oxidationsstufe II und den Liganden NH_3 und Chlorid in der *cis*-Konfiguration. Die Aufnahme von Cisplatin in die Zelle erfolgt über verschiedene zelluläre Vorgänge, einschließlich passive Diffusion, erleichterte Diffusion durch Transportproteine und aktiver Transport [10-12]. Der Kupfertransporter CTR (*Copper transport protein*) 1 scheint an der zellulären Aufnahme sowie am intrazellulären Transport von Platin-basierten Medikamenten beteiligt zu sein [13, 14]. Des Weiteren wird die zelluläre Aufnahme von Cisplatin durch organische Kationentransporter (OCTs – *Organic cation transporter*) in den proximalen Nierentubulus vermittelt. Einer der Haupttransporter von Cisplatin ist OCT2, der hauptsächlich in der basolateralen

Membran des proximalen Nierentubulus exprimiert wird und für die Nephrotoxizität von Cisplatin verantwortlich ist [15-17].

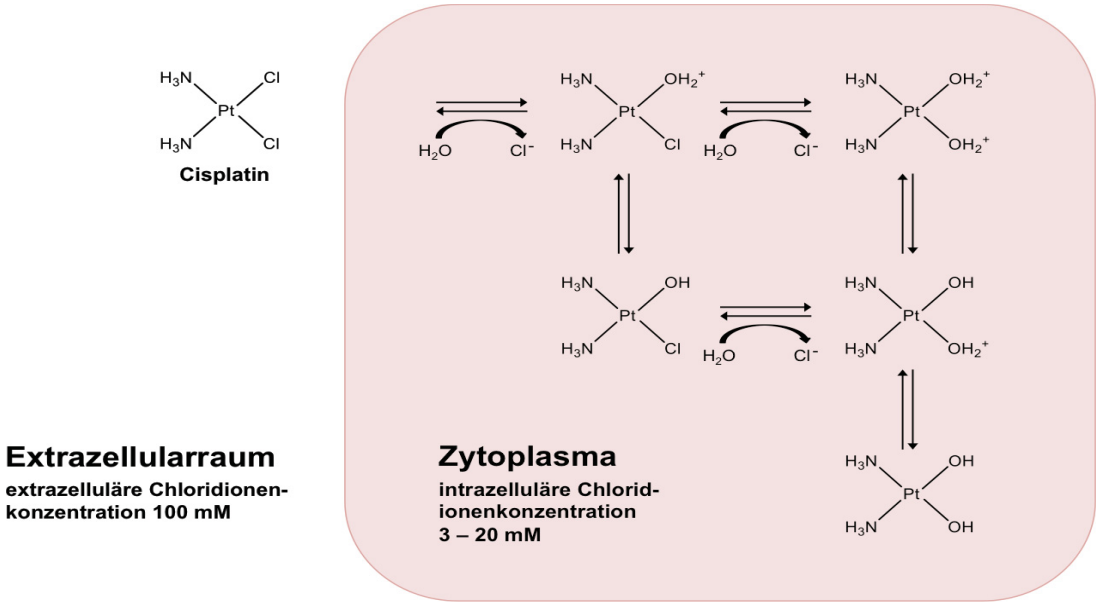

Abbildung 5: Schematische Darstellung der Hydrolyse von Cisplatin mit Ausbildung hochreaktiver Diaquakomplexe im Zytoplasma der Zelle (modifiziert nach [10]).

Cisplatin selbst ist unwirksam und wird erst durch die Hydrolyse im intrazellulären Raum in die Wirkform überführt, begünstigt durch eine niedrige Chloridionenkonzentration von 3-20 mM gegenüber 100 mM im extrazellulären Raum (Abbildung 5) [18]. Durch die hohe H_2O-Konzentration können beide Chlorid-Liganden abgespalten werden und es entstehen in zwei Schritten positiv geladene Mono- und Diaquakomplexe [12]. Bei einer nukleophilen Substitution stellt Wasser eine gute Abgangsgruppe dar, so dass dieser Komplex gut mit Nukleophilen in der Zelle reagieren kann. Cisplatin reagiert bevorzugt mit dem nukleophilen Stickstoffatom 7 des Guanins in der DNA (Desoxyribonukleinsäure). Bei dieser Reaktion entstehen mono- und bifunktionale Cisplatin-DNA-Addukte, wobei die bifunktionalen DNA-Cisplatin Addukte in intra- und intermolekulare Quervernetzungen unterteilt werden (Abbildung 6) [19]. Die zytotoxische Wirkung des Cisplatins basiert hauptsächlich auf der 1,2-intramolekularen Quervernetzung. Hierzu wurde die Häufigkeit der 1,2-intramolekularen Quervernetzung herangezogen, die hervorgerufene Strukturveränderung der DNA als verantwortliche Läsion für die Zytotoxizität angesehen, die minimale Anzahl an

monofunktionalen und interkalierenden Addukten sowie das Stereoisomer Transplatin, das ein begrenztes therapeutisches Wirkungsspektrum aufweist [20]. Insgesamt reagieren nur etwa 1% des intrazellulären Cisplatins mit der DNA [21]. Daher wird angenommen, dass Cisplatin eine hohe Affinität zu schwefelhaltigen Aminosäuren wie Cystein und Methionin hat [22] und gut mit Proteinen, Phospholipiden, Filamenten des Zytoskeletts und thiolhaltigen Molekülen wie Glutathion (GSH) reagieren kann [23, 24].

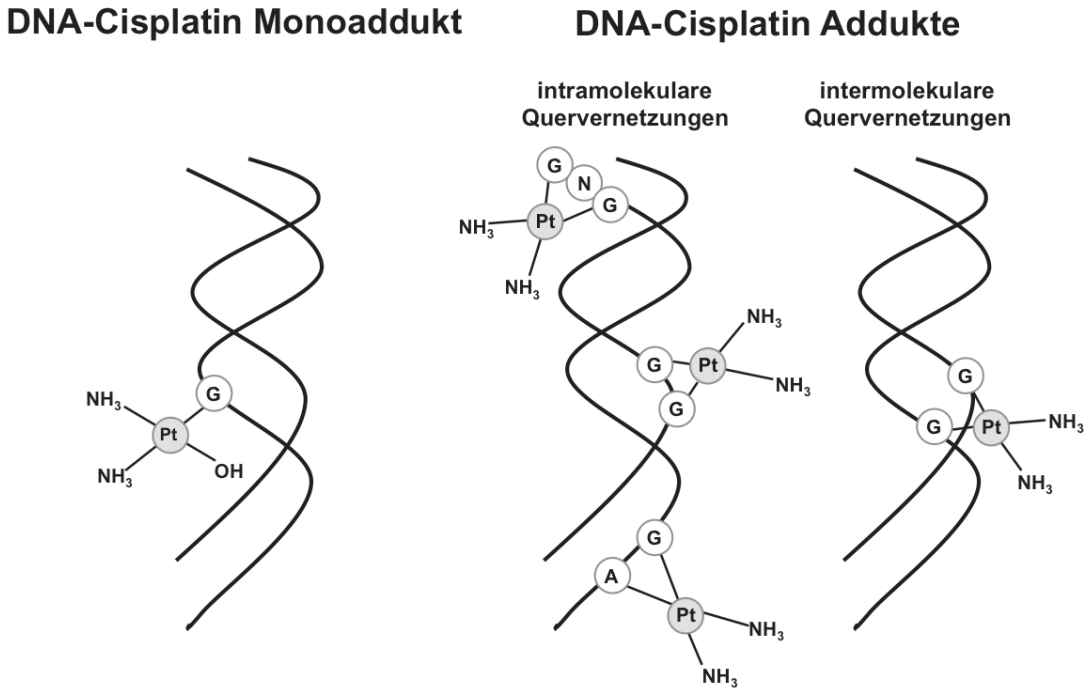

Abbildung 6: Mono- und bifunktionale Cisplatin-DNA-Addukte mit ihrer jeweiligen Prävalenz (modifiziert nach [25, 26]). Pt = Platin, NH_3 = Ammonium, OH = Hydroxid, A = Adenin, G = Guanin, N = Nucleosid

Seit den 1970er Jahren ist Cisplatin ein breit eingesetzter Wirkstoff in der Krebstherapie. Gegenwärtig erfolgt eine Behandlung mit Cisplatin bei Plattenepithelkarzinomen an Kopf und Hals, Lungen-, Harnblasen-, Hoden- und Ovarialkarzinom [27-29]. Die Wirksamkeit von Cisplatin ist durch toxische Nebenwirkungen wie z.B. Oto-, Neuro- und Nephrotoxizität sowie durch die Resistenz von Tumorzellen gegenüber Cisplatin limitiert. Die Toxizität sowie die Resistenz von Tumorzellen gegenüber Cisplatin haben die Entwicklung von weiteren Platin-basierten Zytostatika initiiert, die weniger oder tolerierbare Nebenwirkungen hervorrufen und/oder einen oder mehrere Resistenzmechanismen überwinden können. Seit der Zulassung von Cisplatin

wurden für weitere 23 Platin-basierte Zytostatika klinische Studien durchgeführt, wovon nur Carboplatin (Abbildung 4B) und Oxaliplatin (Abbildung 4C) eine weltweite Zulassung erhielten. Nedaplatin (Japan), Lobaplatin (China) und Heptaplatin (Korea) sind dagegen nur in einzelnen Länder zugelassen.

1.4 RESISTENZMECHANISMEN

1.4.1 ERWORBENE RESISTENZ

Eine Platin-basierte Chemotherapie scheitert häufig an der Resistenz der Tumorzellen [30, 31]. Die 5-Jahres-Überlebensrate beim OC liegt bei etwa 40%, so dass die Mehrzahl der Patientinnen ein Rezidiv des OCs erleiden [1]. Bei einem platinrefraktären Rezidiv ist die Prognose in der Regel besonders ungünstig [32, 33]. Die Resistenz der Tumorzellen gegenüber Cisplatin hat vielfache Gründe [34] und ruft Veränderungen von Signalkaskaden sowie gegenregulierende Mechanismen hervor, wobei antiapoptotische oder proliferative Reize überwiegen und die Tumorzelle weiter teilungs- und lebensfähig bleibt. Bei der Entwicklung von Strategien zur Vermeidung bzw. Überwindung einer Cisplatinresistenz kann somit an unterschiedlichen Punkten angesetzt werden. Für einen umfassenden Überblick der Resistenzmechanismen eignet sich die Klassifizierung nach Galluzzi et *al*. in *pre-target*, *on-target*, *post-target* und *off-target* Resistenz (Abbildung 7) [30, 31].

1.4.1.1 *PRE-TARGET* RESISTENZ

Für die zytotoxische Wirkung von Cisplatin ist die intrazelluläre Konzentration von reaktivem Cisplatin ausschlaggebend [35]. Die *pre-target* Resistenz ist einerseits auf eine verminderte Zufuhr und/oder erhöhten Efflux von Cisplatin zurückzuführen sowie durch eine erhöhte Inaktivierung von Cisplatin durch thiolhaltige Moleküle.

Der Kupfertransporter CTR1 hat einen signifikanten Anteil an der zellulären Aufnahme von Cisplatin [36-40]. CTR1 ist in cisplatinresistenten Tumorzellen vermindert exprimiert und eine Depletion von CTR1 erhöht die Cisplatinresistenz [36, 37, 39]. Kupferchelatoren können hingegen die Aufnahme und zytotoxische Wirksamkeit von Cisplatin erhöhen [38]. Dagegen steigern MRP2 (*Multidrug resistance-associated protein 2*) [41-43] und der Kupfertransporter ATP7B (*Copper-transporting P-type adenosine triphosphatase 7B*) [39, 44] signifikant den

Efflux von Cisplatin und sind in cisplatinresistenten Tumorzellen erhöht exprimiert [45-47]. Zudem zeigen cisplatinresistente Tumorzellen erhöhte Expressionslevel von GSH, γ-Glutamylcystein-Synthetase (Enzym der GSH-Synthese), Glutathion-S-Transferase (Enzym konjugiert Cisplatin und GSH) und Metallothionein [48-51].

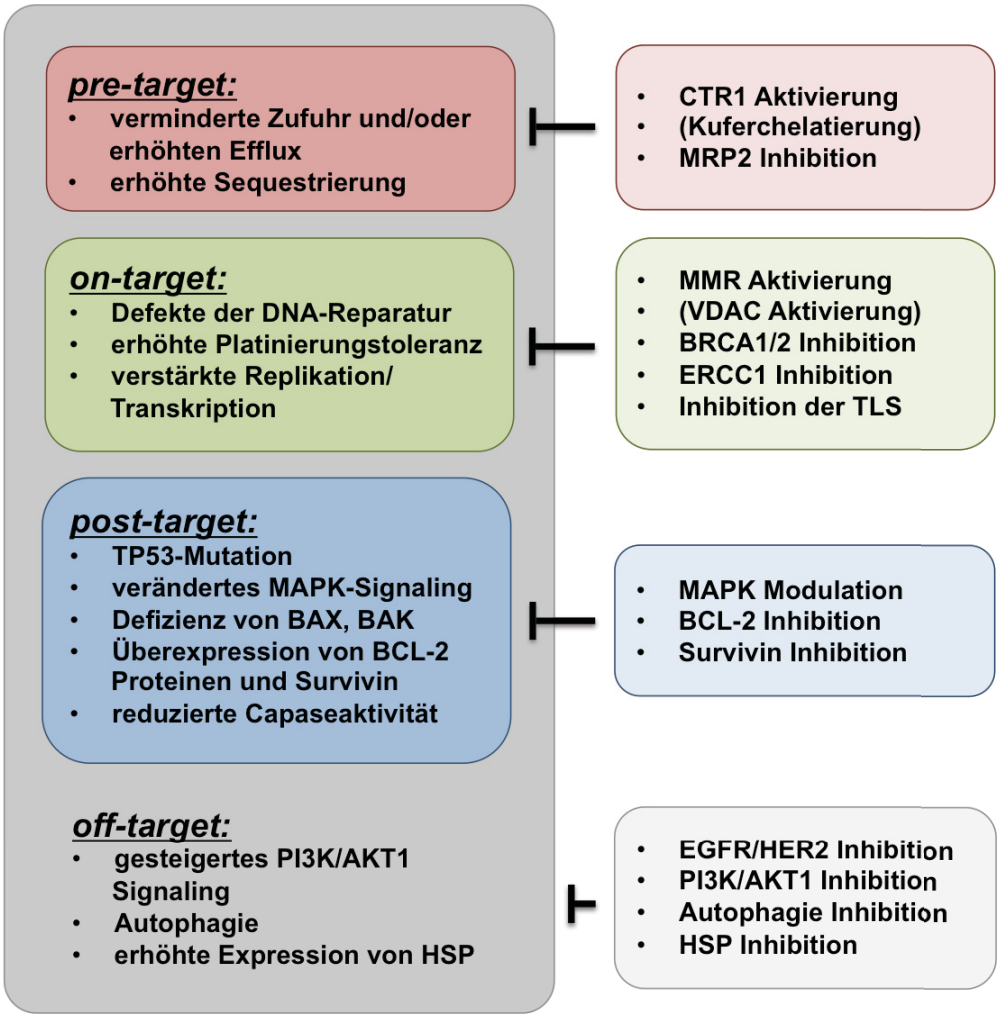

Abbildung 7: Mögliche pharmakologische Angriffspunkte zur Chemosensitivierung (modifiziert nach [30]). Die Cisplatinresistenz hat vielfache Gründe, weshalb gezielte Therapien eine sehr geringe Chance zur Chemosensitivierung haben. Daher sollten Kombinationsstrategien zur Blockierung der Cisplatinresistenz entwickelt werden. Hierzu könnten detaillierte Informationen zum genetischen und epigenetischen Hintergrund des Patienten hilfreich sein, um die Cisplatinresistenz vollständig umgehen zu können. CTR1 = *Copper transport protein 1*, MRP2 = *Multidrug resistance-associated protein 2*, MMR = *Mismatch Repair System*, VDAC = *voltage-dependent anion channel* BRCA = *Breast Cancer*, ERCC = *Excision repair cross-complementing*, TLS = transläsionale DNA-Synthese, MAPK = *Mitogen-activated protein kinase*, BCL-2 = *B-cell lymphoma 2*, EGFR/HER2 = *human Epidermal Growth Factor Receptor*, PI3K/AKT1 = *Phosphatidylinositol-3-Kinase/RAC-alpha serine/threonine-protein kinase*, HSP = *heat shock protein*

1.4.1.2 *ON-TARGET* RESISTENZ

Die zytotoxische Wirkung von Cisplatin in Tumorzellen ist in Gegenwart kompetenter Reparaturmechanismen begrenzt. Es wird angenommen, dass *on-target*-Mechanismen wie die Nukleotidexzisionsreparatur (NER) zur Cisplatinresistenz beitragen. Das NER-System entfernt eine Vielzahl durch Cisplatin hervorgerufene DNA-Läsionen über eine Heterodimerisierung von ERCC (*Excision repair cross-complementing*) 1 und ERCC4/XRF [52, 53]. Die Kapazität des NER-Systems reicht jedoch nicht aus, um alle DNA-Läsionen zu beseitigen.

Die transläsionale DNA-Synthese (TLS) - auch als replikativer Bypass bekannt - ist ein vermeintlicher Reparaturmechanismus und ermöglicht den Tumorzellen eine DNA-Replikation auch bei Vorhandensein von DNA-Schäden. Tumorzellen mit einem ausgeprägten replikativen Bypass verfügen über einen Überlebensvorteil, da Strangbrüche häufig zur Apoptose führen. Die DNA-Polymerasen POLI, POLK, REV1, REV3 und REV7 vermitteln den replikativen Bypass bei der DNA-Synthese, bei der es aber auch zu Basenfehlpaarungen kommen kann [54]. Das *Mismatch Repair* System (MMR) ist ein weiterer zellulärer Mechanismus, das fehlerhafte Insertionen sowie Deletionen von Basen während der DNA-Replikation detektiert [55]. Dieses MMR erkennt auch durch Cisplatin hervorgerufene DNA-Läsionen. Nach der Detektierung von Cisplatin-DNA-Addukten sind die DNA-*Mismatch*-Reparaturproteine MSH2 (*Mismatch Repair Protein 2*) und MLH1 (*MutL homolog 1*) für die Induzierung von Apoptoseprozesse verantwortlich [56]. Eine Mutation oder verminderte Expression von MSH2- und MLH1-Proteinen wird gelegentlich mit der erworbenen Cisplatinresistenz assoziiert [57-59].

Die Reparatur eines Doppelstrangbruchs kann über homologe Reparatur-mechanismen erfolgen, in denen die Gene *BRCA1* und *BRCA2* involviert sind. BRCA-exprimierte Proteine sind an zahlreichen Prozessen der DNA-Reparatur beteiligt und wirken als Tumorsuppressoren [60, 61]. Tumorzellen mit einer BRCA-Mutation können durch Cisplatin und Carboplatin hervorgerufene DNA-Läsionen daher nicht ausreichend durch homologe Rekombination beseitigen. Die DNA-Reparatur in BRCA-mutierten Zellen erfolgt meist durch das NER-System und kann als pharmakologischer Ansatzpunkt genutzt werden, da das Enzym PARP an diesem Mechanismus mitwirkt und fehlerhafte Basen ausschneidet und ersetzt [8].

Außerdem bindet Cisplatin sowohl an mitochondriale DNA als auch an den spannungsabhängigen Anion-Austauscher VDAC (*voltage-dependent anion channel*) [62]. VDAC vermittelt wichtige zelluläre Funktionen [63], zudem konnte eine erhöhte Cisplatinresistenz bei einem VDAC1-*Knockdown* in NSCLC(*Non-small cell lung cancer*)-Zellen nachgewiesen werden [64]. Bisher ist nicht eindeutig geklärt, ob das mitochondriale Protein VDAC direkt durch die Cisplatinbindung (*on-target*) oder durch proapoptotische Signale (*post-target*) reguliert wird.

1.4.1.3 *POST-TARGET* RESISTENZ

Der führende *post-target* Resistenzmechanismus ist die Inaktivierung des Tumorsuppressors 53 (TP53) [65]. Folglich verleiht der Verlust des proapoptotischen Signals Tumorzellen häufig eine Cisplatinresistenz [66]. OC, die eine *TP53*-Mutation aufweisen, zeigen dann meist ein geringeres Ansprechen auf eine Platin-basierte Chemotherapie [67]. Diskutiert wird auch die Mitwirkung der proapoptotischen MAPKs (Mitogen-aktivierten Proteinkinasen) bei einer erworbenen Cisplatinresistenz [68]. Die Defizienz der Proteine BAX (Co-Faktor des Tumorsupressor-Proteins p53) und BAK (*Bcl-2 homologous antagonist*) sowie die Überexpression der antiapoptotischen Proteine der BCL-2 (*B-cell lymphoma 2*) Familie wie BCL-2, BCL-X_L (*B-cell lymphoma-extra large*) und MCL-1 (*myeloid cell leukemia sequence 1*) werden ebenfalls mit der Cisplatinresistenz in Kopf-, Hals-, Ovarial- und nichtkleinzelligem Lungenkrebs in Verbindung gebracht [69-71]. Die Überexpression des Caspase-Inhibitors Survivin (BIRC5) und die damit korrelierende PI3K/AKT(*Phosphatidylinositol-3-Kinase*/*RAC-alpha serine/threonine -protein kinase*)-Signaltransduktion wurde in einigen Tumoren mit einer Chemoresistenz assoziiert [30, 72]. Modifikationen der Initiator- (Caspase-9 und -8) und Exekutivcaspasen (Caspase-3, -6 und -7), die in der Apoptose den Abbau der Proteine einleiten, werden auch mit einer erworbenen Cisplatinresistenz beschrieben [73].

1.4.1.4 *OFF-TARGET* RESISTENZ

O*ff-target* Resistenzmechanismen werden nicht direkt mit Cisplatin in Verbindung gebracht, sondern kompensieren die zytotoxische Wirkung von Cisplatin durch Veränderungen der Signalwege. Das Protoonkogen ERBB2 (HER-2 – *human epidermal growth factor receptor 2*) gehört zur Familie der epidermalen Wachstumsfaktorrezeptoren (EGF-Rezeptor) und ist bei einer Platin-basierten

Chemotherapie in OC hochreguliert [74, 75]. ERBB2 induziert den PI3K/AKT1 Signalweg, das zur Hochregulierung von CDKN1A (*cyclin-dependent kinase inhibitor 1A*) führt [76]. Ein AKT1-abhängiger Mechanismus zur Phosphorylierung verhindert aber die nukleare Transaktivierung von CDKN1A und führt somit zu einer erhöhten Proliferation von Tumorzellen [72, 77]. Der Autophagie-Mechanismus, der den lysosomalen Abbau von zytoplasmatischen Organellen oder zytosolischen Komponenten beinhaltet, wird von Tumorzellen als Reaktion auf eine Platin-basierte Chemotherapie eingesetzt und wird mit der Cisplatinresistenz in OC beschrieben [78]. Zudem reduzieren molekulare Chaperone wie z.B. das HSP 27 (*heat shock 27 kDa protein 1*) das Ansprechen von Tumorzellen auf eine Platin-basierte Chemotherapie [30].

1.4.2 INTRAZELLULÄRE BINDUNG ALS MECHANISMUS DER RESISTENZ

In einer Tumorzelle gibt es für Cisplatin eine Vielzahl von potentiellen Bindungspartnern. Aufgrund der hohen Affinität zu schwefelhaltigen Aminosäuren wurden das Tripepetid GSH und kleine, zytoplasmatische Proteine der Metallothionein-Familie als Bindungspartner von Cisplatin identifiziert [49, 79-81]. Die Resistenz von Tumorzellen gegenüber Cisplatin wurde oftmals auf eine erhöhte Konzentration von GSH sowie auf einen erhöhten Efflux von Cisplatin zurückgeführt [82]. Im Jahr 2009 konnte aber Kasherman et *al.* zeigen, dass bei der OC-Zelllinie A2780*cis* zwei Drittel der Cisplatin-Addukte eine Molekularmasse von mehr als 3 kDa aufwiesen. Daher spielt GSH bei der Inaktivierung von Cisplatin wohl nur eine untergeordnete Rolle [22]. In den letzten Jahren ist die intrazelluläre Bindung von Cisplatin an Proteine in den Fokus der Forschung gerückt, da die Wechselwirkung mit Proteinen die intrazelluläre Verteilung, Eliminierung und Zytotoxizität von Cisplatin beeinflussen kann [83]. Für die Identifizierung und Charakterisierung von Pt-bindenden Proteinen wurden Massenspektrometrie-basierte Analysen hinsichtlich der Erhaltung von Pt-Proteinbindungen mit den Standardproteinen Albumin, Transferrin, Carboanhydrase, Myoglobin und Cytochom c entwickelt [84-88]. Das reaktive Cisplatin interagiert bevorzugt mit schwefelhaltigen Aminosäuren, aber zusätzlich konnten Histidin, Serin, Threonin, Tyrosin, Glutaminsäure und Asparaginsäure als mögliche Bindungsstelle für Cisplatin identifiziert werden [84-89]. Der Wachstumsfaktor IGF-1 (*Insulin-like growth factor-1*) wird in OC-Zelllinien mit der

Cisplatinresistenz in Verbindung gebracht [90]. Daher erforschten Zhang et *al. in vitro* die Wechselwirkung zwischen Cisplatin und IGF-1 und identifizierten drei potentielle Bindungsstellen (Met59, Arg56 und Cys6) von Cisplatin. Die Wechselwirkung zwischen Cisplatin und IGF-1 kann nicht nur die Pharmakokinetik und die intrazelluläre Verteilung von Cisplatin beeinflussen, sondern auch die Bioaktivität von IGF-1 [91].

In der Krebsforschung konnte mittels der quantitativen Proteomik tausende potentielle Biomarker, aufgrund von unterschiedlich exprimierten Proteinen bzw. Peptiden, identifiziert werden [92-97]. Ungeachtet dessen ist die Resistenz der Tumorzellen gegenüber Cisplatin bis heute nicht vollständig verstanden. Seit einigen Jahren wird die Bindung von Cisplatin an Proteine als Resistenzmechanismus diskutiert. Massenspektrometrie-basierte Analysen zur Identifizierung von Pt-bindenden Proteinen konnten mittels Standardproteine etabliert werden [84-88]. In biologischen Proben sind Pt-bindende Proteine bzw. Pt-bindende Peptide normalerweise in geringen Konzentrationen vorhanden, weshalb ihr Nachweis weiterhin sehr schwierig bleibt.

1.5 CFDA-CISPLATIN - EIN MODELLKOMPLEX

Seit etwa zwei Jahrzehnten werden bildgebende Technologien zusammen mit Fluoreszenzfarbstoffen eingesetzt, um intrazelluläre Prozesse sichtbar zu machen und zu beobachten. Im Jahr 2000 setzte Molenaar et *al.* erstmals ein fluoreszierendes CFDA-Cisplatin (Abbildung 8) als Modellsubstanz in der Forschung ein. Durch eine kovalente Bindung ist der Fluoreszenzfarbstoff Carboxyfluoresceindiacetat (CFDA) an Cisplatin gebunden [98]. CFDA ist ein unpolares fluorogenes Fluorescein-Derivat, dass in veresterter Form die Zellmembran lebensfähiger Zellen passieren kann. In der Zelle werden die beiden Acetylgruppen des CFDA durch intrazelluläre Esterasen entfernt, was im Zytoplasma zu einem fluoreszierenden Produkt führt. Die intrazelluläre Verteilung von CFDA-Cisplatin hängt hauptsächlich von Cisplatin ab und das fluoreszierende CFDA-Cisplatin ermöglicht die zelluläre Verteilung von Cisplatin in Krebszellen zu untersuchen [98].

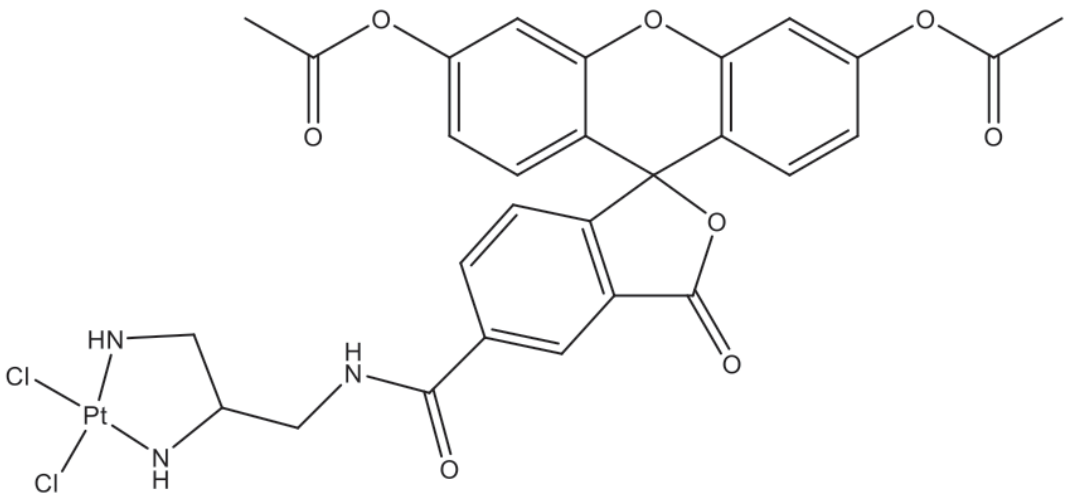

Abbildung 8: Chemische Struktur von CFDA-Cisplatin.

1.6 ZIELE DER ARBEIT

Die Resistenzentwicklung der Tumorzellen gegenüber Cisplatin hat vielfache Gründe und bis heute nicht ganz verstanden [30, 31, 34]. Da nur etwa 1% des intrazellulären Cisplatins mit der DNA reagiert [21], ist seit einigen Jahren die Bindung von Cisplatin an Proteine im Fokus. Die Interaktion mit Proteinen kann die intrazelluläre Verteilung, Eliminierung und Zytotoxizität von Cisplatin beeinflussen. Pt-bindende Proteine sind in komplexen biologischen Proben in niedriger Konzentration vorhanden, weshalb ihr Nachweis bislang erfolglos war. Daher waren die Ziele dieser Arbeit:

- Entwicklung eines methodischen Ansatzes zur Identifizierung von intrazellulären Cisplatin-Proteinaddukten, die an den Mechanismen der Resistenz von Cisplatin beteiligt sein können [99, 100].
- Reduktion der Komplexizität der Proteinproben sowie Verbesserung der Resuspendierung zytosolischer Proteine [99, 100].
- Identifizierung von cisplatinhaltigen Proteinaddukten [99].
- Untersuchung des Beitrages identifizierter Proteine zur Cisplatinresistenz (durchgeführt von Dr. M. Kullmann, Universität Bonn) [101, 102].

Ein platinresistentes OC ist üblicherweise mit einem Überleben von weniger als einem Jahr assoziiert. Daher wurde die humane OC-zelllinie A2780 (malignes

endometrioides Karzinom) und deren cisplatinresistente Tochterzelllinie A2780*cis* für die Identifizierung intrazellulärer Reaktionsprodukte von Cisplatin verwendet.
Ein wichtiger Aspekt der Methodenetablierung zur Trennung und Identifizierung der Cisplatin-Proteinaddukte war die Reproduzierbarkeit und die spezifische Detektion der Cisplatin-Proteinaddukte. Zur Visualisierung intrazellulärer Cisplatin-Proteinaddukte, die in der humanen OC-zelllinie A2780 und deren cisplatinresistenter Tochterzelllinie A2780*cis* in Wechselwirkung stehen, wurde daher das fluoreszierende Cisplatin-Analogon (CFDA-Cisplatin) verwendet [98]. Die Verwendung ermöglicht es, CFDA-Cisplatin-Proteinaddukte von den nicht modifizierten Proteinen zu unterscheiden.
Für die Trennung und Detektion der zytosolischen CFDA-Cisplatin-Proteinaddukte wurde die 2D-Gelelektrophorese mit Fluoreszenzdetektion verwendet. Zur Reduktion der Komplexizität der Proben sowie zur Verbesserung der Auflösung zytosolischer Proteine erfolgte die Auftrennung getrennt für zwei verschiedene pH-Bereiche 4 - 7 und 6 - 10. Die Identifizierung der detektierten CFDA-Cisplatin-Proteinaddukte erfolgte mittels Massenspektrometrie.
Basierend auf den Ergebnissen wurde im Anschluss ein siRNA-vermittelter *Knockdown* einzelner Bindungspartner herbeigeführt, um deren Beitrag zur Resistenzentwicklung in A2780*cis* Zellen zu untersuchen. Im Anschluss wurde die Cisplatin-vermittelte Zytotoxizität mittels MTT(3-(4,5-Dimethylthiazol-2-yl)-2,5-diphenyltetrazoliumbromid)-Assay und die Apoptoseinduktion mittels eines Apoptose-Assays mit Annexin V bestimmt [101, 102].

2 PUBLIKATIONEN

2.1 COMBINATION OF TWO-DIMENSIONAL GEL ELECTRO-PHORESIS AND A FLUORESCENT CARBOXYFLUORESCEIN-DIACETATE-LABELED CISPLATIN ANALOGUE ALLOWS THE IDENTIFICATION OF INTRACELLULAR CISPLATIN-PROTEIN ADDUCTS

Sandra Kotz, Maximilian Kullmann, Barbara Crone, Ganna V. Kalayda, Ulrich Jaehde, Sabine Metzger, Electrophoresis 2015, 00, 1 - 9

Persönlicher Beitrag:

Der persönliche Beitrag für diese Veröffentlichung war die Optimierung der 2D-Gelelektrophorese (pH 4 - 7) zur Identifizierung von intrazellulären Cisplatin-Proteinaddukten, die Identifizierung der detektierten CFDA-Cisplatin-Proteinaddukte mittels Massenspektrometrie sowie das Verfassen der Publikation.

Düsseldorf, Juli 2019

_____

Dr. Sabine Metzger

Electrophoresis 2015, *00*, 1–9

Sandra Kotz[1]
Maximilian Kullmann[2]
Barbara Crone[3]
Ganna V. Kalayda[2]
Ulrich Jaehde[2]
Sabine Metzger[1,4]

[1]Biocenter MS Platform, Department of Biology, University of Cologne, Cologne, Germany
[2]Department of Clinical Pharmacy, Institute of Pharmacy, University of Bonn, Bonn, Germany
[3]Institute of Inorganic and Analytical Chemistry, University of Münster, Münster, Germany
[4]IUF-Leibniz Research Institute for Environmental Medicine, IUF, Düsseldorf, Germany

Received April 12, 2015
Revised June 27, 2015
Accepted July 13, 2015

Research Article

Combination of two-dimensional gel electrophoresis and a fluorescent carboxyfluorescein-diacetate-labeled cisplatin analogue allows the identification of intracellular cisplatin–protein adducts

Cisplatin is one of the most widely used anticancer agents, but a major problem for successful chemotherapy is the development of drug resistance of tumor cells against cisplatin. Resistance to cisplatin is a multifactorial problem. A method to detect and identify intracellular cisplatin–protein adducts was developed using a fluorescent carboxyfluorescein-diacetate-labeled cisplatin analogue (CFDA–cisplatin), 2DE, and ESI-MS/MS. We identified several CFDA–cisplatin–protein adducts including members of the protein disulfide isomerase family (PDI). These are the first results of the detection of intracellular CFDA–cisplatin–protein adducts, which may help to understand the resistance mechanism of cisplatin.

Keywords:
Carboxyfluorescein-diacetate-labeled cisplatin analogue / Cisplatin / Cisplatin–protein adducts / Protein marker grid / Two-dimensional gel electrophoresis
DOI 10.1002/elps.201500188

Additional supporting information may be found in the online version of this article at the publisher's web-site

1 Introduction

Cisplatin is a widely employed platinum-based compound that is currently used for treatment of solid neoplasms, including head and neck, lung, colorectal, bladder, testicular, and ovarian cancers [1–3]. But the effectiveness of cisplatin is limited by two major drawbacks: toxic side effects, such as nephrotoxicity, ototoxicity, and neurotoxicity [4, 5], and resistance of tumor cells to the drug [6].

Resistance to cisplatin is a multifactorial problem including reduced intracellular concentrations of cisplatin by decreased drug influx and/or increased drug efflux, increased repair of DNA damage, adapted apoptotic signaling pathways, and inactivation by cisplatin–glutathione complexes [7,8]. The platination of DNA is seen as a key step of the cytotoxic effect [9], but only a small fraction of cellular cisplatin binds to its pharmacological target [10]. It is assumed that cisplatin has a much higher affinity to the sulfur-containing amino acids cysteine and methionine than to the nitrogen donors of the nuclear DNA [11]. Inside a tumor cell, there are a number of potential binding partners for cisplatin. Increased intracellular formation of biologically inactive adducts with proteins or peptides appears to be involved in drug resistance [6]. Consequently, the interaction of cisplatin with proteins could be an important factor affecting its intracellular distribution, elimination, and cytotoxicity.

The aim of this study was the identification of intracellular cisplatin–protein adducts that may be involved in the mechanisms of cisplatin resistance. For the development of an analytical method, we used the fluorescent carboxyfluorescein-diacetate-labeled cisplatin analogue (CFDA–cisplatin, Fig. 1), which permits easy tracking of the intracellular distribution and the detection of intracellular cisplatin–protein adducts.

CFDA–cisplatin was first introduced by Molenaar et al. [12], and they also showed that the cellular distribution

Correspondence: Dr. Sabine Metzger, Biocenter MS Platform, Department of Biology, University of Cologne, Zülpicher Straße 47b, 50674 Cologne, Germany
E-mail: s.metzger@uni-koeln.de
Fax: +49-221-470-8521

Abbreviations: CFDA–cisplatin, carboxyfluorescein-diacetate-labeled cisplatin analogue; **ER**, endoplasmic reticulum; **GRP**, glucose-regulated protein; **LA**, laser ablation; **PDI**, protein disulfide isomerase

Colour Online: See the article online to view Figs. 1–4 in colour.

© 2015 WILEY-VCH Verlag GmbH & Co. KGaA, Weinheim

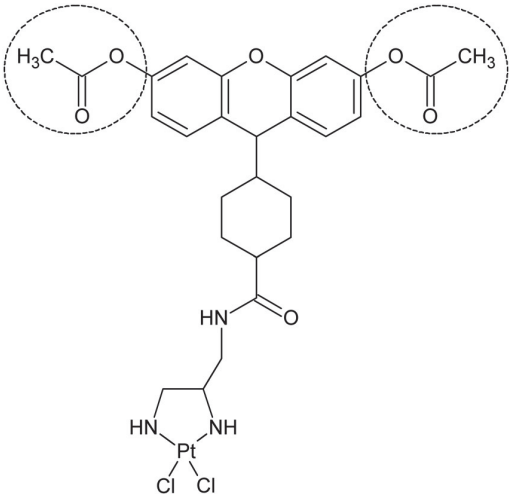

Figure 1. The chemical structure of CFDA–cisplatin. The circles mark the two acetyl groups that were deacetylated intracellularly and therefore allow the fluorescence detection of CFDA–cisplatin–protein adducts.

pattern of CFDA–cisplatin was significantly different to the nonplatinum-containing fluorescein derivative CFDA-boc. These results revealed that the intracellular trafficking of CFDA–cisplatin depends mainly on the platinum moiety. Further studies reported that CFDA–cisplatin reflected the biological behavior of cisplatin [13]. Thus, CFDA–cisplatin represents a suitable model substance for cisplatin. In order to visualize CFDA–cisplatin–protein adducts, CFDA–cisplatin was synthesized as described previously [12, 14]. Intracellularly, the two acetyl groups of CFDA–cisplatin (Fig. 1, see dashed marker) are deacetylated, which allow the fluorescence detection of CFDA–cisplatin–protein adducts following 2DE. 2DE is a powerful tool for the separation of complex protein mixtures enabling the separation and visualization of hundreds to thousands of proteins within a gel. We intended to reduce the complexity of the protein mixture and to enhance the resolution of acidic-neutral proteins. Therefore, narrow pH gradient strips (pH 4–7) were used for the first dimension instead of the common pH gradient strips ranging 3–10. The 2DE analysis with an optimized protocol for the pH range 4–7 showed that the assignment of the CFDA–cisplatin–protein adducts is difficult due to the few existing fluorescent landmarks. A simultaneous on-gel generation of a fluorescent reference protein spot grid during the second dimension of the 2DE separation of the sample allowed a more precise assignment of the CFDA–cisplatin–protein adducts [15].

2 Materials and methods

2.1 Chemicals and materials

Fetal bovine serum, penicillin, RPMI 1640 medium, and streptomycin were purchased from Pan-Biotech (Aidenbach, Germany). Ammonium persulfate, 4′,6-diamidino-2-phenylindole, dimethylformamide, disodium hydrogen phosphate, ethanol, formic acid, glycerine, glycine, HEPES, leupeptin, magnesium chloride, methanol, orthophosphoric acid 85%, potassium chloride, potassium dihydrogen phosphate, pepstatin, SDS, Tergitol® solution Type NP-40, thiourea, and urea were received from Sigma–Aldrich (Steinheim, Germany). Tris PUFFERAN® was from Roth (Karlsruhe, Germany). ACN and ammonium bicarbonate were purchased from Fluka (Steinheim, Germany). Aluminum sulfate-18-hydrate, chloroform, iodoacetamide, and TEMED were obtained from Merck (Darmstadt, Germany). CHAPS was from G-Biosciences (St. Louis, USA). Bromphenole blue and CBB G-250 were purchased from Serva (Heidelberg, Germany). DryStrip cover fluid was from GE Healthcare (Mannheim, Germany). HPLC-grade ACN and DTT were from VWR International (Darmstadt, Germany). Pierce® 660 nm Protein Assay was purchased from Thermo Fisher Scientific (Rockford, USA). NaCl was from Grüssing (Filsum, Germany).

2.2 Synthesis and purification of CFDA–cisplatin

CFDA–cisplatin was synthesized according to Molenaar et al. [12] with a slight modification, which has been described in Zabel et al. [14]. After purification on a semipreparative HPLC (System Gold, Beckman Coulter, Germany) using a Nucleodur C18 HTec column (5 μm; 250 × 10 mm), a purity of 95% was achieved.

2.3 Cell culture, harvesting, and precipitation of proteins

The human ovarian carcinoma cell line A2780 and the cisplatin-resistant subline A2780cis (European Collection of Cell Cultures, UK) were cultured in RPMI 1640 medium (supplemented with 10% fetal bovine serum, 100 I.E./mL penicillin, and 0.1 mg/mL streptomycin) at 37°C and 5% CO_2. Cells were treated with 25 μM of CFDA–cisplatin (dissolved in dimethylformamide) in serum-free medium for 2 h. After washing twice with PBS, the cells were scraped in PBS and centrifuged (160 × *g*, 4 min). The pellet was resuspended in cell lysis buffer (10 mM HEPES (pH 7.4), 40 mM potassium chloride, 3 mM magnesium chloride, 5% glycerine, and 0.5% NP-40) supplemented with pepstatin (2 μM) and leupeptin (1 μM). Afterward, the cells were sonicated three times for 5 s at 25% power with 30-s breaks (Bandelin HD 2070/UW 2070, Bandelin electronic, Germany). Lysates were centrifuged at 700 × *g* for 15 min, and the supernatant was centrifuged at 15 000 × *g* for 20 min. The final supernatant was further analyzed. Protein concentrations were determined using the Pierce® 660 nm Protein Assay. Afterward, 150 μg protein of each sample was precipitated with chloroform–methanol [16].

© 2015 WILEY-VCH Verlag GmbH & Co. KGaA, Weinheim

2.4 Two-dimensional gel electrophoresis

The 2DE experiments were performed using the Ettan IPGphor 3 IEF system (GE Healthcare) in the first dimension. For SDS-PAGE gels in the second dimension ($100 \times 100 \times 1.0$ mm^3), the PerfectBlue^{TM} dual gel system Twin S (Peqlab Biotechnologie, Germany) was used.

2.4.1 Isoelectric focusing

We used narrow pH gradient strips (pH 4–7) for the separation in the first dimension. In the acidic-neutral pH range, 150 μg precipitated proteins were solubilized in 7 M urea, 2 M thiourea, 2% CHAPS, 65 mM DTT, and 2% SERVALYT^{TM} 4–7 (Serva) for at least 1 h to ensure complete solubilization and denaturation, and were then applied to Serva IPG BlueStrips pH 4–7 ($70 \times 3 \times 0.5$ mm; Serva) overnight by in-gel rehydration. IEF was performed with a maximum current of 50 μA and a total of 14.4 kVh using the following focusing protocol (300 V for 2.0 h (step and hold), 1000 V for 0.5 h (gradient mode), 3000 V for 1.5 h (gradient mode), and 3000 V for 3.5 h (step and hold)). Finally, all focused IPG strips were stored at −20°C until equilibration and application to SDS-PAGE.

2.4.2 SDS-PAGE and generation of a reference protein spot grid

The IPG strips were subjected to reduction and alkylation using 1% DTT and 2.5% iodoacetamide in 2.5 mL equilibration solution (6 M urea, 50 mM Tris–HCl (pH 8.8), 30% glycerol, and 2% SDS) per strip. On the top of a self-made 12% SDS-PAGE resolving gel, first an IPG strip was applied. Then, a 4% stacking gel containing bromphenol blue was polymerized over it. Here, V-shaped well combs were used to generate a reference protein spot grid according to Ackermann et al. [15] with the following slight modifications. The Protein Test Mixture 6 for SDS-PAGE (Serva) was labeled according to the manufacturer's instructions with Serva Lightning Red for 1D SDS-PAGE (Serva), and 3 μL was applied to each lane. Proteins were separated for 2.5 h, starting at 50 V for 30 min followed by 150 V until the dye front reached the bottom of the gel.

2.5 Detection, staining, and image analysis

The Typhoon^{TM} 9400 laser scanner (GE Healthcare, UK) was used to scan SDS-PAGEs. CFDA–cisplatin–protein adducts were detected at excitation/emission 488/532 nm and the fluorescent reference protein spot grid at 532/580 nm. Afterward, the colloidal Coomassie G-250 staining protocol according to Kang et al. [17] with slight modifications according to Dyballa and Metzger [18] was used to visualize the proteins. The image analysis was performed with the Delta2D software version 4.3 (DECODON, Germany). Briefly, the image from a fluorescence scan and the gel image from a Coomassie-stained gel were mapped for a master image in order to detect CFDA–cisplatin–protein adducts.

2.6 Analysis of platinum in 2DE gels

For the laser ablation (LA) ICP-MS (LA-ICP-MS) measurements, the Coomassie-stained 2DE gels were treated for 2 min with glycerine and dried on filter paper (Whatman, Germany) using a gel dryer (70°C, 2 h). Afterward, the 2DE gels were divided into several parts to position the relevant sections with fluorescence detection onto a target holder. LA-ICP-MS imaging experiments were performed using the LA system LSX-213 (CETAC Technologies, USA) coupled to a quadrupole-based ICP-mass spectrometer iCAP Q (Thermo Fisher Scientific, Germany). The ablation was performed in a multiline scan, whereby the selected gel fragments were ablated line by line with laser energy of 12 J/cm^2 (90% of the maximum laser energy), 20 Hz laser shot frequency, 200 μm spot diameter, and 50 μm/s scan speed. The produced aerosol was transported to the ICP using Helium as the carrier gas, which was mixed with Argon downstream the ablation cell. A rhodium solution as an internal standard (10 ng/L, SCP SCIENCE, France) was simultaneously introduced via a PFA (Perfluoralkoxy) nebulizer and a cyclonic spray chamber. This improved the plasma stability, and allowed to compensate drift effects. For the maximum sensitivity and to minimize possible interferences of $(^{40}Ar^{154}Gd)^+$, the measurement was performed by utilizing a collision/reaction cell with Helium as the cell gas was in kinetic energy discrimination mode. The isotopes ^{194}Pt, ^{195}Pt, and ^{103}Rh were detected with dwell times of 1.75, 1.75, and 0.5 s, respectively. The recorded ablation profiles were converted into 2D distribution images and evaluated with ImageJ (National Institutes of Health, USA).

2.7 Sample preparation for MS

The protein spots of interest were manually excised from Coomassie-stained 2DE gels, completely destained and incubated with 0.033 μg/μL sequencing-grade modified trypsin (Promega, USA) in 25 mM ammonium bicarbonate (pH 8.0) for 12–16 h at 37°C. The extracted peptides were dried in a vacuum centrifuge (Eppendorf, Germany) and stored at −20°C until analyzed by MS. Prior to ESI-MS/MS analyses, the peptides were desalted using StageTips (C18 material, 20-μL tip, SP201, Thermo Fisher Scientific, USA), and the tryptic peptides were eluted three times with 10 μL of 1% formic acid and 60% methanol in water. For the nano-HPLC ESI-MS/MS analyses, the tryptic peptides were dissolved in 17 μL using 5% TFA in water.

© 2015 WILEY-VCH Verlag GmbH & Co. KGaA, Weinheim

2.8 Protein identification by MS

ESI-MS/MS analyses were performed with an ESI Qq-TOF instrument (QSTAR XL, Applied Biosystems, Germany), which was equipped with an offline nanospray source (Proxeon Biosystems, Denmark). The full MS scans from 350 to 1500 m/z were recorded using the Analyst QS version 1.1 (Applied Biosystems), and at least five peptides per sample were further fragmented. The protein identification was performed using the MASCOT MS/MS ions search 1.6b27 (Matrix Science, UK) using the following parameters: database, Swiss-Prot; protease, trypsin; missed cleavages, 1; variable modifications, carbamidomethyl (C) and oxidation (M); peptide tolerance, ± 1.2 Da; and MS/MS tolerance, ± 0.6 Da.

Protein spots with low protein content were analyzed on a hybrid ion trap-Orbitrap mass spectrometer (Orbitrap Elite, Thermo Scientific, Germany), which was coupled with a nano-HPLC system (UltiMate™ 3000 HPLC system, Dionex, Thermo Scientific). Peptides were preconcentrated on an Acclaim® PepMap™ C18 column (2 cm × 100 μm × 5 μm, 100 Å; Thermo Fisher Scientific) and desalted for 10 min by using 0.1% TFA as mobile phase. Afterward, the peptides were separated on an Acclaim® PepMap™ RSLC (Rapid Separation Liquid Chromatography C18 column (25 cm × 75 μm × 2 μm, 100 Å, Thermo Fisher Scientific) with a gradient (A: 0.1% formic acid in water; B: 0.1% formic acid and 84% ACN in water), 2 min from 4 to 10% B, 17 min to 20% B, 18 min to 30% B, 17 min to 40% B, and 1 min to 95% B. For the Orbitrap, following parameters were used: ion transfer tube temperature, 275°C; spray voltage, 1.4 kV; MS scan range, 350–1700 m/z; and MS resolution, 60 000. The 15 most intense $\geq 2^+$ charged peptide ions were isolated and transferred to the linear ion trap. Protein identification was performed by using the Proteome Discoverer™ 1.4 in combination with MASCOT MS/MS ions search 2.4.1 (Matrix Science) using the following settings: database, Swiss-Prot; protease, trypsin; missed cleavages, 2; static modification, carbamidomethyl (C); dynamic modification, oxidation (M); false detection rate, 1%; precursor mass tolerance, 10 ppm; and fragment mass tolerance, ± 0.4 Da.

3 Results

The aim of this study was the identification of protein adducts with CFDA–cisplatin in the human ovarian carcinoma cell lines A2780 and A2780cis, which may be involved in cisplatin resistance. To detect the adducts, we combined the application of the fluorescent CFDA–cisplatin with the 2DE for the separation of proteins.

3.1 Separation and detection of protein adducts of CFDA–cisplatin

2DE consists of two separation steps: the first dimension, in which the proteins are separated according to their p*I*, and the second dimension, where separation is based on their molecular weight. First, A2780 and A2780cis cells were treated with CFDA–cisplatin, and the cytosolic proteins were extracted. Generally, protein sample prefractionation before 2DE reduced the sample complexity. The optimization of the solubilization power as well as the focusing protocol within the 2DE led to enhanced resolution and visualization of the cytosolic proteins in the pH range 4–7. The comparison of fluorescence scans (Fig. 2A and B) shows that fluorescence signals could only be detected in CFDA–cisplatin-treated samples. This confirms the suitability of our experimental approach. The most intense fluorescence signals were detected in the range of 40–75 kDa. In order to assign CFDA–cisplatin–protein adducts, we used the Delta2D software for the image analysis, which allows the alignment of several images. Hence, the images of the fluorescence (Fig. 2A) and Coomassie stain (Fig. 2C) were overlaid so that several CFDA–cisplatin–protein adducts (black spots) could be detected. The fluorescence signals of the CFDA–cisplatin–protein adducts were assigned on the basis of protein spot pattern. Nevertheless, some of the fluorescence signals could not be assigned to a protein spot with high confidence (see arrows in Fig. 2D).

3.2 Introduction of a simultaneous on-gel generation of a protein marker grid

In order to find a solution to the above-mentioned problems, we used a simultaneous on-gel generation of a reference protein marker grid [15]. This method combines elements of the 1DE and 2DE. While the cytosolic proteins are separated according to p*I* and molecular weight, a fluorescence-labeled protein marker solution was separated in the second dimension according to molecular weight. The use of two different fluorescent stains permitted the distinction between CFDA–cisplatin–protein adducts (Fig. 3A) and the reference protein spot grid (Fig. 3B) within a single minigel. For the generation of a protein marker grid, we used V-shaped sample wells in a stacking gel on top of the p*I* strip to obtain sharp and distinct spots. Only a small volume (3 μL) of the fluorescence-labeled protein marker solution was applied into the V-shaped sample wells in order to improve spot size and shape. Twenty-four spots generated a protein marker grid following electrophoresis. The comparison of Coomassie-stained 2DE gels showed that the introduction of a protein marker grid does not lead to any changes in the protein spot patterns (Fig. 2C and 3C).

3.3 Evaluation of CFDA–cisplatin–protein adducts with image analysis

In order to detect CFDA–cisplatin–protein adducts, the fluorescence signals (Fig. 3A) must be assigned to the corresponding protein spots (Fig. 3C). For this, we used the Delta2D software, which allowed a fast visual analysis and reliable

© 2015 WILEY-VCH Verlag GmbH & Co. KGaA, Weinheim

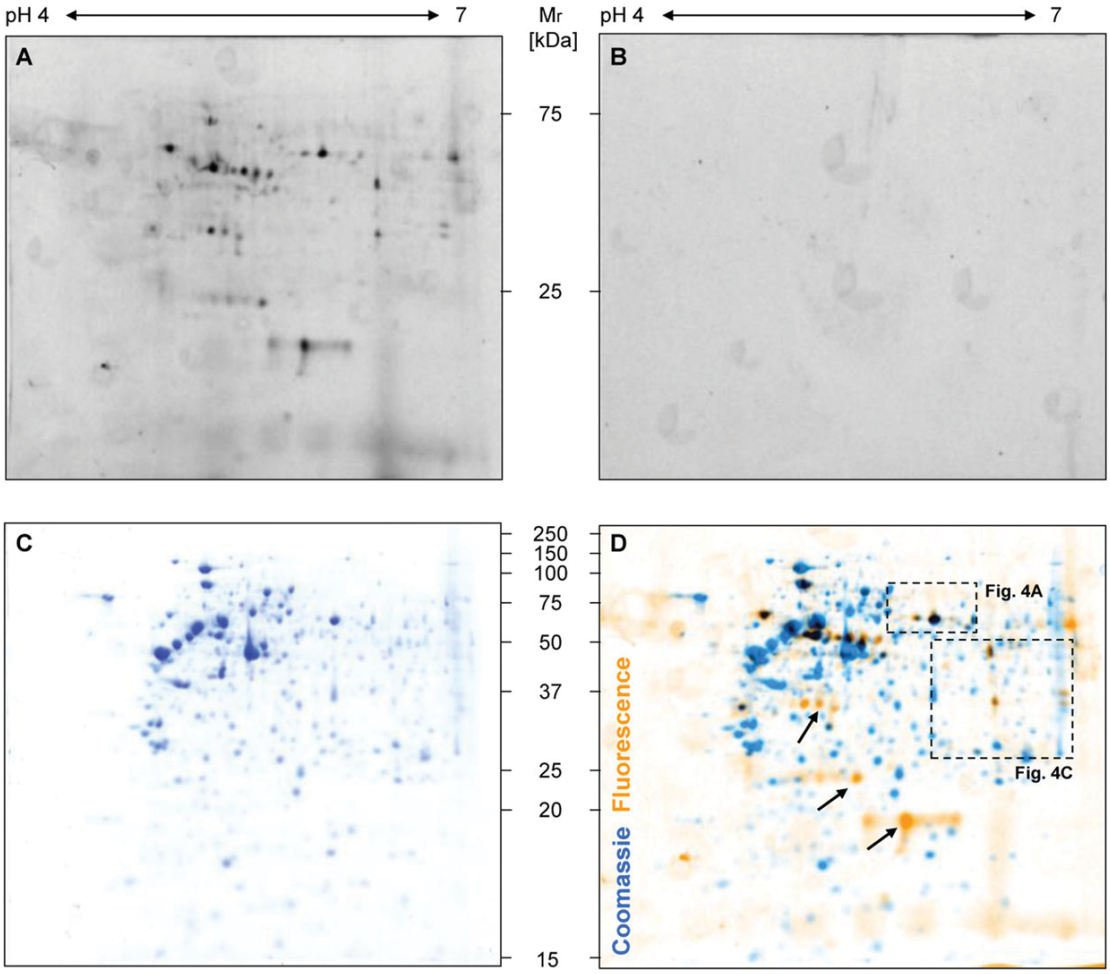

Figure 2. Visualization of CFDA–cisplatin–protein adducts by 2DE. A2780 was treated with (A) and without 25 μM CFDA–cisplatin (B) for 2 h. The 2DE experiment (pH range 4–7) was performed with 150 μg of cytosolic proteins. Afterward, a fluorescence scan was recorded (excitation/emission: 488/532 nm; [A and B]), and the proteins were visualized with Coomassie staining (C). The CFDA–cisplatin–protein adducts (black spots) were assigned on a master image (D).

spot matching. First, the fluorescence scans from CFDA–cisplatin–protein adducts (Fig. 3A) and protein marker grid (Fig. 3B) were fused into one image. Afterward, this fused image was merged with the Coomassie staining image (Fig. 3C) to gain a master image. The fluorescence signals of the CFDA–cisplatin–protein adducts were matched to the corresponding Coomassie-stained spots. The inspection of both master images (Fig. 2D and 3D) showed that the new anchor points improved and strengthened the assignment of the CFDA–cisplatin–protein adducts. Without a protein marker grid, we assigned the fluorescence signals of the CFDA–cisplatin–protein adducts on the basis of protein spot pattern. But the introduction of a protein marker grid showed that the previous assignment was not always correct (Fig. 4A–D). Some fluorescence signals were assigned to other protein spots (Fig. 4A and B), but there were also unassigned fluorescence signals (Fig. 4C and D). These examples demonstrate the necessity of the protein marker grid.

3.4 Detection of platinum in 2DE gels with LA-ICP-MS

LA-ICP-MS is a suitable method for metal imaging in 2DE [19–21]. LA-ICP-MS measurements in the line scanning mode were used to detect platinum in the protein spots that were previously separated by 2DE. Relevant section of 2DE gels, with and without fluorescence signals of the CFDA–cisplatin–protein adducts, was analyzed. The LA-ICP-MS clearly confirms the presence of platinum in distinct spots, which correlates clearly with the fluorescence spot pattern (Supporting Information Fig. 1). This analysis is an

© 2015 WILEY-VCH Verlag GmbH & Co. KGaA, Weinheim

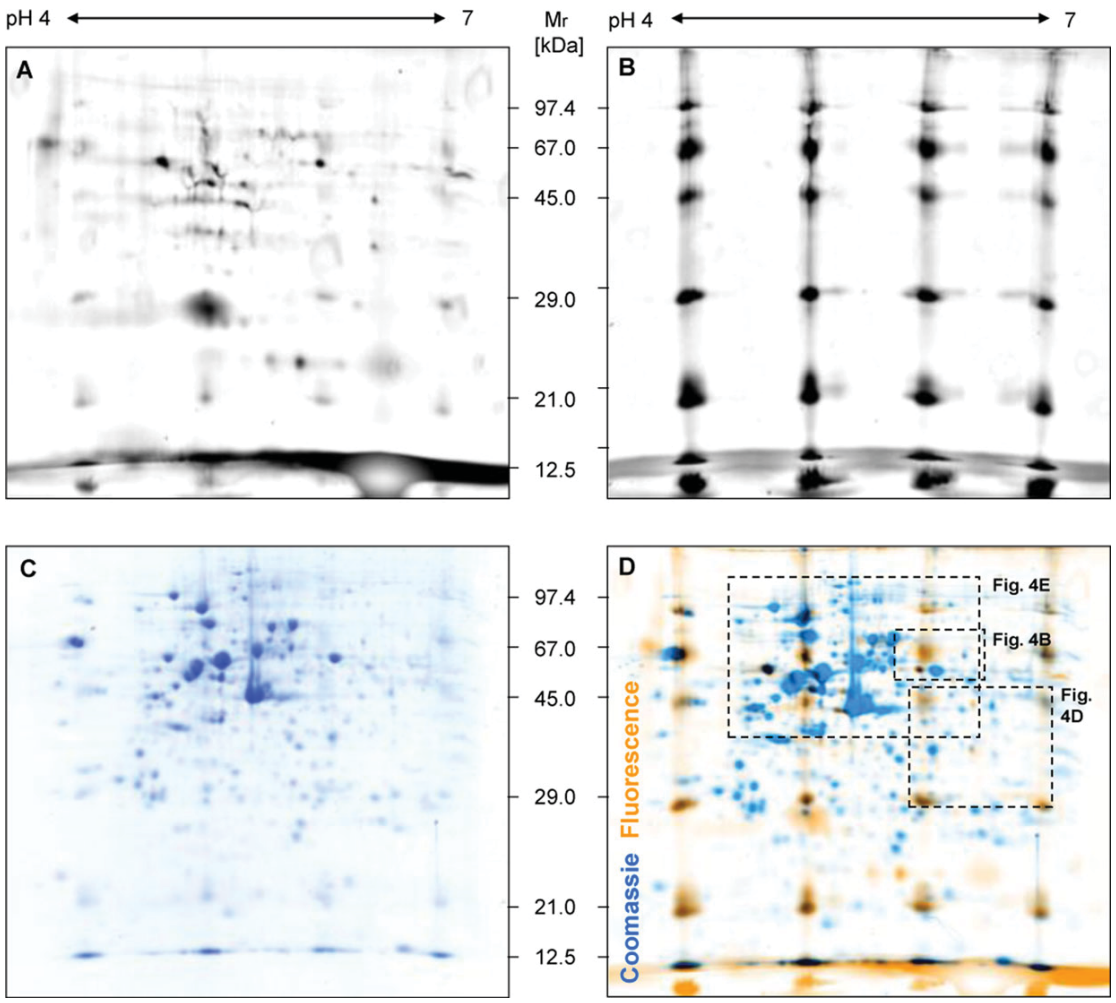

Figure 3. Precise visualization of CFDA–cisplatin–protein adducts through 2DE by using a simultaneous on-gel generation of a reference protein spot grid. A2780cis was treated with (A) 25 μM CFDA–cisplatin for 2 h. A generation of a reference protein spot grid (B) allowed the separation in parallel with 150 μg cytosolic proteins through 2DE. A fluorescence scan was recorded (CFDA–cisplatin, excitation/emission: 488/532 nm [A]; Serva Lightning Red for 1D SDS-PAGE, excitation/emission: 532/580 nm [B]), and the proteins were visualized with Coomassie staining (C). For the image analysis, the fluorescence scans from CFDA–cisplatin–protein adducts (A) as well as from protein marker grid (B) and the Coomassie staining image (C) were fused to a master image (D).

additional proof to the fluorescence scans that CFDA–cisplatin binds to specific proteins.

3.5 Identification of CFDA–cisplatin–protein adducts

The bottom-up approach using the 2DE allows the separation and visualization of hundreds of proteins. In the experiment, it was possible to detect a total of 440 protein spots in the pH range 4–7. The subsequent image analysis in the pH range 4–7 revealed that five spots were detected as CFDA–cisplatin–protein adducts (Fig. 4). 2DE can reveal modifications of a protein, since even small charge and molecular weight changes lead to altered migration behavior of proteins. The posttranslational modifications of a protein could be recognized by horizontal or vertical shifting of a protein spot. In order to verify possible p*I* or molecular weight shifts of the CFDA–cisplatin–protein adducts, nearby lying protein spots were additionally excised from the 2DE Coomassie-stained gels and then analyzed by ESI-MS/MS (see Table 1). On average, each protein spot was identified from three biological samples of three separate gels, respectively.

In the pH range 4–7, the protein disulfide isomerase (PDI) A1, glucose-regulated protein 78 (GRP78), PDIA6, and PDIA3 were identified as CFDA–cisplatin-containing proteins, corresponding to spots 1*–5* in Fig. 4E. Interestingly, PDIA1 was only found as CFDA–cisplatin-containing protein (Fig. 4E, spot 1*), while the other CFDA–cisplatin-containing proteins shifted slightly in their p*I* value

© 2015 WILEY-VCH Verlag GmbH & Co. KGaA, Weinheim

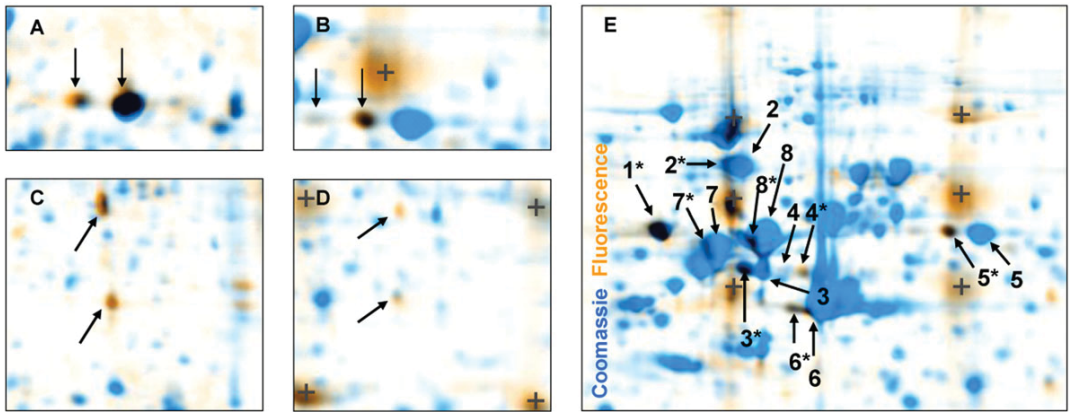

Figure 4. Detection of CFDA–cisplatin–protein adducts (black spots). The reference protein spot grid (+) improves the assignment of the CFDA–cisplatin–protein adducts in the image analysis (A–D); (E): 1* = PDIA1; 2* and 2 = GRP78; 3*, 3, 4*, and 4 = PDIA6; 5* and 5 = PDIA3; 6* and 6 = β-actin; 7*, 7, 8*, and 8 = vimentin.

Table 1. Proteins were identified by ESI-MS/MS or nano-HPLC-ESI-MS/MS after 2DE

Sample and spot number	Protein identification	Accession number	M_r (kDa) experimental/ theoretical	p*I* experimental/ theoretical	Sequence coverage (%)
1*	PDIA1	P07237	60.00/57.08	4.75/4.76	22.60[a)]
2*	78 kDa GRP78	P11021	75.00/72.28	5.05/5.07	20.00[a)]
2	GRP78	P11021	75.00/72.28	5.10/5.07	45.00[a)]
3*	PDIA6	Q15084	52.00/48.12	5.10/4.95	57.88[b)]
3	PDIA6	Q15084	52.00/48.12	5.15/4.95	23.90[a)]
4*	PDIA6	Q15084	52.00/48.12	5.20/4.95	45.15[b)]
4	PDIA6	Q15084	52.00/48.12	5.35/4.95	52.47[b)]
5*	PDIA3	P30101	60.50/56.07	5.90/5.96	70.69[b)]
5	PDIA3	P30101	60.50/56.07	6.00/5.96	37.20[a)]
6*	β-Actin	P60709	43.50/41.74	5.35/5.29	30.70[a)]
6	β-Actin	P60709	43.50/41.74	5.40/5.29	30.70[a)]
7*	Vimentin	P08670	56.00/53.65	5.00/5.05	53.90[a)]
7	Vimentin	P08670	56.00/53.65	5.05/5.05	42.95[a)]
8*	Vimentin	P08670	60.00/53.65	5.10/5.05	48.30[a)]
8	Vimentin	P08670	60.00/53.65	5.15/5.05	43.30[a)]

Numbers refer to the spots and are picked from 2DE Coomassie-stained gels (Fig. 4E).
a) Proteins identified by ESI-MS/MS after 2DE.
b) Proteins identified by nano-HPLC-ESI-MS/MS after 2DE. M_r relative molecular mass.

compared to unmodified proteins (Fig. 4E; spots 2, 3, and 5). The CFDA–cisplatin-containing proteins showed a lower p*I* compared to the unmodified protein spot, with the exception of PDIA6. CFDA–cisplatin-modified PDIA6 was identified in two protein spots; however, only one of these CFDA–cisplatin-containing adducts shifted to a lower p*I* value compared to the unmodified protein (Fig. 4E, shift from 3 to 3*), whereas the other protein representative shifted to a higher p*I* value (compare protein spots 4 and 4*). Besides proteins of the PDI family, we additionally identified two structural components of the cytoskeleton, β-actin and vimentin (spots 6, 7, and 8), to be modified by CFDA–cisplatin (spots 6*, 7*, and 8* in Fig. 4E).

Due to the altered migration behavior of the so far identified CFDA–cisplatin-containing proteins, we could show for the first time that CFDA–cisplatin causes a small change of the net charge within the protein, which can be adequately detected and identified by this fluorescence-based 2DE method.

4 Discussion

4.1 Detection of intracellular CFDA–cisplatin–protein adducts

For the identification of cisplatin–protein adducts within tumor cells, we used the fluorescence model substance CFDA–cisplatin, which has been shown to be a suitable agent for the study of intracellular trafficking of cisplatin [12, 13].

© 2015 WILEY-VCH Verlag GmbH & Co. KGaA, Weinheim

We successfully applied 2DE for the analysis of CFDA–cisplatin–protein adducts in the tumor cell line A2780. A precise image analysis could not be performed because the distribution of fluorescence spot and total number of protein spots, especially in the low molecular weight region, was not sufficient enough. To circumvent this problem, we successfully introduced a protein marker grid. This marker grid was introduced by Ackermann et al. [15] in 2012, who reported that gel size (circa 25 × 19 cm) and run time are important for the formation of protein marker spots in the second dimension of the 2DE. However, we analyzed the cytosolic proteins in the second dimension in a minigel (circa 8 × 8 cm^2) and were able to show that the use of this popular format is completely sufficient in order to form a protein marker grid. The introduced protein marker grid enabled a precise detection of intracellular CFDA–cisplatin-containing proteins. However, it also showed that several fluorescence signals have no corresponding protein spots. One reason could be that the applied Coomassie staining was not sensitive enough to stain very low abundant proteins.

In the procedure of the presented analytical method, the samples were treated with denaturing (urea and thiourea), reducing (DTT) and alkylating (jodacetamide, IAA), and enzymatic (trypsin) agents [22]. Mena et al. [23] showed that the electric field during the electrophoretic separation, as well as staining and destaining of proteins, in the gel had no effect on cisplatin binding to proteins. Therefore, we assume that CFDA–cisplatin remained bound to proteins during sample preparation. To verify that the fluorescence signals in the protein spots are really related to CFDA–cisplatin, we used LA-ICP-MS to detect platinum in the corresponding protein spots of 2DE gels.

4.2 CFDA–cisplatin binding proteins

Using our newly developed method, we identified a set of endoplasmic reticulum (ER) stress proteins as CFDA–cisplatin-containing proteins, including PDIA1, PDIA3, PDIA6, and GRP78. Since cancer cells require a global increase in protein synthesis to manage ER stress and to support rapid proliferation, this could be expected [24, 25]. GRP78 as well as PDI have a C-terminal ER-retention amino acid sequence KDEL, but significant amounts of both proteins were also detected at other locations, such as cell surfaces, nucleus, and the cytosol, suggesting that the GRP78 and PDI can escape from the ER [25–29]. GRP78 and PDI are master regulators of the unfolded protein response, which is activated by accumulation of misfolded proteins in the ER caused by exogenous and/or endogenous stress signals [30–32]. It has been shown that GRP78 and PDI may play a role in cisplatin resistance in some cancers [33–35]. PDI is a member of the thioredoxin-like superfamily of redox proteins. The canonical function of these proteins is the disulfide-bond formation in nascent proteins and protein folding in the ER [36]. GRP78 contains two cysteines, whereas PDIA1, PDIA3, and PDIA6 contain seven cysteines each. It has been shown that cysteine residues are the preferential binding sites of cisplatin in peptides and proteins [22]. Sobierajska et al. [37] showed that PDI is released from subcellular compartments to the cytosol and form a disulfide bond with β-actin Cys^{374}. β-Actin contains six cysteine residues, but only one of them (Cys^{374}) is exposed on the surface of the protein [38].

4.3 Binding of CFDA–cisplatin

The reactive cisplatin interacts preferentially with the sulfur-containing amino acids cysteine and methionine, which are present on the surface of the proteins. It is therefore possible that cysteine-rich proteins such as PDI and GRP78 form covalent complexes in the cytosol with CFDA–cisplatin. The same holds true for the detection and identification of a small amount of CFDA–cisplatin β-actin and vimentin complexes. However, histidine, serine, threonine, tyrosine, glutamic acid, and aspartic acid were also identified as binding sites for cisplatin [39, 40]. The accessibility of the protein side chains determines which amino acids bind to cisplatin. Furthermore, it is conceivable that the binding of CFDA–cisplatin to an amino acid leads to an altered migration behavior of the CFDA–cisplatin-containing proteins in the 2DE gels because CFDA–cisplatin can cause a small change in the net charge of the protein. The p*I* of a protein is a crucial parameter that supports the identity of a protein. The theoretical p*I* often corresponds to the p*I* of unmodified proteins. Among the identified CFDA–cisplatin-containing proteins, PDIA3 and GRP78 were also detected as unmodified proteins, while PDIA1 could only be detected as CFDA–cisplatin adduct. It is possible that upon binding of CFDA–cisplatin to PDIA1, no change in p*I* takes place or the whole amount of the protein has bound CFDA–cisplatin. The protein PDIA6 was identified in four protein spots (spots 3, 3*, 4, and 4* in Fig. 4E). Different isoforms of this protein may be the result of alternative splicing (according to uniprot.org), which usually differ in the p*I* and molecular weight. Moreover, a significant p*I* shift usually suggests posttranslational modification. It is therefore possible that the binding of CFDA–cisplatin impairs the function of the respective protein. Such inactive CFDA–cisplatin protein/peptide adducts may, on the one hand, limit the amount of reactive cisplatin in tumor cells [37], and on the other hand, negatively influence cell viability through the impairment of protein functions.

Elucidation of the cisplatin-binding sites of the identified proteins by ESI-MS/MS is the next step to improve our understanding of the binding stability. Cisplatin shows a characteristic isotope distribution in the mass spectrum, which modifies the characteristic isotope patterns of a peptide. The binding site of cisplatin within a peptide generates a characteristic-altered isotopic pattern and is detectable in the MS. However, the detection of cisplatin-binding sites within a peptide by ESI-MS/MS could be difficult because of the low abundance of platinated peptides in comparison to the unplatinated ones. In this case, preconcentration steps or

© 2015 WILEY-VCH Verlag GmbH & Co. KGaA, Weinheim

in vitro studies of the identified CFDA–cisplatin-containing proteins may be helpful.

4.4 Concluding remarks

We established an analytical method that allows detecting and identifying intracellular CFDA–cisplatin-containing proteins. CFDA–cisplatin in combination with 2DE and subsequent fluorescence detection provides new insights into the cellular processing of this drug and may, therefore, contribute to the understanding of the resistance mechanism of cisplatin. With our method, six previously unknown intracellularly binding partners of CFDA–cisplatin were identified. CFDA–cisplatin intracellular binding to these proteins implies that cisplatin is seized, and therefore, the cells develop a resistance to cisplatin. GRP78 and the three PDI proteins are described to be associated with cancer progression and development of resistance to chemotherapy. Pharmacological studies will reveal their specific contribution to cisplatin resistance.

S. K. wishes to thank A. Stefanski for performing the Orbitrap MS analysis. This project was supported by the Deutsche Forschungsgemeinschaft (ME 1799/2-1).

The authors have declared no conflict of interest.

5 References

[1] Galanski, M., *Recent Pat. Anticancer Drug Discov.* 2006, *1*, 285–295.

[2] Lebwohl, D., Canetta, R., *Eur. J. Cancer* 1998, *34*, 1522–1534.

[3] Prestayko, A. W., D'Aoust, J. C., Issel, B. F., Crooke, S. T., *Cancer Treat Rev.* 1979, *6*, 17–39.

[4] Cvitkovic, E., Spaulding, J., Bethune, V., Martin, J., Whitmore, W. F., *Cancer* 1977, *39*, 1357–1361.

[5] Kelland, L., *Nat. Rev. Cancer* 2007, *7*, 573–584.

[6] Galluzzi, L., Senovilla, L., Vitale, I., Michels, J., Martins, I., Kepp, O., Castedo, M., Kroemer, G., *Oncogene* 2012, *31*, 1869–1883.

[7] Kartalou, M., Essigmann, J. M., *Mutat. Res.* 2001, *478*, 23–43.

[8] Siddik, Z. H., *Oncogene* 2003, *22*, 7265–7279.

[9] Jamieson, E. R., Lippard, S. J., *Chem. Rev.* 1999, *99*, 2467–2498.

[10] Cepeda, V., Fuertes, M. A., Castilla, J., Alonso, C., Quevedo, C., Pérez, J. M., *Anticancer Agents Med. Chem.* 2007, *7*, 3–18.

[11] Kasherman, Y., Sturup, S., Gibson, D., *J. Med. Chem.* 2009, *52*, 4319–4328.

[12] Molenaar, C., Teuben, J. M., Heetebrij, R. J., Tanke, H. J., Reedijk, J., *J. Biol. Inorg. Chem.* 2000, *5*, 655–665.

[13] Kalayda, G. V., Wagner, C. H., Buss, I., Reedijk, J., Jaehde, U., *BMC Cancer* 2008, *8*, 175.

[14] Zabel, R., Kullmann, M., Kalayda, G. V., Jaehde, U., Weber, G., *Electrophoresis* 2015, *36*, 509–517.

[15] Ackermann, D., Wang, W., Streipert, B., Geib, B., Grün, L., König, S., *Electrophoresis* 2012, *33*, 1406–1410.

[16] Wessel, D., Flügge, U. I., *Anal. Biochem.* 1984, *138*, 141–143.

[17] Kang, D., Gho, S. G., Suh, M., Kang, C., *Bull. Korean Chem. Soc.* 2002, *11*, 1511–1512.

[18] Dyballa, N., Metzger, S., *J. Vis. Exp.* 2009, *30*, 1-4.

[19] Becker, J. S., Lobinski, R., Becker, J. S., *Metallomics* 2009, *1*, 312–316.

[20] Becker, J. S., Mounicou, S., Zoriy, M. V., Becker, J. S., Lobinski, R., *Talanta* 2008, *76*, 1183–1188.

[21] Raab, A., Pioselli, B., Munro, C., Thomas-Oates, J., Feldmann, J., *Electrophoresis* 2009, *30*, 303–314.

[22] Moreno-Gordaliza, E., Cañas, B., Palacios, M. A., Gómez-Gómez, M. M., *Analyst* 2010, *135*, 1288–1298.

[23] Mena, M. L., Moreno-Gordaliza, E., Moraleja, I., Cañas, B., Gómez-Gómez, M. M., *J. Chromatogr. A* 2011, *1218*, 1281–1290.

[24] Ron, D., Walter, P., *Nat. Rev. Mol. Cell Biol.* 2007, *8*, 519–529.

[25] Xu, S., Sankar, S., Neamati, N., *Drug Discov. Today* 2014, *19*, 222–240.

[26] Ni, M., Zhang, Y., Lee, A. S., *Biochem. J.* 2011, *434*, 181–188.

[27] Rigobello, M. P., Donella-Deana, A., Cesaro, L., Bindoli, A., *Biochem. J.* 2001, *356*, 567–570.

[28] Turano, C., Coppari, S., Altieri, F., Ferraro, A., *J. Cell Physiol.* 2002, *193*, 154–163.

[29] Yoshimori, T., Semba, T., Takemoto, H., Akagi, S., Yamamoto, A., Tashiro, Y., *J. Biol. Chem.* 1990, *265*, 15984–15990.

[30] Hersey, P., Zhang, X. D., *Pigment Cell Melanoma Res.* 2008, *21*, 358–367.

[31] Zhang, K., Kaufman, R. J., *J. Biol. Chem.* 2004, *279*, 25935–25938.

[32] Lovat, P. E., Corazzari, M., Armstrong, J. L., Martin, S., Pagliarini, V., Hill, D., Brown, A. M., Piacentini, M., Birch-Machin, M. A., Redfern, C. P., *Cancer Res.* 2008, *68*, 5363–5369.

[33] Li, J., Lee, A. S., *Curr. Mol. Med.*, 2006, *6*, 45–54.

[34] Tufo, G., Jones, A. W., Wang, Z., Hamelin, J., Tajeddine, N., Esposti, D. D., Martel, C., Boursier, C., Gallerne, C., Migdal, C., Lemaire, C., Szabadkai, G., Lemoine, A., Kroemer, G., Brenner, C., *Cell Death Differ.* 2014, *21*, 685–695.

[35] Xu, S., Butkevich, A. N, Yamada, R., Zhou, Y., Debnath, B., Duncan, R., Zandi, E., Petasis, N. A, Neamati, N., *Proc. Natl. Acad. Sci. USA* 2012, *109*, 16348–16353.

[36] Noiva, R., *Semin. Cell Dev. Biol.* 1999, *10*, 481–493.

[37] Sobierajska, K., Skurzynski, S., Stasiak, M., Kryczka, J., Cierniewski, C. S., Swiatkowska, M., *J. Biol. Chem.* 2014, *289*, 5758–5773.

[38] Dalle-Donne, I., Giustarini, D., Rossi, R., Colombo, R., Milzani, A., *Free Radic. Biol. Med.* 2003, *34*, 23–32.

[39] Moreno-Gordaliza, E., Cañas, B., Palacios, M. A., Gómez-Gómez, M. M., *Talanta* 2012, *88*, 599–608.

[40] Will, J., Sheldrick, W. S., Wolters, D., *J. Biol. Inorg. Chem.* 2008, *13*, 421–434.

© 2015 WILEY-VCH Verlag GmbH & Co. KGaA, Weinheim

Supporting information

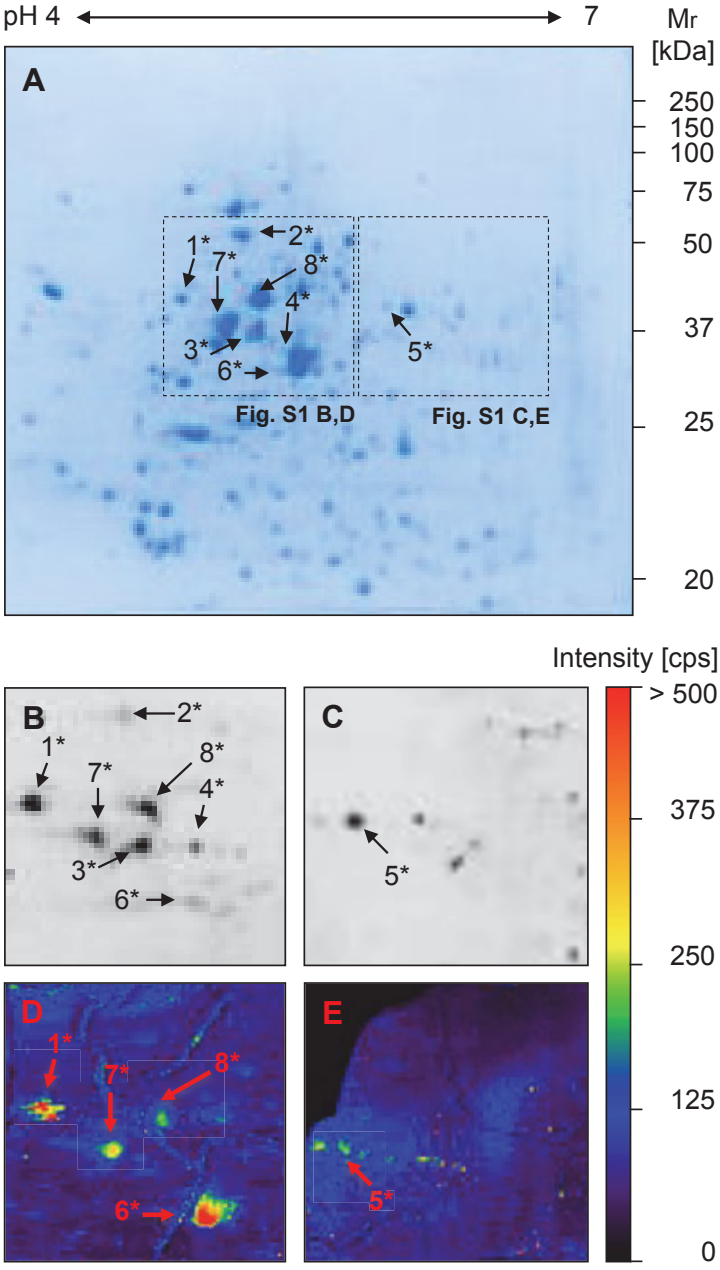

Figure S1: Detection of platinum in protein spots. (A) Coomassie stained 2DE gel, indicated the identified proteins. (B, C) Corresponding fluorescence scan (CFDA-cisplatin: excitation/ emission: 488 nm/532 nm). (D, E) LA-ICP-MS image, showing the distribution of platinum in the 2D gel. (A-E) 1* = PDIA1; 2* = GRP78; 3* and 4* = PDIA6; 5* = PDIA3; 6* = β-actin; 7* and 8* = Vimentin.

2.2 ASSESSING THE CONTRIBUTION OF THE TWO PROTEIN DISULFIDE ISOMERASES PDIA1 AND PDIA3 TO CISPLATIN RESISTANCE

Maximilian Kullmann, Ganna V. Kalayda, Malte Hellwig, Sandra Kotz, Ralf A. Hilger, Sabine Metzger, Ulrich Jaehde, *J. Inorg. Biochem.* 2015, 153: 247-252

Persönlicher Beitrag:

Der persönliche Beitrag für diese Veröffentlichung war die Identifizierung der cisplatinhaltigen Proteine PDIA1 und PDIA3.

Düsseldorf, Juli 2019

_____

Dr. Sabine Metzger

Journal of Inorganic Biochemistry 153 (2015) 247–252

Contents lists available at ScienceDirect

Journal of Inorganic Biochemistry

journal homepage: www.elsevier.com/locate/jinorgbio

Assessing the contribution of the two protein disulfide isomerases PDIA1 and PDIA3 to cisplatin resistance

Maximilian Kullmann [a], Ganna V. Kalayda [a], Malte Hellwig [a], Sandra Kotz [b], Ralf A. Hilger [c], Sabine Metzger [b,d], Ulrich Jaehde [a,*]

[a] University of Bonn, Institute of Pharmacy, Department of Clinical Pharmacy, An der Immenburg 4, 53121 Bonn, Germany
[b] University of Cologne, Cologne Biocenter, Zülpicherstraße 47b, 50674 Cologne, Germany
[c] Department of Medical Oncology, West German Cancer Center, University Hospital Essen, University Duisburg-Essen, Hufelandstraße 55, 45147 Essen, Germany
[d] IUF–Leibniz Research Institute for Environmental Medicine, Aufm Hennekamp 50, 40225 Düsseldorf, Germany

ARTICLE INFO

Article history:
Received 4 May 2015
Received in revised form 25 August 2015
Accepted 28 August 2015
Available online 5 September 2015

Keywords:
Cisplatin
Resistance
SiRNA knockdown
PDIA1
PDIA3
PACMA31

ABSTRACT

Intracellular binding of cisplatin to non-DNA partners, such as proteins, has received increasing attention as an additional mode of action and as mechanism of resistance. We investigated two cisplatin-interacting isoforms of protein disulfide isomerase regarding their contribution to acquired cisplatin resistance using sensitive and resistant A2780/A2780cis ovarian cancer cells. Cisplatin cytotoxicity was assessed after knockdown of either protein disulfide isomerase family A member 1 (PDIA1) or protein disulfide isomerase family A member 3 (PDIA3). Whereas PDIA1 knockdown led to increased cytotoxicity in resistant A2780cis cells, PDIA3 knockdown showed no influence on cytotoxicity. Coincubation with propynoic acid carbamoyl methyl amide 31 (PACMA31), a PDIA1 inhibitor, resensitized A2780cis cells to cisplatin treatment. Determination of the combination index revealed that the combination of cisplatin and PACMA31 acts synergistically. Our results warrant further evaluation of PDIA1 as promising target for chemotherapy, and its inhibition by PACMA31 as a new therapeutic approach.
© 2015 Elsevier Inc. All rights reserved.

1. Introduction

Cisplatin is among the most widely used chemotherapeutic drugs for several cancer entities, e.g. testicular and ovarian cancer. However, its use is limited by severe toxicity such as nephro-, neuro- and ototoxicity. Chemoresistance, which can be either intrinsic or acquired during therapy, is another limiting factor. The acquired drug resistance is a major setback to successful therapy and compromises effective outcome. Several mechanisms underlying chemoresistance have been postulated and experimental evidence points to a multifactorial nature. Most of the mechanisms prevent cisplatin from reaching its therapeutic target, the genomic DNA (reviewed in Ref. [1]). These "pre-target effects" include but are not limited to reduced cellular uptake, increased efflux and increased inactivation of cisplatin before binding to DNA. This inactivation can occur, for example, by binding to glutathione [2], metallothioneins [3,4] or proteins [5]. On-target mechanisms such as the nucleotide excision repair (NER) and the replicative bypass are also contributing to resistance. Several genetic and epigenetic alterations, e.g. inactivation of TP53, can be classified as "post-target resistance" (reviewed in Ref. [6]).

In order to elucidate the increased inactivation of cisplatin as one of the pre-target mechanisms of resistance, we screened ovarian tumor cells (A2780 and its cisplatin-resistant subline A2780cis) for proteins interacting with cisplatin using a fluorescent cisplatin analog (CFDA-Pt) [7,8]. After cell lysis, 2D gel electrophoresis of cytosolic proteins was performed [9]. With this technique, the separation of complex protein mixtures and visualization of hundreds to thousands of proteins is possible. Several fluorescent spots colocalizing with Coomassie-stained spots were detected indicating the interaction of CFDA-Pt with a protein. The presence of platinum in the spots was confirmed by LA–ICP–MS analysis. Some of the proteins interacting with CFDA-Pt were identified by ESI–MS/MS analysis, among them two isoforms of the protein disulfide isomerase (PDIA1, PDIA3). Here, we report the results of experiments intended to assess the relevance of these two proteins for acquired cisplatin resistance. PDI are compartmentalized mainly to the endoplasmic reticulum (ER) where they exert an oxidoreductase activity catalyzing the formation, isomerization and reduction of disulfides [10]. Most PDI isoforms contain a KDEL (lysine, aspartic acid, glutamic acid, leucine) amino acid sequence for ER retention, but were also localized in other cellular compartments, e.g. the cytosol [11]. PDIA1 (or PDI, P4HB or p55) and PDIA3 (or GRP58, ERp57, ERp60) are highly homologous sharing similar amino acid sequences (CGHC) at their active sites [10,12]. PDIA1 and PDIA3 carry seven cysteines, thus presenting a possible target for irreversible coordination of platinum complexes, as

* Corresponding author.
E-mail address: u.jaehde@uni-bonn.de (U. Jaehde).

http://dx.doi.org/10.1016/j.jinorgbio.2015.08.028
0162-0134/© 2015 Elsevier Inc. All rights reserved.

cisplatin binds preferably to cysteine residues [13]. The role of PDIA1 in cancer was recently reviewed in detail [12]. PDIA3 is highly expressed in the serous ovarian cancer cell line YDOV-139 and may be a potential biomarker for this cancer entity [14]. In cervical cancer, PDIA3 overexpression in 73% of patients was associated with low overall survival and recurrence-free survival [15]. Several studies suggest a link between some of the known PDI, such as PDIA3, PDIA4, and PDIA6, and stress tolerance and chemoresistance [16–18].

In order to study the contribution of PDIA1 and PDIA3 to acquired cisplatin resistance in ovarian cancer cells we accomplished a siRNA-mediated knockdown of PDIA1 and PDIA3 in A2780 and A2780cis cells and evaluated the effect thereof on cisplatin cytotoxicity. Subsequently we used a pharmacological inhibitor of PDIA1, a propynoic acid carbamoyl methyl amide known as PACMA31 (Fig. 1), to arrest the intracellular isomerase function [19].

2. Materials and methods

2.1. Reagents

Cis-diamminedichloridoplatinum(II) (cisplatin) and MTT (3-(4,5-dimethylthiazol-2-yl)-2,5-diphenyl-2 H-tetrazolium bromide) were obtained from Sigma (Steinheim, Germany). Protein Disulfide Isomerase Inhibitor III (PACMA31) was from Merck Millipore (Darmstadt, Germany). Cisplatin was dissolved in 0.9% NaCl solution. PACMA31 stock solution was prepared in DMSO.

2.2. Cell culture

The human ovarian carcinoma cell line A2780 and the cisplatin-resistant subline A2780cis were from the European Collection of Cell Cultures (ECACC). They were cultured in RPMI1640 supplemented with 10% FBS, 100 I.E./mL penicillin and 0.1 mg/mL streptomycin at 37 °C and 5% CO_2.

2.3. MTT assay

Cells were seeded in colorless flat bottom 96 well-plates (Sarstedt AG & Co., Nümbrecht, Germany) at a density of 1×10^4 cells per well in 90 μL medium and were allowed to attach overnight. Cells were exposed to increasing concentrations of cisplatin for either 72 h (cisplatin and PACMA31) or for 48 h for knockdown experiments. The assays were developed by adding 20 μL of MTT solution in PBS (5 mg/mL) per well for approximately 1 h. Viable cells convert MTT into a purple formazan product. The supernatant was discarded and the cells were dissolved in 100 μL of DMSO. Absorbance was measured at 570 nm with background subtraction at 690 nm using a plate reader (Thermomultiscan EX, Thermo, Schwerte, Germany). The results were analyzed and the pEC_{50}, EC_{50} and EC_{10} values ($pEC_{50} = -\log EC_{50}$, EC_{50} is the drug concentration that produces 50% of the maximum response, EC_{10} is the concentration that produces 10% of the maximum response) were determined with the GraphPad Prism® analysis software package (GraphPad Software, San Diego, USA) using non-linear regression (sigmoidal dose response, variable slope). Resistance factor was calculated as a ratio of EC_{50} of A2780cis to that of A2780 cells.

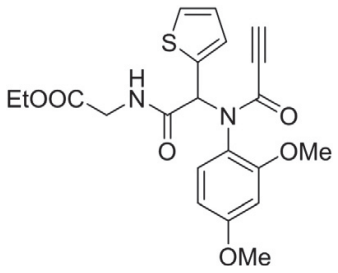

Fig. 1. Structure of PACMA31 [20].

2.4. Combination index

The combination index (CI) of cisplatin and PACMA31 was calculated with the CompuSyn® software (ComboSyn, Paragon, NJ, USA) as described by Chou [20].

Cells were seeded in 96-well plates and treated with 10, 20, 40, 60, 80, 100, 200, 400 and 800% of the previously determined EC_{50} concentration of cisplatin, of PACMA31 or a fix combination of cisplatin and PACMA31. The ratio of cisplatin to PACMA31 in the combination was 5.7 for A2780 and 21.3 for A2780cis cells. After 72 h, the interaction was assessed by an MTT assay as described in 2.3. CI values of <1, $= 1$, or >1 were considered as synergism, additivity and antagonism, respectively.

2.5. Small-interfering RNA knockdown

A2780 and A2780cis cells were seeded in 6-well plates at 0.5×10^6 cells per well and incubated for 24 h. The siRNA against PDIA1 (Hs_P4HB_5 FlexiTube, SI02662100) and PDIA3 (Hs_GRP58_6 FlexiTube, functionally verified siRNA, SI02654778), and the negative control siRNA (AllStars Negative Control siRNA, SI03650318) were obtained from Qiagen (Hilden, Germany). Cells were transfected using the K2® transfection system (Biontex Laboratories GmbH, München, Germany). First, 15 μL/mL K2® multiplier was added to wells 2 h before siRNA treatment. Then, cells were treated with 40 nM siRNA in antibiotics-free medium. After 24 h the medium was changed to full medium and the cells were incubated for another 48 h. Efficiency of knockdown was assessed by Western blot analysis.

2.6. Western blot analysis

Cells grown in 6-well plates were lysed in 200 μL RIPA buffer (25 mM Tris–HCl, 150 mM NaCl, 1% Triton X100, 1% sodium deoxycholate, 0.1% SDS). Protein concentration was determined using the Novagen® BCA assay (Merck Millipore, Darmstadt, Germany). Lysates were separated by SDS–PAGE using a 10% gel and transferred to PVDF membrane (Carl Roth, Karlsruhe, Germany). The membrane was blocked in 5% skim milk in tris-buffered saline (TBS) with 0.2% Tween 20 for 1 h. After washing, membranes were incubated at 4 °C overnight with primary antibodies against PDIA1 (GTX101468, Genetex, Irvine, USA) or PDIA3 (GTX113719). Next, membranes were washed twice and incubated with GAPDH antibody (GTX100118) for 1 h. Secondary goat anti-rabbit antibody (4030–05, SouthernBiotech, Birmingham, USA) was used. Chemiluminescence was detected after incubation with Pierce ECL Western blotting substrate (Thermoscientific, Rockford, USA) on a ChemiDoc™ XRS + System (Bio-Rad, Hercules, USA). Densitometric analysis was performed with ImageLab (Bio-Rad, Hercules, USA). Relative expression of the proteins to the loading control GAPDH was calculated.

2.7. Apoptosis analysis

Apoptosis was evaluated using the FITC Annexin V Apoptosis Detection Kit with PI® (BioLegend, San Diego, USA) according to the protocol provided by the manufacturer. Cells were seeded in 6-well plates at a density of 0.5×10^6 cells per well and the knockdown was performed as described in 2.5. Cells were treated with 10 μM cisplatin for 24 h. After staining with Annexin V and propidium iodide (PI), cells were analyzed by flow cytometry (FACScalibur®, BD Biosciences, San Jose, USA). Intact cells were gated with FlowJo® v10 (TreeStar, Ashland, USA) in the forward/side scatter to exclude small debris. Annexin V FITC-positive and propidium iodide-negative (Annexin FITC-V (+)/PI (−)) cells

were gated to identify the early apoptotic (EA) population, Annexin FITC-V (+)/PI (+) cells to identify the late apoptotic (LA) population.

2.8. Statistical analysis

Statistical comparisons between groups were carried out using a one-way analysis of variance (ANOVA) with the post-hoc Holm–Sidak test. Differences were considered statistically significant for $p < 0.05$.

3. Results

3.1. Effect of transient PDIA1 and PDIA3 knockdown on cisplatin cytotoxicity

In order to address the question to which extent the identified protein disulfide isomerases are involved in acquired resistance, we studied the effect of PDIA1 and PDIA3 siRNA knockdown on cisplatin cytotoxicity. In A2780 and A2780cis cells, the expression of PDIA1 and PDIA3 was reduced to below 50% (PDIA1) and to around 20–30% (PDIA3) of its basal level in untreated cells, respectively (Fig. 2).

A2780cis cells showed a cisplatin resistance factor of 3.5 ± 0.2 (n = 16). After PDIA1 knockdown, the MTT assay revealed for A2780 cells a slight but not significant sensitization to cisplatin treatment. A knockdown of PDIA3 had no influence on cisplatin cytotoxicity. Cisplatin-resistant A2780cis cells were significantly sensitized to cisplatin after PDIA1 knockdown compared to either negative knockdown controls ($p = 0.019$) or controls without knockdown ($p = 0.046$). Knockdown of PDIA3 showed no influence on cisplatin cytotoxicity in both cell lines (Fig. 3).

3.2. Effect of transient PDIA1 and PDIA3 knockdown on apoptosis induction after cisplatin treatment

The induction of apoptosis is regarded as the final step in the mechanism of action of cisplatin [21]. Therefore, we investigated the degree of apoptosis induction after knockdown of PDIA1 or PDIA3 and a subsequent treatment with 10 μM cisplatin for 24 h. In order to compensate for the apoptosis-inducing effect of the knockdown procedure, we calculated the ratio of the percentage of apoptotic cells after knockdown and subsequent cisplatin incubation to the percentage of apoptotic cells in corresponding control experiments without cisplatin. As internal control, we simultaneously tested cells without knockdown using the same procedure. In order to investigate the cisplatin effect on both stages of apoptosis, we analyzed the early apoptotic (EA) and late apoptotic (LA) cell population (Fig. 4).

As expected, cisplatin exposure generally induced early and late apoptosis in A2780 cells (ratio EA: 3.5 ± 0.3; LA: 3.9 ± 0.6) and to a lower extent in A2780cis (EA: 2.1 ± 0.5; LA: 2.4 ± 0.3). Within the same cell type no significant differences in early and late apoptosis induced by cisplatin were found between the different knockdown experiments. However, some trends were observed.

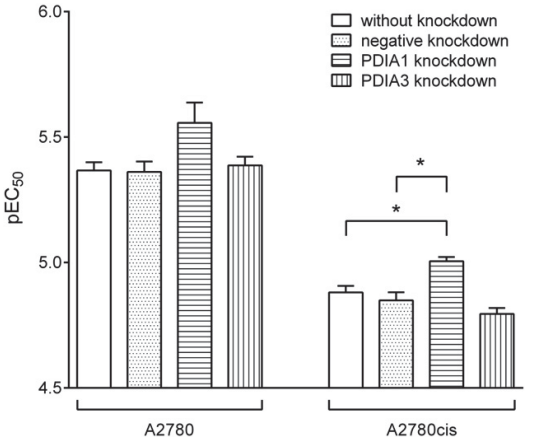

Fig. 3. Cisplatin cytotoxicity in A2780 and A2780cis cells assessed without knockdown, after negative, PDIA1 and PDIA3 knockdown (mean ± SEM, n = 3–6, $^*p < 0.05$).

In sensitive A2780 cells, apoptosis induction of cisplatin was not affected by PDIA1 knockdown exhibiting comparable EA and LA ratios than negative knockdown cells. After PDIA3 knockdown the effect of cisplatin treatment was lower (EA: 1.4 ± 0.1; LA: 1.3 ± 0.1) due to a stronger effect of PDIA3 knockdown alone without cisplatin compared to negative knockdown (not shown). Still, the cisplatin effect was detectable as the ratio was above 1.

In resistant A2780cis cells, PDIA1 knockdown led to higher ratios of EA and LA cells (EA: 3.5 ± 1.2; LA: 2.2 ± 0.6) compared to negative knockdown cells (EA: 1.4 ± 0.4; LA: 1.4 ± 0.4) which is in accordance with a cisplatin-sensitizing effect of PDIA1 knockdown in these cells. In contrast, PDIA3 knockdown showed comparable ratios for EA and LA cells than after negative knockdown indicating no cisplatin-sensitizing effect of PDIA3 knockdown.

3.3. Effect of pharmacological inhibition of PDI by PACMA31 on cisplatin cytotoxicity

To better understand the role of PDIA1 and PDIA3 we studied the effect of the recently described irreversible PDI inhibitor PACMA31 (Fig. 1) on cisplatin cytotoxicity [19]. PACMA31 has been reported to be selective for PDIA1 over other protein families, but its selectivity over other PDI isoforms is not yet known [12]. First, we analyzed the

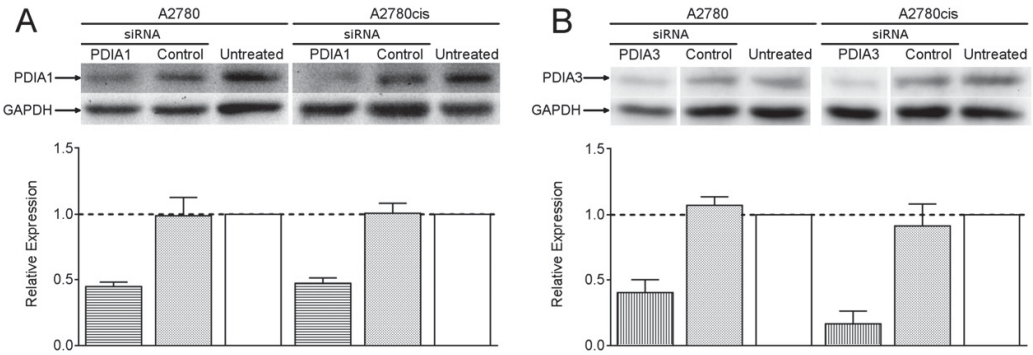

Fig. 2. Representative Western blot and corresponding densitometric quantification of the expression (bar graph) of (A) PDIA1 and (B) PDIA3 in A2780 and A2780cis cells either without knockdown (untreated), or treated with the respective siRNA (PDIA1, PDIA3 or negative control). GAPDH was used as housekeeping protein (mean ± SEM, n = 3).

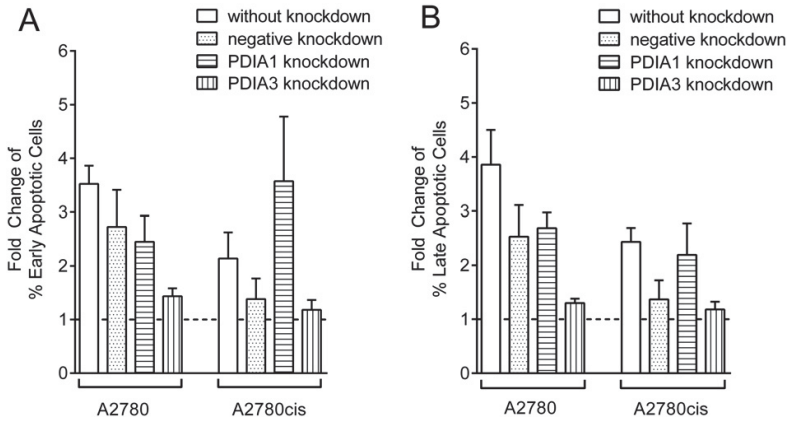

Fig. 4. Apoptosis induction in A2780 and A2780cis cells assessed without knockdown, after negative, PDIA1 or PDIA3 knockdown. Fold change of the percentage of (A) early apoptotic (EA) and (B) late apoptotic (LA) cells after a 24 h incubation with 10 μM cisplatin related to a corresponding control experiment without cisplatin treatment (mean ± SEM, $n = 3–6$).

effect of PACMA31 on A2780 and A2780cis cells alone and then in combination with cisplatin. We determined the EC_{50} and EC_{10} of PACMA31 (Table 1). The results show that PACMA31 is highly cytotoxic in A2780 and A2780cis cells with markedly lower EC_{50} values than cisplatin. The resistance factor for PACMA31 was 1.2.

In a second experiment, we investigated the combination of PACMA31 at a concentration of 0.2 μM (which is lower than its EC_{10} concentration) together with cisplatin. Whereas sensitivity of A2780 cells did not change, A2780cis cells were significantly sensitized to cisplatin treatment ($p = 0.015$) (Fig. 5). The resistance factor of A2780cis cells decreased from 4.3 ± 0.06 to 2.5 ± 0.27 (mean ± SEM, $n = 3–6$, $p = 0.0032$) upon addition of PACMA31 at a concentration of 0.2 μM.

3.4. Determination of the combination index of cisplatin and PACMA31

In order to further assess the potential of PACMA31 to overcome cisplatin resistance, we determined the combination index according to Chou [20]. For the combination of PACMA31 with cisplatin in sensitive A2780 cells we found a synergistic effect at effective concentration combinations higher than EC_{90} with the strongest synergism at EC_{95}. This effect was even more pronounced in resistant A2780cis cells where we determined CI values lower than 1 already at EC_{75} (Fig. 6). Again, the strongest effects were found at EC_{95}.

4. Discussion

Acquired drug resistance is one of the major obstacles in cancer chemotherapy. In our cell model consisting of a sensitive parental cell line (A2780) and a cisplatin-resistant subline (A2780cis), the resistance was previously attributed to a reduced drug uptake, and elevated glutathione levels [22]. Our approach focuses on the interference with intracellular proteins interacting with cisplatin, namely the protein disulfide isomerases PDIA1 and PDIA3.

Protein disulfide isomerases exhibit intracellular functions, which mainly support cellular homeostasis. Depending on the substrate, they form (oxidize), break (reduce) or rearrange (isomerize) disulfide bonds in proteins [12]. The role of PDIA1 seems to be cell-type specific. It has been shown that PDIA1 knockdown has no significant effect on HeLa cells whereas it inhibits viability of MCF-7 cells [23]. It has been recently shown that an upregulation of PDIA1 in glioblastoma is associated with resistance against temozolomide. Again, the effect of a PDIA1 knockdown on cytotoxicity was cell-line dependent [24].

The results on cisplatin cytotoxicity obtained with the MTT assay suggest a sensitizing effect of PDIA1 knockdown in the resistant A2780cis cells. In sensitive cells we only observed a tendency for a sensitization to cisplatin treatment by PDIA1. In contrast, PDIA3 knockdown had no influence on cisplatin cytotoxicity, even though we achieved a higher knockdown efficiency for PDIA3. Therefore, PDIA1 (and not PDIA3) may be an interesting target to investigate as one possible mechanism of acquired cisplatin resistance.

The results on cisplatin-induced apoptosis, however, are less clear. We observed a non-significant tendency to increased apoptosis induction upon cisplatin treatment in A2780cis cells after PDIA1 knockdown compared to negative knockdown. Although this observation is in accordance with a cisplatin-sensitizing effect it may also fall within biological variability. Knockdown of PDIA3 alone strongly increased apoptosis in A2780 cells, thus reducing the cisplatin effect. It is important to consider that the apoptosis experiments were limited to a cisplatin

Table 1
Cytotoxicity of PACMA31 in A2780 and A2780cis cells (mean ± SEM, $n = 9$).

	A2780	A2780cis
pEC_{50}	6.47 ± 0.05	6.40 ± 0.06
EC_{50} [μM]	0.37	0.46
pEC_{10}	6.62 ± 0.07	6.50 ± 0.05
EC_{10} [μM]	0.29	0.35

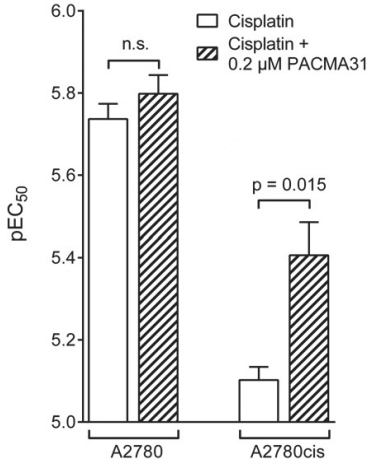

Fig. 5. Cisplatin cytotoxicity in A2780 and A2780cis cells without and with coincubation with 0.2 μM PACMA31 (mean ± SEM, $n = 3–6$, n.s. not significant).

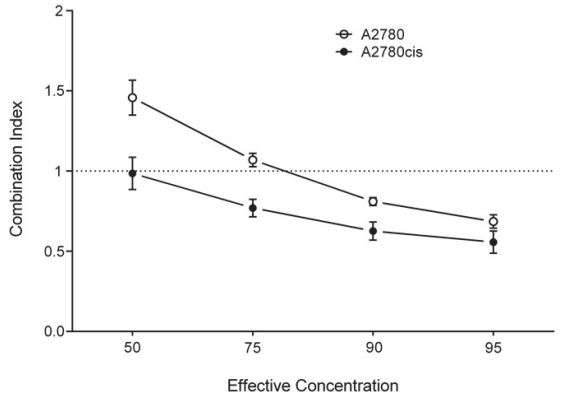

Fig. 6. Combination index (CI) of PACMA31 and cisplatin cytotoxicity in A2780 and A2780cis cells. CI was determined for EC_{50} to EC_{95}. (mean ± SEM, $n = 9$).

exposure of 24 h. Therefore, it may be interesting to investigate the time-dependence of the effect of PDIA1 knockdown on cisplatin-induced apoptosis.

Transient genetic modifications by siRNA treatment have been highly investigated in preclinical settings. The next step would be in vivo treatment with siRNA which is already under investigation [25]. However, at the moment, the most common therapeutic option is still a pharmacological inhibition. Thus, we investigated the potential of the recently developed PDIA1 inhibitor PACMA31 to reverse acquired cisplatin resistance. PACMA31 covalently binds to Cys397/Cys400 at the CGHC motif of PDIA1's active site, abolishing its intracellular function [19]. At the same time, this binding may block a predominant binding site of cisplatin [26]. For a different small molecule PDI inhibitor (16F16) it was shown, that it binds the two isoforms of PDI (also known as PDIA1) and PDIA3 investigated here [27]. We suspect that this may also hold true for PACMA31. Further studies to identify the PACMA31 binding site in PDIA3 and cisplatin binding sites in PDIA1 and PDIA3 are required.

PACMA31 shows comparable cytotoxicity in A2780/A2780cis cells as in the OVCAR-3 cell line for which an EC_{50} of 0.32 μM was determined [19]. Interestingly, A2780cis cells did not show any resistance to PACMA31 with a resistance factor of only 1.2. Our results further suggest that PACMA31 increases cisplatin cytotoxicity in A2780cis cells. The sensitizing effect by PACMA31 was even stronger than after PDIA1 knockdown. One may speculate that a knockdown to just 50% of the baseline level may be too low to reduce the protein function sufficiently. However, the results also suggest that beside irreversible PDIA1 inhibition there may be additional or alternative underlying mechanisms, e.g. an elevation of the ER stress level. The assumption of an alternative mechanism is also supported by the fact that PACMA31 is per se highly cytotoxic on these cells.

Nevertheless, this is the first study that manifests a synergistic interaction of PACMA31 and cisplatin in their ability to inhibit the growth of cancer cells. As postulated by Chou, it is of paramount importance for drug combinations in cancer therapy to exhibit synergy especially at high EC concentrations (higher than EC_{90}) [28], in the best case eradicating all cancer cells. Our results show a synergistic effect of PACMA31 and cisplatin for concentrations above the respective EC_{75} in resistant cells. Given this synergism, the administered dose of both substances may be decreased, with equal effectivity. Since the toxic side effects of cisplatin are dose-dependent dose reduction may diminish the systemic toxicity (for example neuro-, nephro- and ototoxicity). Additionally, these results suggest that a combined treatment of cisplatin and PACMA31 may improve the therapy outcome in resistant ovarian cancer. This, however, should be confirmed in future investigations.

5. Conclusions

In conclusion, siRNA knockdown of PDIA1 increases cisplatin cytotoxicity in cisplatin-resistant A2780cis cells. The effect of PDIA1 knockdown on apoptosis induction by cisplatin remains unclear and deserves further investigation. Most interestingly, A2780cis cells are resensitized to cisplatin treatment by combination with the PDIA1 inhibitor PACMA31.

Our results justify further investigation of the potential of this combination to control cisplatin resistance which still poses a major threat to the success of platinum-based therapy in ovarian cancer.

Abbreviations

BCA	Bicinchoninic acid
CFDA-Pt	[{1-([5-(and-6)-Carboxyfluorescein-diacetate]aminomethyl)-1,2-ethylenediamine}-dichlorideplatinum(II)]
DMSO	Dimethylsulfoxide
EA	Early apoptotic cells
ESI-MS	Electrospray ionization mass spectrometry
GAPDH	Glyceraldehyde 3-phosphate dehydrogenase
LA	Late apoptotic cells
MTT	3-(4,5-Dimethylthiazol-2-yl)-2,5-diphenyl-2H-tetrazolium bromide
PACMA	Propynoic acid carbamoyl methyl amide
PDIA1	Protein disulfide isomerase family A member 1
PDIA3	Protein disulfide isomerase family A member 3
PVDF	Polyvinylidine fluoride
RIPA buffer	Radio immunoprecipitation assay buffer
SDS–PAGE	Sodium dodecyl sulfate polyacrylamide gel electrophoresis
TBS	Tris-buffered saline

Acknowledgments

This project was supported by the Deutsche Forschungsgemeinschaft (JA 817/4-1).

References

[1] R. Mezencev, Interactions of cisplatin with non-DNA targets and their influence on anticancer activity and drug toxicity: the complex world of the platinum complex, Curr. Cancer Drug Targets 14 (2015) 794–816.
[2] D. Hagrman, J. Goodisman, A.K. Souid, Kinetic study on the reactions of platinum drugs with glutathione, J. Pharmacol. Exp. Ther. 308 (2004) 658–666.
[3] K. Kasahara, Y. Fujiwara, K. Nishio, T. Ohmori, Y. Sugimoto, K. Komiya, T. Matsuda, N. Saijo, Metallothionein content correlates with the sensitivity of human small cell lung cancer cell lines to cisplatin, Cancer Res. 51 (1991) 3237–3242.
[4] D. Hagrman, J. Goodisman, J.C. Dabrowiak, A.K. Souid, Kinetic study on the reaction of cisplatin with metallothionein, Drug Metab. Dispos. 31 (2003) 916–923.
[5] T. Zhao, F.L. King, Direct determination of the primary binding site of cisplatin on cytochrome C by mass spectrometry, J. Am. Soc. Mass Spectrom. 20 (2009) 1141–1147.
[6] L. Galluzzi, L. Senovilla, I. Vitale, J. Michels, I. Martins, O. Kepp, M. Castedo, G. Kroemer, Molecular mechanisms of cisplatin resistance, Oncogene 31 (2011) 1869–1883.
[7] C. Molenaar, J.M. Teuben, R.J. Heetebrij, H.J. Tanke, J. Reedijk, New insights in the cellular processing of platinum antitumor compounds, using fluorophore-labeled platinum complexes and digital fluorescence microscopy, J. Biol. Inorg. Chem. 5 (2000) 655–665.
[8] R. Zabel, M. Kullmann, G.V. Kalayda, U. Jaehde, G. Weber, Optimized sample preparation strategy for the analysis of low molecular mass adducts of a fluorescent cisplatin analogue in cancer cell lines by CE-dual-LIF, Electrophoresis 36 (2015) 509–517.
[9] S. Kotz, M. Kullmann, B. Crone, G.V. Kalayda, U. Jaehde, S. Metzger, Combination of two-dimensional gel electrophoresis and a fluorescent carboxyfluorescein diacetate labeled cisplatin analogue allows the identification of intracellular cisplatin-protein adducts, Electrophoresis (2015). http://dx.doi.org/10.1002/elps.201500188 (e-pub ahead of print).
[10] C.E. Jessop, R.H. Watkins, J.J. Simmons, M. Tasab, N.J. Bulleid, Protein disulphide isomerase family members show distinct substrate specificity: P5 is targeted to BiP client proteins, J. Cell Sci. 122 (2009) 4287–4295.
[11] C. Turano, S. Coppari, F. Altieri, A. Ferraro, Proteins of the PDI family: unpredicted non-ER locations and functions, J. Cell. Physiol. 193 (2002) 154–163.

[12] S. Xu, S. Sankar, N. Neamati, Protein disulfide isomerase: a promising target for cancer therapy, Drug Discov. Today 19 (2014) 222–240.
[13] T. Zimmermann, M. Zeizinger, J.V. Burda, Cisplatin interaction with cysteine and methionine, a theoretical DFT study, J. Inorg. Biochem. 99 (2005) 2184–2196.
[14] D. Chay, H. Cho, B.J. Lim, E.S. Kang, Y.J. Oh, S.M. Choi, B.W. Kim, Y.T. Kim, J.-H. Kim, ER-60 (PDIA3) is highly expressed in a newly established serous ovarian cancer cell line, YDOV-139, Int. J. Oncol. 37 (2010) 399–412.
[15] C.J. Liao, T.I. Wu, Y.H. Huang, T.C. Chang, C.S. Wang, M.M. Tsai, C.H. Lai, Y. Liang, S.M. Jung, K.H. Lin, Glucose-regulated protein 58 modulates cell invasiveness and serves as a prognostic marker for cervical cancer, Cancer Sci. 102 (2011) 2255–2263.
[16] H. Okudo, H. Kato, Y. Arakaki, R. Urade, Cooperation of ER-60 and BiP in the oxidative refolding of denatured proteins in vitro, J. Biochem. 138 (2005) 773–780.
[17] D. Xu, R.E. Perez, M.H. Rezaiekhaligh, M. Bourdi, W.E. Truog, Knockdown of ERp57 increases BiP/GRP78 induction and protects against hyperoxia and tunicamycin-induced apoptosis, Am. J. Physiol. Lung Cell. Mol. Physiol. 297 (2009) L44–L51.
[18] G. Tufo, A. Jones, Z. Wang, J. Hamelin, N. Tajeddine, D.D. Esposti, C. Martel, C. Boursier, C. Gallerne, C. Migdal, C. Lemaire, G. Szabadkai, A. Lemoine, G. Kroemer, C. Brenner, The protein disulfide isomerases PDIA4 and PDIA6 mediate resistance to cisplatin-induced cell death in lung adenocarcinoma, Cell Death Differ. 21 (2014) 685–695.
[19] S. Xu, A.N. Butkevich, R. Yamada, Y. Zhou, B. Debnath, R. Duncan, E. Zandi, N.A. Petasis, N. Neamati, Discovery of an orally active small-molecule irreversible inhibitor of protein disulfide isomerase for ovarian cancer treatment, Proc. Natl. Acad. Sci. 109 (2012) 16348–16353.
[20] T.-C. Chou, Theoretical basis, experimental design, and computerized simulation of synergism and antagonism in drug combination studies, Pharmacol. Rev. 58 (2006) 621–681.
[21] V.M. Gonzalez, M.A. Fuertes, C. Alonso, J.M. Perez, Is cisplatin-induced cell death always produced by apoptosis? Mol. Pharmacol. 59 (2001) 657–663.
[22] J. Zisowsky, S. Koegel, S. Leyers, K. Devarakonda, M.U. Kassack, M. Osmak, U. Jaehde, Relevance of drug uptake and efflux for cisplatin sensitivity of tumor cells, Biochem. Pharmacol. 73 (2007) 298–307.
[23] T. Hashida, Y. Kotake, S. Ohta, Protein disulfide isomerase knockdown-induced cell death is cell-line-dependent and involves apoptosis in MCF-7 cells, J. Toxicol. Sci. 36 (2011) 1–7.
[24] S. Sun, D. Lee, A.S. Ho, J.K. Pu, X.Q. Zhang, N.P. Lee, P.J. Day, W.M. Lui, C.F. Fung, G.K. Leung, Inhibition of prolyl 4-hydroxylase, beta polypeptide (P4HB) attenuates temozolomide resistance in malignant glioma via the endoplasmic reticulum stress response (ERSR) pathways, Dev. Oncol. 15 (2013) 562–577.
[25] X. Xu, K. Xie, X.-Q. Zhang, E.M. Pridgen, G.Y. Park, D.S. Cui, J. Shi, J. Wu, P.W. Kantoff, S.J. Lippard, R. Langer, G.C. Walker, O.C. Farokhzad, Enhancing tumor cell response to chemotherapy through nanoparticle-mediated codelivery of siRNA and cisplatin prodrug, Proc. Natl. Acad. Sci. 110 (2013) 18638–18643.
[26] A.K. Boal, A.C. Rosenzweig, Crystal structures of cisplatin bound to a human copper chaperone, J. Am. Chem. Soc. 131 (2009) 14196–14197.
[27] B.G. Hoffstrom, A. Kaplan, R. Letso, R.S. Schmid, G.J. Turmel, D.C. Lo, B.R. Stockwell, Inhibitors of protein disulfide isomerase suppress apoptosis induced by misfolded proteins, Nat. Chem. Biol. 6 (2010) 900–906.
[28] T.-C. Chou, Drug combination studies and their synergy quantification using the Chou–Talalay method, Cancer Res. 70 (2010) 440–446.

2.3 GRP78 KNOCKDOWN DOES NOT AFFECT CYTOTOXICITY OF CISPLATIN IN OVARIAN CANCER CELLS

Kullmann M, Kotz S, Hellwig M. Kalayda GV, Hilger RA, Metzger S, Jaehde U., *Int J Clin Pharmacol Ther.* 2015, 53(12): 1038-40.

Persönlicher Beitrag:

Der persönliche Beitrag für diese Veröffentlichung war die Identifizierung des cisplatinhaltigen Proteins GRP78.

Düsseldorf, Juli 2019

_____

Dr. Sabine Metzger

International Journal of Clinical Pharmacology and Therapeutics, Vol. 53 – No. 12/2015 (1038-1040)

Extended Abstracts

©2015 Dustri-Verlag Dr. K. Feistle
ISSN 0946-1965

DOI 10.5414/CPXCES14EA02
e-pub: November 2, 015

GRP78 knockdown does not affect cytotoxicity of cisplatin in ovarian cancer cells

Maximilian Kullmann[1], Sandra Kotz[2], Malte Hellwig[1], Ganna V. Kalayda[1], Sabine Metzger[2], and Ulrich Jaehde[1]

[1]Institute of Pharmacy, Department of Clinical Pharmacy, University of Bonn, Bonn, and [2]Cologne Biocenter, University of Cologne, Cologne, Germany

Key words
GRP78 – siRNA – knockdown – cisplatin – resistance

Correspondence to
Prof. Dr. U. Jaehde
Institute of Pharmacy,
Department of Clinical Pharmacy, University of Bonn,
An der Immenburg 4,
53121 Bonn, Germany
u.jaehde@uni-bonn.de

Introduction

Cisplatin is an effective treatment in a variety of cancer entities. However, in addition to toxic side effects, the occurrence of acquired resistance frequently compromises therapy outcome, and several resistance mechanisms are the focus of current research efforts. Of these mechanisms, an increased intracellular formation of biologically inactive adducts with proteins and peptides seems to be a relevant factor contributing to the acquisition of resistance [1]. It has been shown, for example, that cisplatin, after entering the cell, can react with water molecules and readily bind to nucleophilic species such as glutathione (GSH), metallothioneins, and other proteins prior to reaching the cell DNA [1, 2].

In a previous project, we used CFDA-Pt, a fluorescent cisplatin analogue [3], to identify other intracellular binding partners of cisplatin. Following 2D gel electrophoresis of cytosolic proteins, an ESI-MS/MS analysis of fluorescent adducts revealed several proteins binding CFDA-Pt [4]. One of these was glucose-regulated protein 78 kDa (GRP78). In several cancer cell line models of a variety of tumor types it has been shown that GRP78 up-regulation occurs intrinsically or can be induced by cisplatin treatment [5, 6]. Recently, Cali et al. [7] reported an increased GRP78 expression in endometrial tumors. Melanoma cells were sensitized to cisplatin treatment after siRNA-mediated knockdown of GRP78 [8]. Lin et al. [9] showed an upregulation of GRP78 in ER stress-tolerant lung cancer cells (A460et and A549et). In these cells, cisplatin resistance could be reversed by knockdown of GRP78.

Since GRP78 has been identified as an important binding partner for CFDA-Pt we hypothesized that it may contribute to cisplatin resistance by deactivating reactive platinum species in the cytoplasm before these can reach their target, the cell DNA. We therefore investigated the effect of siRNA-mediated knockdown of GRP78 on the cytotoxicity of cisplatin in A2780 ovarian cancer cells and their cisplatin-resistant variant A2780cis.

Material and methods

Cell culture

The human ovarian carcinoma cell line A2780 and the cisplatin-resistant variant A2780cis were cultivated as monolayers in RPMI-1640™ medium with 10% fetal calf serum, 0.6 mM L-glutamine, 100 I.E./mL penicillin, and 0.1 mg/mL streptomycin at 37 °C with 5% CO_2.

Small-interfering RNA knockdown of GRP78

A2780 and A2780cis cells were seeded in 6-well plates at 0.5×10^6 cells per well and incubated for 24 hours. The siRNA against GRP78 (Hs-HSPA5-6 Flexi tube, functionally verified siRNA, SI02780554) and the negative control siRNA (AllStars Negative Control siRNA, SI03650318) were obtained from Qiagen GmbH, Hilden, Germany. Cells were transfected using the K2™ transfection system (Biontex Laboratories GmbH, Planegg, Germany) with 50 pmol/well of siRNA in antibiotic-free medium. Efficiency of knockdown was assessed using western blot analysis.

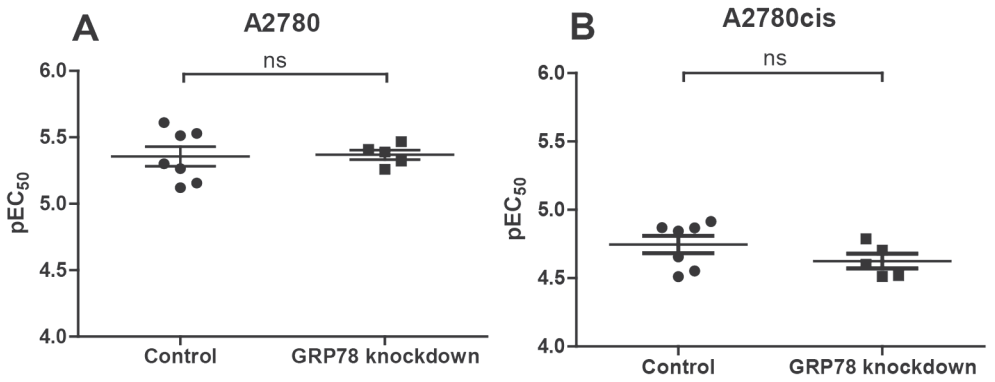

Figure 1. Cisplatin cytotoxicity in (A) A2780 and (B) A2780cis cells (mean ± SEM, n = 5 – 7, ns = not significant) without and after GRP78 knockdown.

Cytotoxicity

The cytotoxicity of cisplatin after siRNA knockdown of GRP78 was determined using an MTT-based assay (MTT = 3-(4,5-Dimethyl-2-thiazolyl)-2,5-diphenyl-2H-tetrazolium bromide). Cells were allowed to attach in 96-well plates overnight prior to carrying out the knockdown. Subsequently, cells were incubated with increasing concentrations of cisplatin for 48 hours. The EC_{50} (drug concentration which produces 50% of the maximum possible response) and pEC_{50} (= –log EC_{50}) values were estimated using the GraphPad Prism™ analysis software package (GraphPad Software, San Diego, CA, USA) by means of non-linear regression (sigmoidal dose response). Resistance factors were calculated by the ratio of EC_{50} values of A2780cis to A2780 cells.

Western blot analysis

Cells were lysed in RIPA buffer, separated by SDS/PAGE, and transferred to polyvinylidene difluoride (PVDF) membranes. Non-specific binding to the membranes was blocked using 5% skim milk in Tris-buffered saline (TBS) with 0.2% Tween for 1 hour. After washing, membranes were incubated overnight with antibodies against GRP78 at 1 : 1,000 (GTX102580, GeneTex Inc., Irvine, CA, USA) and GAPDH at 1 : 10,000 (GTX100118, GeneTex Inc.) dilutions. Secondary antibody goat anti-rabbit (4030-05, SouthernBiotech, Birmingham, AL, USA), was used at 1 : 2,000 and 1 : 20,000, respectively. Chemiluminescence was detected after incubation with Pierce™ ECL western blotting substrate (Thermo Scientific, Rockford, IL, USA) on a ChemiDoc™ XRS+ System (Bio-Rad, Hercules, CA, USA). Densitometric analysis was carried out using Image Lab™ software (Bio-Rad).

Results

We first determined the basal expression of GRP78 and the effect of cisplatin treatment on GRP78 expression in A2780 and A2780cis cells. In contrast to previous findings [5, 6], there was no significant effect of cisplatin on GRP78 expression detectable by western blot analysis. After treatment with 5 – 20 µM of cisplatin for 6 – 48 hours, GRP78 expression in A2780 and A2780cis cells did not change significantly compared to the basal expression without treatment.

To investigate if GRP78 contributes to cisplatin detoxification in the cytoplasm, we performed a transient siRNA-mediated silencing of GRP78 in A2780 and A2780cis cells. The expression of GRP78 compared to untreated control cells was reduced to 59 ± 9% and 37 ± 8% in A2780 and A2780cis cells, respectively.

We next determined cisplatin cytotoxicity using the MTT assay after GRP78 knockdown. Our results showed no significant difference between non-transfected control cells and GRP78 knockdown cells (Figure 1). A2780cis cells exhibited a non-significant ($p = 0.11$) decrease in the pEC_{50} value, rather suggesting an increase in resistance. This is supported by the fact that the resistance fac-

tor was increased by 40% after knockdown ($RF_{control}$ = 4.2 vs. $RF_{GRP78kd}$ = 5.8).

Conclusions

We conclude that cisplatin has no significant effect on GRP78 expression in the cell line model A2780/A2780cis. The influence of GRP78 on resistance seems to be minor since the pEC_{50} did not change significantly after knockdown. In further experiments, the degree of DNA platination after knockdown will be measured in order to examine the possibility that cell signaling adaptations are able to counteract the effects of GRP78 knockdown.

Acknowledgment

This project was supported by the Deutsche Forschungsgemeinschaft (JA 817/4-1).

References

[1] *Galluzzi L, Senovilla L, Vitale I, Michels J, Martins I, Kepp O, Castedo M, Kroemer G*. Molecular mechanisms of cisplatin resistance. Oncogene. 2012; *31:* 1869-1883. CrossRef PubMed

[2] *Kasahara K, Fujiwara Y, Nishio K, Ohmori T, Sugimoto Y, Komiya K, Matsuda T, Saijo N*. Metallothionein content correlates with the sensitivity of human small cell lung cancer cell lines to cisplatin. Cancer Res. 1991; *51:* 3237-3242. PubMed

[3] *Molenaar C, Teuben JM, Heetebrij RJ, Tanke HJ, Reedijk J*. New insights in the cellular processing of platinum antitumor compounds, using fluorophore-labeled platinum complexes and digital fluorescence microscopy. J Biol Inorg Chem. 2000; *5:* 655-665. CrossRef PubMed

[4] *Kotz S, Kullmann M, Crone* B, *Kalayda A, Jaehde U, Metzger S.* Combination of two-dimensional gel electrophoresis and a fluorescent carboxyfluorescein-diacetate-labeled cisplatin analogue allows the identification of intracellular cisplatin-protein adducts. Electrophoresis. 2015; Epub ahead of print.

[5] *Gray MJ, Mhawech-Fauceglia P, Yoo E, Yang W, Wu E, Lee AS, Lin YG*. AKT inhibition mitigates GRP78 (glucose-regulated protein) expression and contribution to chemoresistance in endometrial cancers. Int J Cancer. 2013; *133:* 21-30. CrossRef PubMed

[6] *Xing X, Lai M, Wang Y, Xu E, Huang Q*. Overexpression of glucose-regulated protein 78 in colon cancer. Clin Chim Acta. 2006; *364:* 308-315. CrossRef PubMed

[7] *Calì G, Insabato L, Conza D, Bifulco G, Parrillo L, Mirra P, Fiory F, Miele C, Raciti GA, Di Jeso B, Terrazzano G, Beguinot F, Ulianich L*. GRP78 mediates cell growth and invasiveness in endometrial cancer. J Cell Physiol. 2014; *229:* 1417-1426. CrossRef PubMed

[8] *Jiang CC, Mao ZG, Avery-Kiejda KA, Wade M, Hersey P, Zhang XD*. Glucose-regulated protein 78 antagonizes cisplatin and adriamycin in human melanoma cells. Carcinogenesis. 2009; *30:* 197-204. CrossRef PubMed

[9] *Lin Y, Wang Z, Liu L, Chen L*. Akt is the downstream target of GRP78 in mediating cisplatin resistance in ER stress-tolerant human lung cancer cells. Lung Cancer. 2011; *71:* 291-297. CrossRef PubMed

2.4 OPTIMIZED TWO-DIMENSIONAL GEL ELECTROPHORESIS IN AN ALKALINE pH RANGE IMPROVING THE IDENTIFICATION OF INTRACELLULAR CFDA-CISPLATIN-PROTEIN ADDUCTS IN OVARIAN CANCER CELLS

Sandra Kotz, Maximilian Kullmann, Ganna V. Kalayda, Nadine Dyballa-Rukes, Ulrich Jaehde, Sabine Metzger, *Electrophoresis* 2018, 39, 1488 - 1496.

Persönlicher Beitrag:

Der persönliche Beitrag für diese Veröffentlichung war die Optimierung der 2D-Gelelektrophorese (pH 6 - 10) zur Identifizierung von intrazellulären Cisplatin-Proteinaddukten, die Identifizierung der detektierten CFDA-Cisplatin-Proteinaddukte mittels Massenspektrometrie sowie die Verfassung der Publikation.

Düsseldorf, Juli 2019

_____

Dr. Sabine Metzger

1488 *Electrophoresis* 2018, *39*, 1488–1496

Sandra Kotz[1,2]
Maximilian Kullmann[3]
Ganna V. Kalayda[3]
Nadine Dyballa-Rukes[2]
Ulrich Jaehde[3]
Sabine Metzger[1,2]

[1]MS-Platform Biocenter, Cluster of Excellence on Plant Science (CEPLAS), University of Cologne, Cologne, Germany
[2]IUF-Leibniz Research Institute for Environmental Medicine, Heisenberg-group - Environmentally-induced cardiovascular degeneration, Mass spectrometry Core Unit, Düsseldorf, Germany
[3]Department of Clinical Pharmacy, Institute of Pharmacy, University of Bonn, Bonn, Germany

Received September 26, 2017
Revised April 6, 2018
Accepted April 6, 2018

Research Article

Optimized two-dimensional gel electrophoresis in an alkaline pH range improves the identification of intracellular CFDA-cisplatin-protein adducts in ovarian cancer cells

Intracellular binding of cisplatin to proteins has been associated with acquired resistance to chemotherapy. In our previous study we established an analytical method for the identification of intracellular cisplatin-binding proteins. The method used a fluorescent carboxyfluorescein-diacetate-labeled cisplatin analogue (CFDA-cisplatin), two-dimensional gel electrophoresis (2DE) and mass spectrometry, which allows detecting and identifying intracellular CFDA-cisplatin-containing protein adducts in the acidic pH range (pH 4–7). Based on this analytical method we extended the identification of intracellular cisplatin-protein adducts to the alkaline pH range (pH 6–10) giving chance to discover new important binding partners. 2DE analysis of alkaline proteins is challenging due to the difficult separation of basic proteins during the isoelectric focusing (IEF). The establishment of an optimized IEF protocol for basic proteins enabled us to identify several intracellular CFDA-cisplatin-binding proteins including enzymes of the glucose and serine metabolism like alpha enolase and D-3-phosphoglycerate 1-dehydrogenase.

Keywords:
Alkaline pH-range / CFDA-cisplatin / Cisplatin / Two-dimensional gel electrophoresis
DOI 10.1002/elps.201700377

Additional supporting information may be found in the online version of this article at the publisher's web-site

1 Introduction

Ovarian cancer is the second most common cause of death from gynecological cancer worldwide [1]. Current therapies include a cytoreductive surgery followed by platinum- and taxane-based chemotherapy. Despite the high initial response of ovarian cancer cells to the primary therapy, an important fraction of cisplatin-sensitive tumors develops chemoresistance leading to therapeutic failure [2].

Cisplatin is a widely employed chemotherapeutic drug for treatment of solid neoplasms, including head and neck, lung, colorectal, bladder, testicular and ovarian cancers [3–5]. Resistance to cisplatin is a multifactorial problem including reduction of intracellular concentrations of cisplatin through decreased drug influx and/or increased drug efflux, increased repair of DNA damage, adapted apoptotic signaling pathways, and inactivation of the active species [6, 7]. Inside the cell the low concentration of chloride ions in the cytoplasm enables the aquation of cisplatin, so that the reactive species can interact with DNA, RNA, proteins, membrane phospholipids, cytoskeletal filaments and sulfur-containing molecules. The platination of DNA represents a critical part of the cytotoxic action of cisplatin [8], however only $<1\%$ of the intracellular drug binds to its pharmacological target [9]. Therefore, it is possible that DNA damage is not the only mechanism of cisplatin cytotoxicity. Binding of cisplatin to the sulfur-containing amino acids cysteine and methionine, which have a much higher affinity to platinum than the nitrogen donors of the nuclear DNA [10], may affect the function of various proteins involved in cellular energy metabolism, the regulation of transmembrane transport and the assembly of the cytoskeleton [11]. Currently, it is conceivable that the platination of DNA may be not the only process leading to

Correspondence: Dr. Sabine Metzger, Cologne Biocenter, Zülpicherstraße 47b, University of Cologne, 50674 Cologne, Germany
Fax: +49-221-470-8289
E-mail: s.metzger@uni-koeln.de

Abbreviations: **CFDA-cisplatin**, carboxyfluorescein-diacetate-labeled cisplatin analogue; **EF1A1**, elongation factor 1-alpha 1; **ENOA**, alpha-enolase; **GAPDH**, glyceraldehyde-3-phosphate dehydrogenase; **HED**, hydroxyethyldisulphide; **hn-RNP**, heterogeneous nuclear ribonucleoprotein; **PHGDH**, D-3-phosphoglycerate-dehydrogenase; **PKM**, pyruvate kinase

© 2018 WILEY-VCH Verlag GmbH & Co. KGaA, Weinheim

cisplatin-induced apoptosis. Changes in energy metabolism and oxidative damage on sulfur-containing molecules and cell membrane proteins may contribute significantly to the cisplatin cytotoxicity and associated side effects [12].

Therefore, the identification of intracellular cisplatin-protein adducts, which may be involved in the mechanisms of action of cisplatin and in resistance mechanisms, is of great interest. A method to detect and to identify intracellular cisplatin-protein adducts using a fluorescent carboxyfluorescein-diacetate-labeled cisplatin analog (CFDA-cisplatin), two-dimensional gel electrophoresis (2DE) and mass spectrometry has recently been developed [12]. CFDA-cisplatin represents a suitable model substance for cisplatin, because it reflects the biological behavior of the parent drug [13] and neither 2DE, nor the processes of staining and destaining of proteins in a 2DE gel resulted in the loss of platinum from CFDA-cisplatin-binding proteins [12, 14, 15]. Broad (pH 3–10) and acidic (pH 4–7) pH ranges for 2DE have been widely investigated in ovarian cancer cells, but 2DE analysis specifically designed for the alkaline pH range (pH 6–10) has not been reported so far. An optimal 2DE in the alkaline pH range remains a challenge, because basic proteins are difficult to separate in the IEF due to aggregation, oxidation and precipitation. Several other studies have also tackled these challenges [16–23]. By the use of anodic cup-loading and narrow pH gradient strips (pH 6–10) for the first dimension, the resolution of the separation and therefore the possibility of revealing and identifying new cisplatin-binding proteins can be enhanced. Nevertheless, when pH gradient strips (pH 6–10) are used, extensive horizontal streaking and poor resolution within 2DE gels is a considerable problem. Some strategies have been applied for the reduction of streaking: the use of an alternative reducing agent hydroxyethyldisulphide (HED), the addition of a dithiothreitol (DTT) wick to supplement DTT at the cathode and the optimization of the equilibration conditions between the IPG strip and second dimension SDS-PAGE. HED removes much of the streaking by converting of negatively charged protein thiol groups into neutral ones and prevents the reformation of disulfide bridges [22]. DTT is a weak acid (pK_a close to 9) and diminished the reformation of disulfide bridges due to the oxidation of sulfhydryl groups.

It was the aim of this study to adapt methodical strategies for the 2DE analysis of the alkaline pH range (pH 6–10) enabling the precise detection and identification of new intracellular CFDA-cisplatin-containing proteins. With this, we will extend the current list of cisplatin-protein adducts in ovarian cancer cells.

2 Materials and methods

2.1 Chemicals and materials

2,2′-Dithiodiethanol (2-hydroxyethyl disulfide, HED), ammonium persulfate, ethanol, formic acid, glycerine, glycine, HEPES, magnesium chloride, methanol, ortho-phosphoric acid 85%, SDS, Tergitol® solution Type NP-40, thiourea and urea were received from Sigma Aldrich (Steinheim, Germany). Tris Pufferan® was from Roth (Karlsruhe, Germany). Acetonitrile (ACN) and ammonium bicarbonate were purchased from Fluka (Steinheim, Germany). Aluminiumsulfate-18-hydrate, chloroform, iodoacetamide, and TEMED were obtained from Merck (Darmstadt, Germany). CHAPS was from G-Biosciences® (St. Louis, USA), amidosulfobetaine (ASB-14) from Calbiochem® (San Diego, USA). Bromphenole blue and CBB G250 were purchased from Serva (Heidelberg, Germany). Drystrip Cover Fluid and IPGphor™ sample cups were from GE Healthcare (Freiburg, Germany), Servalyt™ 3–10 from SERVA (Freiburg, Germany). HPLC-grade ACN and DTT were from VWR international (Darmstadt, Germany). Pierce® 660 nm Protein Assay was purchased from Thermo Fisher Scientific (Rockford, USA).

2.2 Synthesis and purification of CFDA-cisplatin

CFDA-cisplatin was synthesized according to Molenaar *et al.* [24] with minor modification described by Zabel *et al.* [25]. The purification of CFDA-cisplatin was performed on a semi-preparative HPLC (System Gold, Beckmann Coulter, Krefeld, Germany) using a Nucleodur® C18 HTec column (5 μm; 250 × 10 mM).

2.3 Cell culture, harvesting and precipitation of proteins

The human ovarian carcinoma cell line A2780 and the cisplatin-resistant subline A2780 *cis* (European Collection of Cell Cultures, United Kingdom) were cultured, treated with 25 μM CFDA-cisplatin for 2 h (due to the short half-life of non-bound cisplatin 50–70 min), harvested and collected as previously described [12].

2.4 Two-dimensional gel electrophoresis (2DE)

The 2DE experiments were performed in two separation steps. For the first dimension, the Ettan™ IPGphor 3 IEF System (GE Healthcare, Sweden) was utilized, and in the second dimension (100 × 100 × 1.0 mm) SDS-PAGE the PerfectBlue™ Dual Gel System Twin S (PEQLAB Biotechnologie GmbH, Erlangen, Germany).

2.4.1 Isoelectric focusing (IEF)

Narrow pH gradient strips (pH 6–10) were used for the separation in the first dimension. 150 μg precipitated proteins were solubilized overnight in 7 M urea, 2 M thiourea, 1% CHAPS, 1% amidosulfobetaine (ASB-14), 60 mM DTT and 0.5% Servalyt™ 3–10 and applied to already rehydrated (7 M urea, 2 M thiourea, 1% CHAPS, 1% ASB-14, 75 mM

© 2018 WILEY-VCH Verlag GmbH & Co. KGaA, Weinheim

HED and 0.5% Servalyt™ 3–10) Serva IPG *Blue*Strips 6–10 (70 × 3 × 0.5 mm, SERVA, Freiburg, Germany) by cup-loading near the anode. IEF was performed with a maximum current of 50 μA and a total of 18.4 kVh using the following focusing protocol: 500 V for 2 h (step and hold), 2500 V in 1.5 h (gradient mode), 3000 V for 0.5 h (gradient mode) and 3000 V for 4.5 h (step and hold). Before reaching 3000 V of the IEF, new paper wicks were soaked in solubilization buffer containing 20 mM DTT and were placed again on the IPG strip at the cathode. Finally, all focused immobilized pH gradient (IPG) strips were stored at −20°C until equilibration and application to SDS-PAGE.

2.4.2 SDS-PAGE and generation of a reference protein spot grid

The IPG strips were subjected to reduction and alkylation using 1% DTT and 2.5% iodoacetamide in 2.5 and 10 mL equilibration solution, respectively (6 M urea, 50 mM Tris-HCl (pH 8.8), 30% glycerol and 10% SDS) per strip. Afterwards, an IPG strip was applied on the top of a self-made 12% SDS-PAGE resolving gel. A 4% stacking gel containing Bromphenol blue was polymerized above that and V-shaped well combs were used to produce a protein spot grid according to Ackermann *et al.* [26] with minor modifications [12]. Proteins were separated for 3 h, beginning at 50 V for 30 min followed by 150 V until the dye front reached the bottom of the gel.

2.5 Detection, staining and image analysis

The Typhoon™ 9400 laser scanner (GE Healthacare, Little Chaltfont, UK) or the ChemiDoc™ MP System (Bio-Rad Laboratories, Watford, UK) was used to scan the SDS-PAGEs. CFDA-cisplatin-protein adducts were detected at excitation/emission 488/532 nm and the fluorescent protein spot grid at 532/580 nm. Then, the colloidal Coomassie G-250 staining protocol according to Kang *et al.* [27] with minor modifications [28] was applied to visualize the proteins. For the image analysis, the Delta2D software (version 4.3, Decodon, Greifswald, Germany) was used as earlier described [12].

2.6 Sample preparation for mass spectrometry (MS)

The protein spots of interest were manually excised from Coomassie-stained 2DE gels. Afterwards, the completely destained gel pieces were incubated with 0.033 μg/μL sequencing grade modified trypsin (Promega, Madison, USA) in 25 mM ammonium bicarbonate (pH 8.0) for 12–16 h at 37°C. Extracted peptides were dried in a vacuum centrifuge (Eppendorf, Hamburg, Germany) and stored at −20°C until analysis by MS. Prior to electrospray ionization tandem mass spectrometry (ESI-MS/MS) analyses the peptides were desalted as previously described [12]. For the nano high-performance liquid chromatography (nano-HPLC)-ESI-MS/MS analysis, the tryptic peptides were resolved in 17 μL 5% trifluoroacetic acid (TFA) (AppliChem, Darmstadt, Germany) in water.

2.7 Protein identification by MS

The MS analysis of protein spots were performed with an ESI Qq-TOF instrument (QSTAR XL, Applied Biosystems, Darmstadt Germany) that was equipped with an offline-nanospray source (Proxeon, Odense, Denmark). The full MS scans from 350 to 1500 m/z were recorded using the Analyst QS version 1.1 (Applied Biosystems), and at least five peptides per sample were further fragmented. The protein identification was performed using the MASCOT MS/MS ions search 1.6b27 (Matrix Science, UK) using the following parameters: database, Swiss-Prot; protease, trypsin; missed cleavages, 1; variable modifications, carbamidomethyl (C) and oxidation (M); peptide tolerance, ±1.2 Da; and MS/MS tolerance, ±0.6 Da. Protein identification was considered positive when at least three peptides were assigned to the protein the protein sequence coverage achieved > 15% and the experimental molecular weight and isoelectric point is in agreement with the theoretical.

Protein spots with low protein content were analyzed on a hybrid ion trap-Orbitrap mass spectrometer (Orbitrap Elite, Thermo Scientific, Bremen, Germany), which was coupled with a nano-HPLC system (UltiMate™ 3000 HPLC system, Dionex/Thermo Scientific, Dreieich, Germany) as previously decribed [12]. The 15 most intense 2+ charged peptide ions were isolated and transferred to the linear ion trap. Protein identification was performed by using the Proteome Discoverer™ 1.4 in combination with MASCOT MS/MSions search 2.4.1 (Matrix Science) using the following settings: database, Swiss-Prot; protease, trypsin; missed cleavages, 2; static modification, carbamidomethyl (C); dynamic modification, oxidation (M); false detection rate, 1%; precursor mass tolerance, 10 ppm; and fragment mass tolerance, ± 0.4 Da. Furthermore, several protein spots with low protein content were analyzed on a Q Exactive™ Plus Hybrid Quadrupole-Orbitrap™ mass spectrometer (Thermo Scientific, Germany), which was used with the same setup (nano-HPLC, colums, solutions and protein identification).

3 Results

3.1 2DE in the alkaline pH range

2DE combines isoelectric focusing (IEF), in which the proteins are separated according to their p*I*, and SDS-PAGE, where separation is based on the molecular weight (M_r). The usage of broad pH gradients (pH 3–10) allows the visualization of most proteins in a single gel but reduces the resolution power over a particular p*I* range. Therefore, narrow pH gradients (pH 4–7, 6–10) enhance resolution and the possibility to identify more proteins. In the present study, we optimized the 2DE in the alkaline pH range (pH 6–10) for the human

© 2018 WILEY-VCH Verlag GmbH & Co. KGaA, Weinheim

ovarian carcinoma cell line A2780 and the cisplatin-resistant subline A2780*cis*.

A broad pH range 3–10 commonly shows unsatisfactory results with respect to the alkaline proteins, whereas the use of alkaline pH range (pH 6–10) reveals two main problems: extensive horizontal streaking and poor resolution. Here we could show that the optimization of the (i) sample extraction, (ii) solubilization power, (iii) the focusing protocol and (iv) the equilibration conditions within the 2DE led to enhanced resolution and visualization of the proteins in the alkaline pH range (Fig. 1). Furthermore, the optimization conditions vary depending on the biological samples.

For the 2DE analysis, the optimization of the solubilization power is an important step as well as keeping proteins in solution during IEF. The detergents CHAPS und ASB-14 are recommended for the solubilization of basic proteins. Therefore, cytosolic protein extracts from ovarian cells were resolved in an improved solubilization buffer containing these both detergents (Supporting Information Fig. S1). Instead of the in-gel rehydration after IPG strip rehydration the anodic cup-loading was used for sample loading, applying a final voltage up to 18.4 kVh.

The use of cup-loading at the anodic side ensured barely sample loss and improved the transfer of basic proteins to the IPG strips. However, the insufficiency of migration from the IPG strip into the SDS-PAGE resulted in an unsatisfactory spot pattern with poor resolution (Fig. 1A). We therefore substituted DTT as a reducing agent to HED in the rehydration buffer. HED neutralizes negatively charged protein thiol groups and prevents the reformation of disulfide bridges. For next 2DE experiment we used 75 mM HED in the rehydration buffer to remove much of the horizontal streaking found in the alkaline pH range of 2DE gels. The 2DE gels resulted in a more simplified spot pattern with slight improved

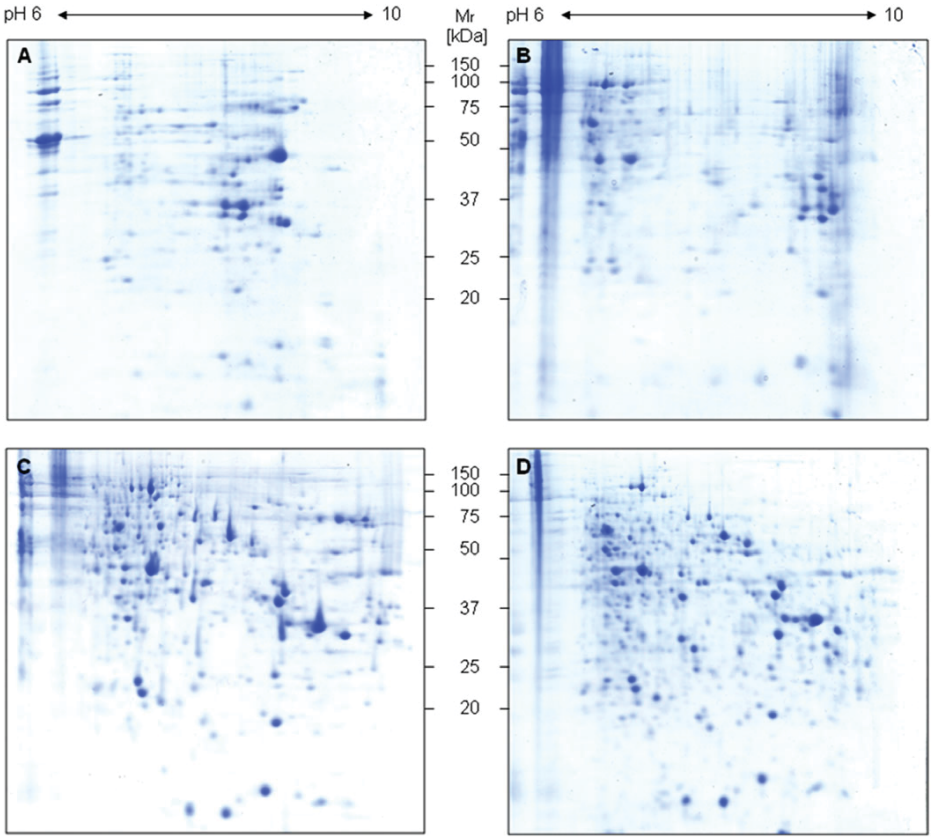

Figure 1. Optimization of 2DE with the human ovarian carcinoma A2780 cell lysate in the alkaline pH range. 150 μg cytosolic proteins were resolved in solubilization buffer, applied to a rehydrated IPG strip 6–10 (7 cm) by cup-loading and finally the focused IPG strip was used for a 12% SDS-PAGE (circa 8 × 8 cm^2). (A) The 2DE experiments were performed as described with the following exceptions: 25 mM HED in the rehydration buffer, without the DTT wick method, a final voltage up to 15.0 kVh and the IPG strips were subjected to reduction and alkylation using 1% DTT and 2.5% iodoacetamide in 2.5 mL equilibration solution. (B) The following changes were made in the next experiment 2DE: 75 mM HED in the rehydration buffer and a final voltage up to 17.0 kVh. (C) The next 2DE experiment was carried out with these changes: introduction of the DTT wick method (20 mM DTT in rehydration buffer) and a total final voltage of 18.4 kVh. (D) Finally, the additional modification of the equilibration conditions (10 mL equilibration buffer) between the IPG strip and second dimension of 2DE showed the greatest resolution and reproducibility of basic proteins of the human ovarian carcinoma cell line A2780.

© 2018 WILEY-VCH Verlag GmbH & Co. KGaA, Weinheim

resolution (Fig. 1B). DTT was used in the solubilization buffer to cleave disulfide bonds, but the reducing agent is deprotonated and negatively charged at alkaline pH. Thereby, DTT migrates towards the anode, results in depletion of DTT at the cathode and can lead to reformation of disulfide bridges due to the oxidation of sulfhydryl groups. This can result in lower solubility of the proteins within the sample, leading to horizontal streaking and poor resolution of the basic proteins in the second dimension of 2DE. To circumvent the problem of DTT migration, we applied the DTT wick method [23]. For the DTT wick method, a paper wick was soaked in solubilization buffer containing 20 mM DTT and was laid again on the IPG strips at the cathode. The effect of using the DTT wick method for protein separation in the first dimension resulted in the lowest level of horizontal streaking and good resolution (Fig. 1C). To get the best resolution of basic proteins, we optimized each step of the 2DE. Optimizing the equilibration step prevents lacking migration of basic proteins from the IPG strip during SDS-PAGE. The volume of both equilibration buffers was increased from 2.5 to 10 mL and also the SDS concentration from 2 to 10% in accordance to J. McDonough and E. Marban [29]. The combined use of CHAPS and ASB-14 in the solubilization buffer, the anodic cup-loading, HED in the rehydration buffer, the DTT wick method, a final voltage up to 18.4 kVh and the modification of the equilibration conditions led to the lowest level of horizontal and vertical streaking, the greatest resolution and reproducibility of the method in the human ovarian carcinoma cell line A2780 (Fig. 1D). This method allowed us to identify CFDA-cisplatin protein adducts up to a theoretical p*I* value of 9.10 (Table 1).

3.2 Evaluation and identification of CFDA-cisplatin-protein adducts

In our previous study, a 2DE and mass spectrometry based analytical method to detect and identify intracellular CFDA-cisplatin-containing proteins was established using fluorescent CFDA-cisplatin. Here, the use of the fluorescent CFDA-cisplatin was also helpful in the visualization of CFDA-cisplatin-protein adducts in the alkaline pH range (pH 6–10) (Fig. 2A), because the fluorescent CFDA-cisplatin binds specifically and reproducibly to certain proteins [12]. The simultaneous use of a protein marker grid permitted the precise detection of intracellular CFDA-cisplatin-containing proteins. Thus, the cytosolic proteins were separated according to p*I* and M_r, while the fluorescence-labeled protein marker solution was separated in the second dimension according to molecular weight solely. The use of two different fluorescent dyes ensured the differentiation between CFDA-cisplatin-protein adducts and the protein spot grid (Fig. 2A and B). For the image analysis, the fluorescence scans (Fig. 2A) from CFDA-cisplatin-protein adducts and the protein marker grid (Fig. 2B) were fused into one image, which was then merged with the Coomassie staining image (Fig. 2C) to create a master image (Fig. 2D).

In the pH range 6–10, it was possible to detect on average a total of 417 protein spots. The most intense fluorescence signals were detected in the range between 35 and 55 kDa, and the subsequent image analysis by Delta 2D software revealed that thirteen spots were detected as CFDA-cisplatin-protein adducts (Fig. 2E).

Table 1. Identified CFDA-cisplatin-containing proteins (*) and proteins from 2DE gels

Sample and spot number	Protein identification	Accession number	Mr (kDa) experimental/ theoretical	p*I* experimental/ theoretical	Sequence count	Sequence coverage (%)
1*	Elongation factor 1-alpha 1 (EF1A1)	P68104	45.00/50.14	9.20/9.10	8	16.90^{+}
2*	EF1A1	P68104	45.00/50.14	9.15/9.10	8	18.60^{+}
3*	EF1A1	P68104	45.00/50.14	9.10/9.10	6	15.60^{+}
4*	Serpin H1	P50454	44.00/46.44	9.00/8.69	6	17.50^{+}
5	Pyruvate kinase (PKM)	P14618	55.00/57.90	7.70/7.84	9	28.80^{+}
6*	PKM	P14618	55.00/57.90	7.60/7.84	26	73.63$^{\#}$
7	Alpha-enolase (ENOA)	P06733	44.00/47.17	7.00/7.01	12	39.90^{+}
8*	ENOA	P06733	44.00/47.17	6.90/7.01	11	35.30^{+}
9	ENOA	P06733	44.00/47.17	6.80/7.01	9	31.30^{+}
10*	D-3-phosphoglycerate- dehydrogenase (PHGDH)	O43175	51.00/56.65	6.80/6.71	16	44.80$^{\#}$
11*	PHGDH	O43175	51.00/56.65	6.70/6.71	11	14.30^{+}
12*	PHGDH	O43175	51.00/56.65	6.60/6.71	21	59.70$^{\#}$
13*	Heterogenous nuclear ribonucleoprotein A/B	Q99729	41.00/36.20	6.70/8.21	11	39.20$^{\#}$
14*	Heterogenous nuclear ribonucleoprotein H3	P31942	37.00/36.90	6.70/6.87	16	90.50$^{\#}$
15*	Heterogenous nuclear ribonucleoprotein H3	P31942	37.00/36.90	6.70/6.87	14	62.70$^{\#}$
16*	Glyceraldehyd-3-phosphate dehyrogenase (GAPDH)	P04406	37.00/36.05	8.40/8.57	3	30.10^{+}
17	GAPDH	P04406	37.00/36.05	8.50/8.57	5	25.40^{+}
18	GAPDH	P04406	37.00/36.05	8.75/8.57	5	28.10^{+}

Proteins were identified by ESI-MS/MS (+) or nano-HPLC-ESI-MS/MS (#) after 2DE. Each protein spot was identified from three biological samples of three separate gels. Numbers refer to the spots in Fig. 2E and were picked from 2DE Coomassie stained gels.

© 2018 WILEY-VCH Verlag GmbH & Co. KGaA, Weinheim

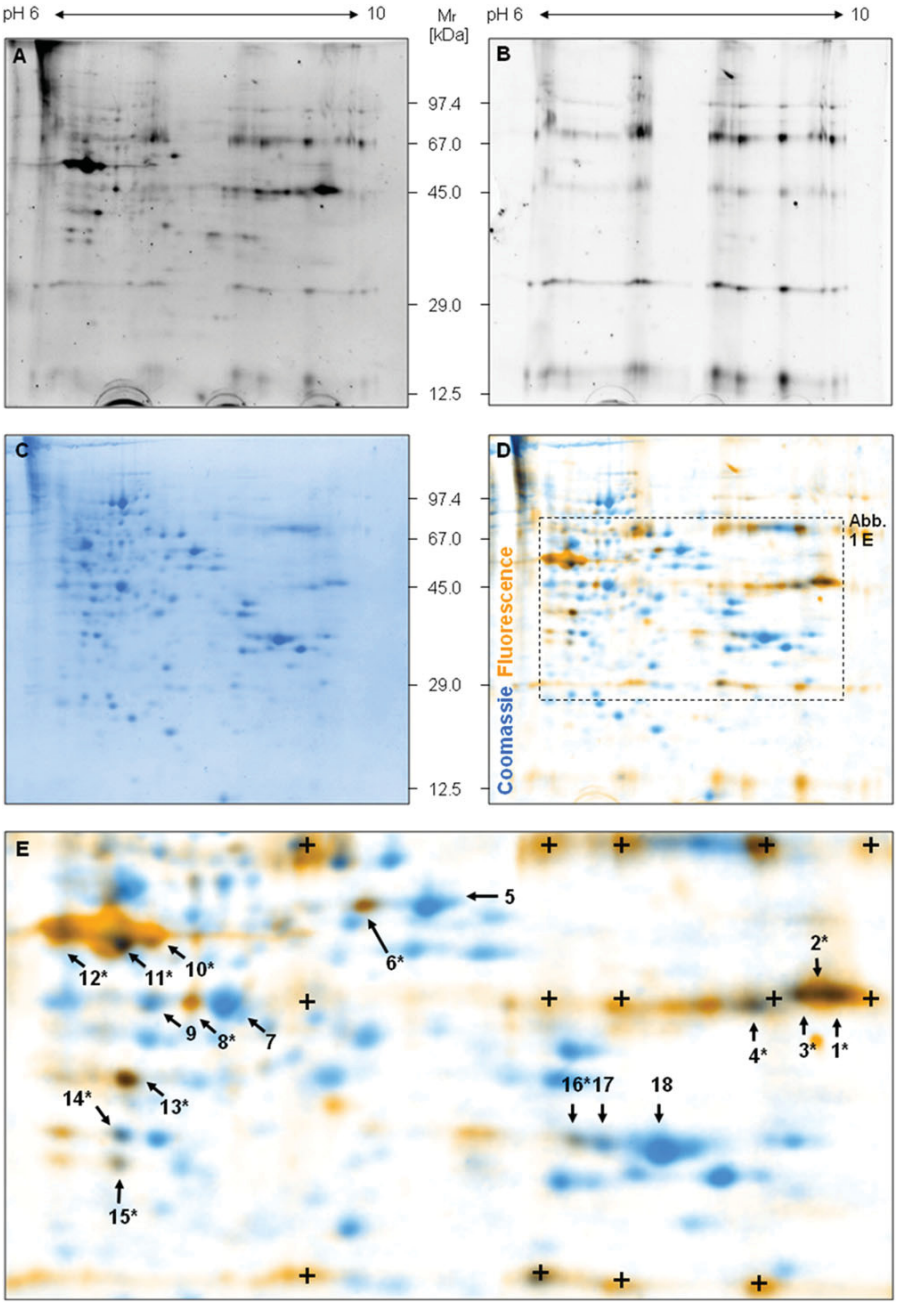

Figure 2. Precise visualization of CFDA-cisplatin-protein adducts through 2DE after using a protein spot grid. A2780 *cis* cells were treated with 25 μM CFDA-cisplatin for 2 h and separated by 2DE according to the optimized steps described in Figure 1 (A). A generation of a protein spot grid (B) allowed the separation parallel with 150 μg cytosolic proteins through 2DE. After the 2DE, a fluorescence scan was recorded (CFDA-cisplatin: ex/em: 488 nm/532 nm (A); SERVA Lightning Red for 1D SDS-PAGE: ex/em: 532 nm/580 nm (B)) and the proteins were visualized with Coomassie staining (C). For the image analysis, the fluorescence scans from CFDA-cisplatin-protein adducts (A) as well as from protein marker grid (B) and the Coomassie staining image (C) were fused to a master image (D). CFDA-cisplatin-protein adducts were detected as black spots (E). The reference protein spot grid (+) improves the assignment of the CFDA-cisplatin-protein adducts in the image analysis (A - D); (E): 1*, 2* and 3* = EF1A1; 4* = serpin H1, 5 and 6* = PKM; 7, 8* and 9 = ENOA, 10*, 11* and 12* = PHGDH; 13* = heterogeneous nuclear ribonucleoprotein A/B; 14*, 15* = heterogeneous nuclear ribonucleoprotein H3; 16*, 17 and 18 = GAPDH.

One strength of 2DE is the possibility to detect protein modifications. Several posttranslational modifications including binding of cisplatin may lead to an altered migration behavior of proteins, because small charge changes induce horizontal p*I* shifting of a protein spot in 2DE gels. For the identification, possible p*I* or molecular weight shifts of CFDA-cisplatin-protein adducts nearby protein spots of interest were additionally excised from the 2DE Coomassie-stained gels and analyzed by mass spectrometry (see Table 1). Each protein spot was identified from three biological samples of three separate gels.

In the pH range 6–10 a total of eight CFDA-cisplatin-containing proteins were identified in both cell lines (Table 1) and they exhibited an altered migration behavior compared to the unmodified proteins. The identified CFDA-cisplatin-containing proteins pyruvate kinase (PKM), alpha-enolase (ENOA), heterogeneous nuclear ribonucleoprotein A/B (hnRNP A/B) and glyceraldehyde-3-phosphate dehydrogenase

© 2018 WILEY-VCH Verlag GmbH & Co. KGaA, Weinheim

(GAPDH) (Fig. 2E, spot 6*, 8* and 14*, 16*) shifted slightly in their p*I* value compared to unmodified proteins (Fig. 2E, spot 5, 7, 8, 17 and 18). Moreover, the CFDA-cisplatin-containing proteins PKM and GAPDH showed a lower p*I* compared to the unmodified protein spot and the p*I* of the CFDA-cisplatin-containing protein spot ENOA (Fig. 2E, spot 8*) was between two other identified ENOA protein spots (Fig. 2E; spot 7, 9). Other CFDA-cisplatin-containing proteins were identified as: elongation factor 1-alpha 1 (EF1A1), serpin H1, hnRNP H3 and D-3-phosphoglycerate 1-dehydrogenase (PHGDH) (Fig. 2E, spot 1* - 4*, 10* - 13*). Interestingly, the CFDA-cisplatin modified EF1A1 and PHGDH were each identified in three protein spots, which differ only in p*I*.

4 Discussion

4.1 Optimization of 2DE conditions in the alkaline range

CFDA-cisplatin, 2DE and mass spectrometry are components of an analytical method to detect and identify intracellular cisplatin-protein adducts. In order to complement our previous data [12] the 2DE was optimized for the analysis of proteins in the alkaline pH range (6–10). 2DE is a superior tool for the separation of complex protein mixtures and was developed over years to get more reproducibility by improvements like IPG strips [30] and the alternative reducing agent HED [22]. Despite these improvements, optimization and standardization of IEF conditions is still a challenge for alkaline proteins due to aggregation, oxidation and precipitation. Former studies have shown that in urea/thiourea based solubilization buffer the combination with the detergents CHAPS and ASB-14 is recommended for alkaline proteins [16, 21]. Further, an incorrect sample application leads to protein instability during the IEF. The use of cup-loading for the alkaline pH range (pH 6–10) improved the transfer of alkaline proteins to the IPG strips. But there are two conceivable causes for the absence of proteins within 2DE gels: (i) the proteins are not focused, as a result of poor denaturation or solubilization, or (ii) the lack of migration from the IPG strip to the SDS-PAGE, due to aggregation, precipitation or associations with the polyacrylamide gel matrix. The migration of the reducing agent DTT towards the anode during IEF results in the loss of DTT at the cathode, promotes reformation of disulfide bonds and leads to blurred and streaky spot pattern in 2DE gels. The effects of using the alternative reducing agent HED in the IPG strip and a DTT wick as supplement at the cathode [23] on protein separation in the first dimension showed the most improvement in the separation of basic proteins. Very basic and hydrophobic proteins remain a challenge within 2DE, while basic proteins are only visible as dense streaks and hydrophobic proteins are almost absent. For very basic proteins the current strategy is to apply high voltages (8000–10000 V) in order to keep the focusing time down [17,31,32], because particularly in the alkaline pH range labile proteins can degrade at their p*I*. However, 3000 V and a final voltage up to 18.4 kVh resulted in the best resolution of very alkaline proteins in 2DE gels. Furthermore, it was shown that hydrophobic proteins often remain in the IPG strips during the SDS-PAGE [29]. The most plausible reason for the lack of migration from the IPG strip to the SDS-PAGE is that the proteins in the IPG strip were not sufficiently soluble. Therefore, incubation volumes of the equilibration buffer were increased to 10 mL and the SDS concentration to 10%, which clearly improved migration and separation of basic proteins. In summary, the optimization of each step of the 2DE method is important.

4.2 Binding of CFDA-cisplatin

The presented analytical method implies protein denaturation prior to 2DE and can nevertheless be used for the detection of intracellular CFDA-cisplatin-binding proteins [12, 14, 15]. 2DE can detect pseudo-covalent CFDA-cisplatin-protein adducts, but non-covalent platinum-protein interactions are lost. The use of fluorescent CFDA-cisplatin allows the visualization of intracellular CFDA-cisplatin-binding proteins by 2DE and the fluorescence signals in the protein spot are indeed related to CFDA-cisplatin, as has been shown previously [12].

Cisplatin reacts preferentially with the sulfur-containing amino acids cysteine and methionine, which are present on the surface of proteins. Therefore, the cysteine- and methionine-rich proteins PHGDH, PKM, ENOA and EF1A1 are able to form complex bonds with CFDA-cisplatin in the cytosol. The proteins annexin, GAPDH, serpin H1, hnRNP A/B and hnRNP H3 contain few cysteines, but more methionines and are also capable to form complex bonds with CFDA-cisplatin. Moreover, aspartic acid, glutamic acid, histidine, serine, threonine and tyrosine were also determined as potential binding sites for cisplatin [15, 33]. It is proven that the binding of CFDA-cisplatin to an amino acid causes a small change in the net charge of the protein, which leads to altered migration behavior of the CFDA-cisplatin-binding protein in the 2DE gels [12]. In addition, the binding of CFDA-cisplatin can impair the function of the CFDA-cisplatin-binding protein. Thus, cisplatin binding to a protein may limit the reactive cisplatin as well as the reactivity of the protein species in tumor cells and might have as well a negative influence on the cell viability through the impairment of protein functions.

4.3 CFDA-cisplatin-binding proteins

An important aspect of cancer is the altered metabolism in tumorigenesis. Rapidly proliferating cancer cells, even in the presence of normal oxygen tension, prefer fermentative glycolysis-based glucose metabolism instead of mitochondrial aspiration (Warburg effect) [11, 34]. The glycolytic shift in cancer cells shows an overexpression of genes of glucose metabolism compensates a mitochondrial dysfunction and may lead to resistance to apoptosis [11, 35]. Several of

© 2018 WILEY-VCH Verlag GmbH & Co. KGaA, Weinheim

the identified CFDA-cisplatin-binding proteins are known to be involved in glucose metabolism, such as GAPDH, ENOA and PKM. ENOA is present on the surface of cells and plays a key role in various processes such as glycolysis, growth control and hypoxia tolerance [36, 37]. It catalyzes the conversion of 2-phosphoglycerate to phosphoenolpyruvate, the second of the two high energy intermediates that produce ATP in the glycolytic pathway [38]. In ovarian cancer cells, ENOA is upregulated at the mRNA and protein level [35]. The increased abundance of ENOA can influence the chemotherapy, as shown in estrogen receptor-positive breast tumors, where ENOA induces tamoxifen resistance [39]. Clinical studies suggest ENOA as an attractive therapeutic target for cancer immunotherapy [40].

A further identified CFDA-cisplatin-binding protein is the PHGDH, which acts as key enzyme of the *de novo* serine biosynthesis. PHGDH, phosphoserine aminotransferase and phosphoserine phosphatase convert the glycolytic intermediate 3-phosphoglycerate into L-serine in a three-step reaction [41]. L-serine is an essential amino acid in the protein synthesis and the synthesis of sphingolipids and phospholipids, that are important components of cellular membranes [42, 43]. In addition, L-serine can be converted into glycine by serine hydroxymethyltransferase, which results in the *de novo* synthesis of nucleotide acid bases [39]. In breast cancer and melanoma cell lines a PHGDH knockdown led to a degradation of serine synthesis and impairment of cell proliferation [44–46]. Further, a PHGDH knockdown in HeLa cells showed a significant inhibition of cell proliferation and increased sensitivity to cisplatin [47]. PHGDH may be a new target promising for anticancer therapy, as the higher level of PHGDH in cancer cells compared to healthy cells could open up a therapeutic window [34, 48].

Another identified protein was EF1A1, a 50 KDa GTPase that catalyzes the binding of aminoacyl tRNAs to the ribosome during protein translation [49, 50]. Previous studies have demonstrated that EF1A1 have essential regulatory roles in cell growth, apoptosis and tumorigenesis [50–55]. EF1A1 was identified as an interacting protein of the transcription factors p53 and p73, which play important role in tumorigenesis including apoptosis [56]. Overexpression of EF1A1 inhibits p53-, p73- and chemotherapy-induced apoptosis, which leads to chemoresistance [56]. Within the p53-family signaling, EF1A1 has anti-apoptotic properties and could be a potential target for cancer chemotherapy [56].

The other identified binding partners are currently not discussed with chemoresistance and the relevance for cisplatin resistance will be addressed in further studies as has been done for GRP78 and PDIA [57].

4.4 Concluding remarks

We complemented our previous data on intracellular binding partners of CFDA-cisplatin in ovarian cancer cells with an established analytical method using CFDA-cisplatin, 2DE and mass spectrometry. The 2DE was performed for proteins in the alkaline pH range (pH 6–10) and it was important to optimize each step, so that the CFDA-cisplatin-binding protein EF1A1 could be identified as most basic protein with a theoretical p*I* of 9.10. The identification of eight previously unknown intracellular binding partners of CFDA-cisplatin provides new insights into the cellular processing of cisplatin and might contribute to the understanding of mechanism of action and among them the reaction mechanism. The identified proteins ENOA, PHGDH and EF1A1 may be potential targets for anticancer therapy of ovarian carcinoma. This approach provides new insights into the cellular processing of cisplatin, which may help to understand the resistance mechanism of this drug.

S. K. thanks A. Stefanski for performing the Orbitrap MS analysis. This project was funded by the Deutsche Forschungsgemeinschaft (ME 1799/2-1) and supported by the Cluster of Excellence on Plant Science, CEPLAS (EXC1028).

The authors have declared no conflict of interest.

5 References

[1] Siegel, R. L., Miller, K. D., Jemal, A., *CA Cancer J. Clin.* 2016, *66*, 7–30.

[2] Koberle, B., Tomicic, M. T., Usanova, S., Kaina, B., *Biochim. Biophys. Acta* 2010, *1806*, 172–182.

[3] Galanski, M., *Recent Pat. Anticancer Drug Discov.* 2006, *1*, 285–295.

[4] Lebwohl, D., Canetta, R., *Eur. J. Cancer* 1998, *34*, 1522–1534.

[5] Prestayko, A. W., D'Aoust, J. C., Issell, B. F., Crooke, S. T., *Cancer Treat Rev.* 1979, *6*, 17–39.

[6] Kartalou, M., Essigmann, J. M., *Mutat. Res.* 2001, *478*, 23–43.

[7] Siddik, Z. H., *Oncogene* 2003, *22*, 7265–7279.

[8] Jamieson, E. R., Lippard, S. J., *Chem. Rev.* 1999, *99*, 2467–2498.

[9] Cepeda, V., Fuertes, M. A., Castilla, J., Alonso, C., Quevedo, C., Pérez, J. M., *Anticancer Agents Med. Chem.* 2007, *7*, 3–18.

[10] Kasherman, Y., Sturup, S., Gibson, D., *J. Med. Chem.* 2009, *52*, 4319–4328.

[11] Maccio, A., Madeddu, C., *Expert Opin. Pharmacother.* 2013, *14*, 1839–1857.

[12] Kotz, S., Kullmann, M., Crone, B., Kalayda, G. V., Jaehde, U., Metzger, S., *Electrophoresis* 2015, *21–22*, 2811–2819.

[13] Kalayda, G. V., Wagner, C. H., Buss, I., Reedijk, J., Jaehde, U., *BMC Cancer* 2008, *8*, Article ID 175.

[14] Mena, M. L., Moreno-Gordaliza, E., Moraleja, I., Benito Cañas, B., Gómez-Gómez, M. M., *J. Chromatogr. A* 2011, *1218*, 1281–1290.

[15] Moreno-Gordaliza, E., Cañas, B., Palacios, M. A., Gómez-Gómez, M. M., *Analyst* 2010, *135*, 1288–1298.

© 2018 WILEY-VCH Verlag GmbH & Co. KGaA, Weinheim

[16] Chevallet, M., Santoni, V., Poinas, A., Rouquié, D., Fuchs, A., Kieffer, S., Rossignol, M., Lunardi, J., Garin, J., Rabilloud, T., *Electrophoresis* 1998, *19*, 1901–1909.

[17] Drews, O., Reil, G., Parlar, H., Görg, A., *Proteomics* 2004, *4*, 1293–1304.

[18] Görg, A., Obermaier, C., Boguth, G., Harder, A., Scheibe, B., Wildgruber, R., Weiss, W., *Electrophoresis* 2000, *21*, 1037–1053.

[19] Kask, L., Larsson, K., Bjellqvist, B., *Proteomics* 2009, *9*, 5558–5561.

[20] Luche, S., Diemer, H., Tastet, C., Chevallet, M., Van Dorsselaer, A., Leize-Wagner, E., Rabilloud, T., *Proteomics* 2004, *4*, 551–561.

[21] Martins-de-Souza, D., Menezes de Oliveira, B., dos Santos Farias, A., Horiuchi, R. S., Crepaldi Domingues, C., de Paula, E., Marangoni, S., Gattaz, W. F., Dias-Neto, E., Camillo Novello, J., *Brief Funct. Genomic Proteomic* 2007, *6*, 70–75.

[22] Olsson, I., Larsson, K., Palmgren, R., Bjellqvist, B., *Proteomics* 2002, *2*, 1630–1632.

[23] Pennington, K., McGregor, E., Beasley, C. L., Everall, I., Cotter, D., Dunn, M. J., *Proteomics* 2004, *4*, 27–30.

[24] Molenaar, C., Teuben, J. M., Heetebrij, R. J., Tanke, H. J., Reedijk, J., *J. Biol. Inorg. Chem.* 2000, *5*, 655–665.

[25] Zabel, R., Kullmann, M., Kalayda, G. V., Jaehde, U., Weber, G., *Electrophoresis* 2015, *36*, 509–517.

[26] Ackermann, D., Wang, W., Streipert, B., Geib, B., Grün, L., König, S., *Electrophoresis* 2012, *33*, 1406–1410.

[27] Kang, D., Gho, Y. S., Suh, M., Kang, C., *Bull. Korean Chem. Soc.* 2002, *11*, 1511–1512.

[28] Dyballa, N., Metzger, S., *J. Vis. Exp.* 2009.

[29] McDonough, J., Marban, E., *Proteomics* 2005, *5*, 2892–2895.

[30] Görg, A., Postel, W., Gunther, S., *Electrophoresis* 1988, *9*, 531–546.

[31] Görg, A., Drews, O., Lück, C., Weiland, F., Weiss, W., *Electrophoresis* 2009, *30*, S122-32.

[32] Wildgruber, R., Reil, G., Drews, O., Parlar, H., Görg, A., *Proteomics* 2002, *2*, 727–732.

[33] Will, J., Sheldrick, W. S., Wolters, D., *J. Biol. Inorg. Chem.* 2008, *13*, 421–434.

[34] Zogg, C. K., *J. Oncol.* 2014, Article ID 524101.

[35] Altenberg, B., Greulich, K. O., *Genomics* 2004, *84*, 1014–1020.

[36] Diaz-Ramos, A., Roig-Borrellas, A., Garcı´a-Melero, A., López-Alemany, R., *J. Biomed. Biotechnol.* 2012, Article ID 156795.

[37] Subramanian, A., Miller, D. M., *J. Biol. Chem.* 2000, *275*, 5958–5965.

[38] Pancholi, V., *Cell Mol. Life Sci.* 2001, *58*, 902–920.

[39] Tu, S. H., Chang, C. C., Chen, C. S., Tam, K. W., Wang, Y. J., Lee, C. H., Lin, H. W., Cheng, T. C., Huang, C. S., Chu, J. S., Shih, N. Y., Chen, L. C., Leu, S. J., Ho, Y. S., Wu, C. H., *Breast Cancer Res. Treat.* 2010, *121*, 539–553.

[40] Capello, M., Ferri-Borgogno, S., Cappello, P., Novelli, F., *FEBS J.* 2011, *278*, 1064–1074.

[41] Snell, K., *Adv. Enzyme Regul.* 1984, *22*, 325–400.

[42] Futerman, A. H., Riezman, H., *Trends Cell Biol.* 2005, *15*, 312–318.

[43] Kuge, O., Nishijima, M., *J. Biochem.* 2003, *133*, 397–403.

[44] Chen, J., Chung, F., Yang, G., Pu, M., Gao, H., Jiang, W., Yin, H., Capka, V., Kasibhatla, S., Laffitte, B., Jaeger, S., Pagliarini, R., Chen, Y., Zhou, P., *Oncotarget* 2013, *4*, 2502–2511.

[45] Locasale, J. W., Grassian, A. R., Melman, T., Lyssiotis, C. A., Mattaini, K. R., Bass, A. J., Heffron, G., Metallo, C. M., Muranen, T., Sharfi, H., Sasaki, A. T., Anastasiou, D., Mullarky, E., Vokes, N. I., Sasaki, M., Beroukhim, R., Stephanopoulos, G., Ligon, A. H., Meyerson, M., Richardson, A. L., Chin, L., Wagner, G., Asara, J. M., Brugge, J. S., Cantley, L. C., *Nat. Genet.* 2011, *43*, 869–874.

[46] Possemato, R., Marks, K. M., Shaul, Y. D., Pacold, M. E., Kim, D., Birsoy, K., Sethumadhavan, S., Woo, H. K., Jang, H. G., Jha, A. K., Chen, W. W., Barrett, F. G., Stransky, N., Tsun, Z. Y., Cowley, G. S., Barretina, J., Kalaany, N. Y., Hsu, P. P., Ottina, K., Chan, A. M., Yuan, B., Garraway, L. A., Root, D. E., Mino-Kenudson, M., Brachtel, E. F., Driggers, E. M., Sabatini, D. M., *Nature* 2011, *476*, 346–350.

[47] Jing, Z., Heng, W., Xia, L., Ning, W., Yafei, Q., Yao, Z., Shulan, Z., *Cancer Biol. Ther.* 2015, *16*, 541–548.

[48] Hamanaka, R. B., Chandel, N. S., *J. Exp. Med.* 2012, *209*, 211–215.

[49] Hershey, J. W., *Annu. Rev. Biochem.* 1991, *60*, 717–755.

[50] Thornton, S., Anand, N., Purcell, D., Lee, J., *J. Mol. Med.* 2003, *81*, 536–548.

[51] Al-Maghrebi, M., Anim, J. T., Olalu, A. A., *Anticancer Res.* 2005, *25*, 2573–2577.

[52] Gross, S. R., Kinzy, T. G., *Nat. Struct. Mol. Biol.* 2005. *12*, 772–778.

[53] Kato, M. V., Sato, H., Nagayoshi, M., Ikawa, Y., *Blood* 1997, *90*, 1373–1378.

[54] Lamberti, A., Caraglia, M., Longo, O., Marra, M., Abbruzzese, A., Arcari, P., *Amino Acids* 2004, *26*, 443–448.

[55] Tatsuka, M., Mitsui, H., Wada, M., Nagata, A., Nojima, H., Okayama, H., *Nature* 1992, *359*, 333–336.

[56] Blanch, A., Robinson, F., Watson, I. R., Cheng, L. S., Irwin, M. S., *PLoS One* 2013, *8*, e66436.

[57] Kullmann, M., Kotz, S., Hellwig, M., Kalayda, G. V., Metzger, S., Jaehde, U., *Int. J. Clin. Pharmacol. Ther.* 2015, *53*, 1038–1040.

© 2018 WILEY-VCH Verlag GmbH & Co. KGaA, Weinheim

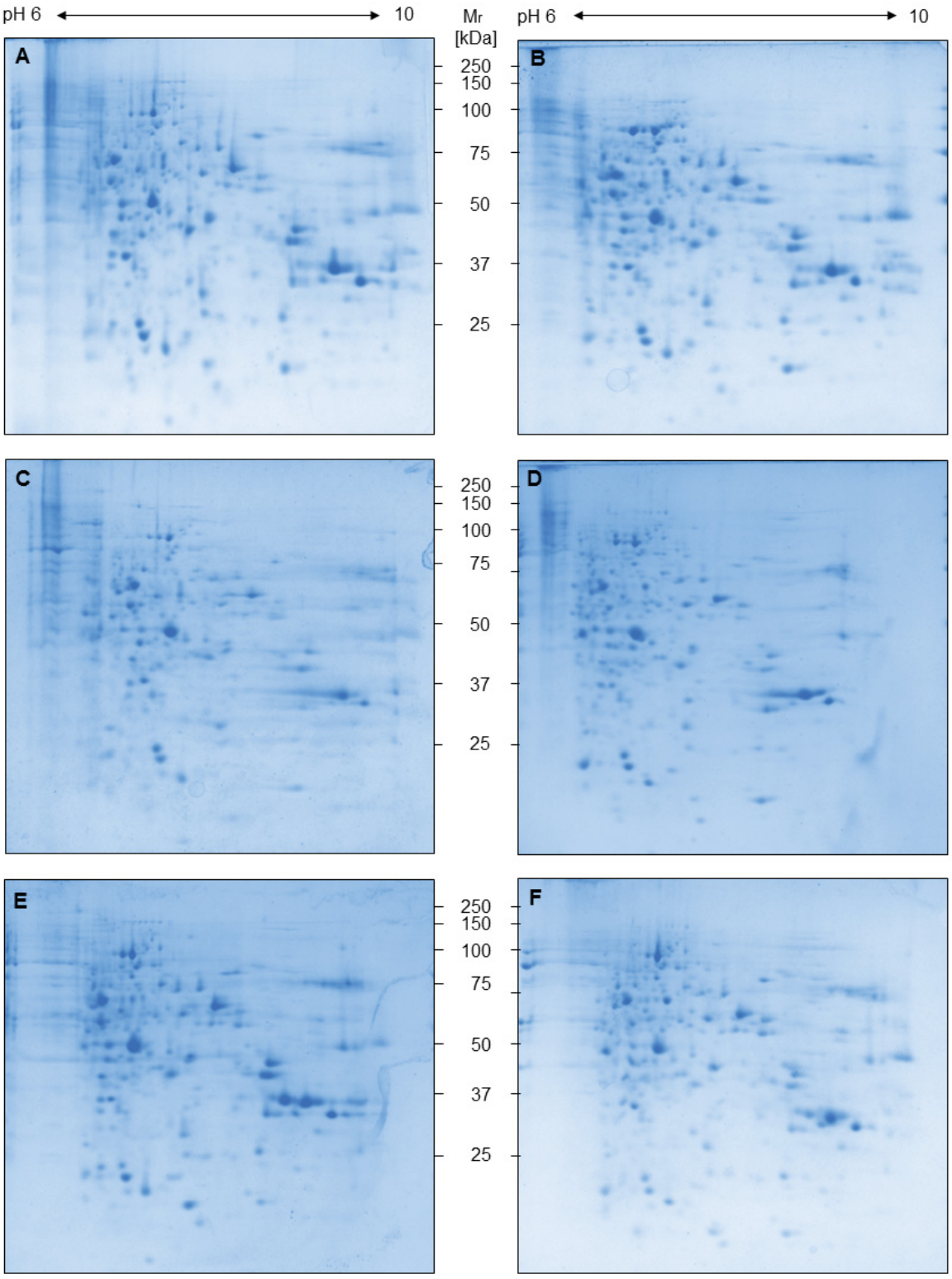
pH 6
10
Mr
[kDa]
A
B
C
D
E
F
250
150
100
75
50
37
25

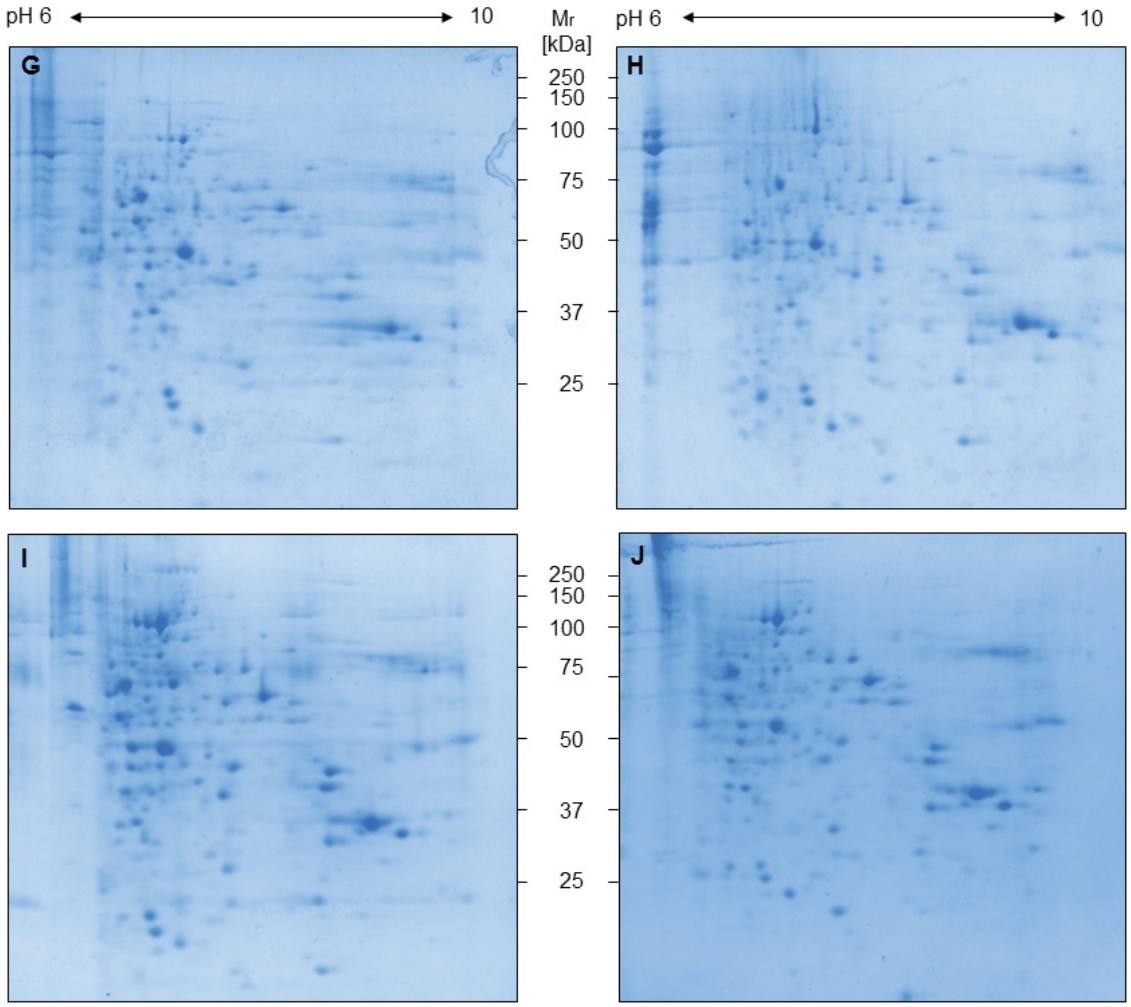

Figure S1: Stability and reproducibility of the optimization of 2DE in the alkaline pH range. 150 µg cytosolic proteins were resolved in solubilization buffer, applied to a rehydrated IPG strip 6-10 (7 cm) by cup-loading and finally the focused IPG strip was used for a 12% SDS-PAGE (circa 8 × 8 cm²).The figure shows 10 replicates containing the human ovarian carcinoma cell line A2780 (A, B, C, E, G and I) and the cisplatin-resistant subline A2780*cis* (D, F, H and J), which have been treated with 25 !M CFDA-cisplatin (A – H) and additionally two controls (I – J).

3 DISKUSSION

Die relative 5-Jahres-Überlebensrate beim Ovarialkarzinom liegt derzeit bei 41,2% [1]. Aufgrund der hohen Sterblichkeitsrate besteht die dringende Notwendigkeit, die pharmakologischen Therapien beim Ovarialkarzinom zu verbessern. Neue Einblicke in die zelluläre Prozessierung von Cisplatin sowie erworbene Resistenzmechanismen gegenüber Cisplatin können potentielle Angriffsziele für pharmakologische Therapien liefern. Daher wurde für die Identifizierung intrazellulärer Cisplatin-Proteinaddukte die humane OC-zelllinie A2780 (malignes endometrioides Karzinom) und deren cisplatinresistente Tochterzelllinie A2780*cis* verwendet.

Die Anwendung der Massenspektrometrie hat einen Fortschritt in der qualitativen und quantitativen Analyse von Biomolekülen wie z.B. Proteinen und Peptiden bewirkt. Grundsätzlich ist das methodische Vorgehen in jedem analytischen Experiment ein entscheidender Schritt. Zudem sollte unter Berücksichtigung der Komplexität der biologischen Probe die richtige Methodik für die Probenvorbehandlung sowie für die MS-basierte Strategie ausgewählt werden.

Bisher wurden Massenspektrometrie-basierte Analysen hinsichtlich der Identifizierung von Pt-Proteinbindungen lediglich mit Standardproteinen entwickelt [84-88]. Daher wurde für die vorliegende qualitative Analyse von Cisplatin-Proteinaddukten aus einer komplexen biologischen Probe die fluoreszierende Modellsubstanz CFDA-Cisplatin verwendet [98, 103].

Erstmalig konnten intrazelluläre cisplatinhaltige Proteine nach Behandlung einer cisplatinsensitiven A2780 und -resistenten A2780*cis* OC-zelllinie mit CFDA-Cisplatin und anschließender Auftrennung der isolierten Proteine mittels 2D-Gelelektrophorese mit MS identifiziert werden. Die Verwendung der 2D-Gelelektrophorese innerhalb der analytischen Methode impliziert die Detektion kovalenter CFDA-Cisplatin-Proteinaddukte. Für deren Identifizierung erfolgte die 2D-Gelelektrophorese getrennt für zwei verschiedene pH-Bereiche 4 - 7 und 6 - 10. Zudem war die Optimierung einzelner Schritte der 2D-Gelelektrophorese notwendig, insbesondere für die Detektion und Identifizierung von Proteinen im alkalischen pH-Wert.

Die Analyse zeigte trotz Optimierung und Reproduzierbarkeit der 2D-Gelelektrophorese nicht alle potentiellen Pt-Proteinbindungen sowie keine

unterschiedliche cisplatinhaltige Proteine zwischen der cisplatinsensitiven A2780 und -resistenten A2780*cis* OC-zelllinie. Insgesamt konnten 14 zytosolische CFDA-cisplatinhaltige Proteine identifiziert werden.

3.1 NACHWEIS VON INTRAZELLULÄREN CFDA-CISPLATIN-PROTEINADDUKTEN

Die 2D-Gelelektrophorese im pH-Bereich 4 - 7 und 6 - 10 konnte erfolgreich zur Analyse von CFDA-Cisplatin-Proteinaddukten in der cisplatinsensitiven A2780 und -resistenten A2780*cis* Tumorzelllinie eingesetzt werden. „Da die Verteilung der detektierten Fluoreszenzsignale auf Basis der Gesamtanzahl der Proteinspots nicht ausreichend war, insbesondere im Bereich des niedrigen Molekulargewichtes, stellte sich in der Bildanalyse eine präzise Detektion der CFDA-Cisplatin-Proteinaddukte als schwierig heraus. Um eine präzise Detektion der CFDA-Cisplatin-Proteinaddukte zu gewährleisten, wurde erfolgreich das Proteinmarkergitter nach Ackermann et *al*. eingeführt. Ackermann et *al*. erachtet die Gelgröße (ca. 25 x 19 cm) und die Laufzeit für die Bildung eines Proteinmarkergitters in der zweiten Dimension der 2D-Gelelektrophorese für wichtig [104]. Für die Analyse von CFDA-Cisplatin-Proteinaddukten wurden in der zweiten Dimension jedoch vertikale Minigele (ca. 8 x 8 cm) eingesetzt und die Ergebnisse zeigten, dass die Verwendung dieses populären Formats völlig ausreichend war, um ein Proteinmarkergitter zu bilden. Das eingeführte Proteinmarkergitter ermöglichte eine genaue Detektion von intrazellulären CFDA-cisplatinhaltigen Proteinen [99]. Die Bildanalyse zeigte aber auch, dass mehrere Fluoreszenzsignale keine entsprechenden Proteinspots aufwiesen. Ein Grund dafür könnte sein, dass die angewandte Coomassie-Färbung nicht empfindlich genug war, um gering abundante Proteine zu färben.“ [1] Eine MS-kompatible Silberfärbung, die eine verbesserte Nachweissensitivität besitzt, könnte hier vermutlich die gering abundante Proteine anfärben.

“Während der Analysemethode zur Detektierung und Identifizierung intrazellulärer Bindungspartner von Cisplatin erfolgte eine Denaturierung (Harnstoff, Thioharnstoff), Reduzierung (Dithiothreitol (DTT)), Alkylierung (Iodacetamid) und ein tryptischer Verdau der Proben [87]. Mena et *al*. konnten zeigen, dass eine

[1] Kotz 2015, S. 8

Gelelektrophorese, Färbung sowie Entfärbung von Proteinen keinen negativen Einfluss auf die Bindung von Cisplatin an Proteine hat [84]. Für den Nachweis, dass CFDA-Cisplatin an Proteine gebunden bleibt, erfolgte eine Verifizierung von Platin in 2D-Gelen mittels LA-ICP-MS (*laser ablation - inductively coupled plasma - mass spectrometry*) [99]. Die LA-ICP-MS bestätigte das Vorkommen von Platin in mehreren Proteinspots, die eindeutig mit den Fluoreszenzsignalen korrelierten. Dies ist als weiterer Hinweis zu werten, dass CFDA-Cisplatin spezifisch an Proteine bindet."[2]

3.2 OPTIMIERUNG DER 2D-GELELEKTROPHORESE IM PH-BEREICH 6-10

„Das fluoreszierende CFDA-Cisplatin, die 2D-Gelelektrophorese und die Massenspektrometrie waren Bestandteile einer analytischen Methode zur Detektion und Identifizierung von intrazellulären Cisplatin-Proteinaddukten im sauren pH-Bereich (pH 4 - 7). Basierend auf dieser analytischen Methode wurde die Identifizierung von intrazellulären Cisplatin-Proteinaddukten auf den alkalischen pH-Bereich (pH 6 - 10) erweitert. Die 2D-Gelelektrophorese ist ein überlegenes Werkzeug zur Trennung komplexer Proteinmischungen. Zahlreiche Verbesserungen wie z. B. immobilisierte pH-Gradienten (IPG-Streifen) [105] und das alternative Reduktionsmittel Hydroxyethyldisulfid (HED) [106] führten in den letzten Jahren zu einer höheren Reproduzierbarkeit. Trotz dieser Verbesserungen ist die Optimierung und Standardisierung der IEF-Bedingungen nach wie vor für basische Proteine eine Herausforderung, und zwar hauptsächlich aufgrund von Protein-Aggregation, -Oxidation und -Präzipitation. Frühere Studien zeigten, dass Solubilisierungspuffer auf Basis von Harnstoff und Thioharnstoff in Kombination mit den Detergenzien CHAPS und ASB-14 für basische Proteine besonders geeignet sind [107, 108]. Des Weiteren führt eine falsche Probenapplikation (z.B. Rehydratisierung des IPG-Streifens) während der IEF zur Proteininstabilität [109]. Die Probenapplikation mittels *Cup-Loading* verbesserte deutlich die Übertragung von basischen Proteinen auf die IPG-Streifen.

Für die Abwesenheit von Proteinen innerhalb der 2D-Gele gibt es zwei denkbare Ursachen: (I) die Proteine werden durch schlechte Denaturierung oder

[2] Kotz 2015, S. 8

Solubilisierung nicht fokussiert, oder (II) mangelnde Migration vom IPG-Streifen zur SDS-PAGE, aufgrund von Aggregation, Ausfällung oder Assoziationen mit der Polyacrylamidgelmatrix. Die Migration des Reduktionsmittels DTT zur Anode führt während der IEF zum Verlust des DTTs an der Kathode und fördert die Reformierung von Disulfidbindungen. Dies führt in 2D-Gelen zu horizontalen Streifen und einem verwischten Spotmuster. Zur Reduzierung der horizontalen Streifen in 2D-Gelen wurden die IPG-Streifen mit HED prähydratisiert und als Ergänzung an der Kathode ein mit DTT getränktes Filterpapierstück verwendet [110]. Die Proteintrennung in der ersten Dimension der 2D-Gelelektrophorese zeigte daraufhin eine äußerst gute Trennung der basischen Proteine. Innerhalb der 2D-Gelelektrophorese bleiben sehr basische Proteine eine Herausforderung, da diese meist nur als dichte Streifen nachgewiesen werden können. Die derzeitige Strategie für die Auftrennung sehr basischer Proteine besteht darin, bei der IEF hohe Spannungen (8000 - 10000 V) anzuwenden, um die Fokussierungszeit zu verringern [111-113], da im alkalischen pH-Bereich bei einer zu langen Fokussierung instabile Proteine an ihrem *pI* degradieren können. In der vorliegenden Arbeit zeigte allerdings eine Maximalspannung von 3000 V und eine Erhöhung der Voltstunden auf bis zu 18,4 kVh im letzten Schritt der IEF eine ausgezeichnete Auflösung von sehr basischen Proteinen in 2D-Gelen. Des Weiteren konnten McDonough et *al*. zeigen, dass hydrophobe Proteine während der zweiten Dimension sehr häufig im IPG-Streifen verbleiben [114]. Folglich wurde der Mangel an Migration vom IPG-Streifen zur SDS-PAGE durch eine ungenügende Äquilibrierung der Proteine verursacht. Daher wurde das Volumen des Äquilibrierungspuffers auf 10 mL sowie die Konzentration von SDS auf 10% erhöht.

Insgesamt führte die kombinierte Verwendung von CHAPS und ASB-14 im Solubilisierungspuffer, die Probenapplikation mittels *Cup-Loading* an der Anode, die Verwendung von HED im Rehydratisierungspuffer, ein mit DTT getränktes Filterpapierstück an der Kathode, die Erhöhung der Voltstunden auf bis zu 18,4 kVh im letzten Schritt der IEF sowie die Optimierung des Äquilibrierungspuffers zu einer deutlichen Verbesserung der Migration und Auftrennung basischer Proteine. Zusammenfassend ist die Optimierung einzelner Schritte für eine

hochauflösenden 2D-Gelelektrophorese unverzichtbar und ermöglicht eine gute Reproduzierbarkeit [100].“[3]

3.3 BINDUNG VON CFDA-CISPLATIN AN PROTEINE

Durch die 2D-Gelelektrophorese impliziert die analytische Methode zur Detektion und Identifizierung von intrazellulären Cisplatin-Proteinaddukten die Denaturierung von Proteinen. Dennoch kann die Methode für den Nachweis von intrazellulären CFDA-Cisplatin-bindenden Proteinen verwendet werden [84, 87], da die 2D-Gelelektrophorese kovalente CFDA-Cisplatin-Proteinaddukte nachweisen kann. Die nicht-kovalenten Wechselwirkungen zwischen CFDA-Cisplatin und Proteinen gehen durch die Verwendung der 2D-Gelelektrophorese verloren.

Cisplatin reagiert bevorzugt mit den schwefelhaltigen Aminosäuren Cystein und Methionin, die auf der Oberfläche von Proteinen vorhanden sind. Daher sind Proteine, die reich an Cystein und Methionin sind, wie Protein-Disulfid-Isomerase (PDI)A1, PDIA3, PDIA6, D-3-phosphoglycerate-dehydrogenase (PHGDH), Pyruvatekinase (PKM), Alpha-Enolase (ENOA) und Elongation factor alpha-1 (EF1A1) in der Lage kovalente Komplexe mit CFDA-Cisplatin im Zytosol zu bilden [99, 100]. PDI ist ein Mitglied der Thioredoxin-Superfamilie, welche die Spaltung und Ausbildung von Disulfidbrücken in Proteinen katalysieren sowie die Proteinfaltung im endoplasmatischen Retikulum (ER) regeln [115]. Sobierajska et *al*. [116] konnten zeigen, dass PDI aus subzellulären Kompartimenten ins Zytosol freigesetzt wird und eine Disulfidbindung mit dem β-Actin Cys^{374} bildet. β-Actin enthält sechs Cystein-Reste, von denen jedoch nur einer (Cys^{374}) auf der Oberfläche des Proteins exponiert ist [117]. Die Proteine Glucose-regulierendes-Protein (GRP) 78, β-Actin, Vimentin, Glyceraldehyd-3-phosphate dehyrogenase (GAPDH), Serpin H1, Heterogenous nuclear ribonucleoprotein (hnRNP) A/B und hnRNP H3 enthalten dagegen weniger Cysteine, dafür mehr Methionine und sind ebenfalls in der Lage Bindungen mit CFDA-Cisplatin zu bilden [99, 118]. Darüber hinaus können auch Asparaginsäure, Glutaminsäure, Histidin, Serin, Threonin und Tyrosin mit CFDA-Cisplatin kovalente Komplexe bilden, da diese Aminosäuren ebenfalls als potentielle Bindungsstellen für Cisplatin identifiziert wurden [87, 89]. Dabei bestimmt die Zugänglichkeit der Seitenketten, die vom Rückgrat aus in den Raum ragen, welche Aminosäuren an Cisplatin binden.

[3] Kotz 2018, S. 1494

Die 2D-Gelelektrophorese zeigte, dass die Bindung des CFDA-Cisplatins an eine Aminosäure eine geringe Veränderung der Nettoladung des Proteins hervorrufen kann, was zu einem veränderten Migrationsverhalten des CFDA-Cisplatin-bindenden Proteins in 2D-Gelen führte. Unter den identifizierten CFDA-cisplatinhaltigen Proteinen wurden PDIA3, PDIA6, GRP78, PKM und ENOA auch als unmodifizierte Proteine nachgewiesen, während PDIA1, EF1A1 und PHGDH nur als CFDA-Cisplatinaddukte identifiziert wurden [99, 100]. Möglicherweise verursachte die Bindung von CFDA-Cisplatin an PDIA1 keine Veränderung im *pI* oder die Gesamtmenge des Proteins hatte CFDA-Cisplatin gebunden. Dagegen wurden die Proteine PDIA6, EF1A1 und PHGDH jeweils auch in unterschiedlichen Proteinspots identifiziert. Dies könnte durch das Vorliegen verschiedener Isoformen des PDIA6 als Ergebnis des alternativen Spleißens bedingt sein, die sich gewöhnlich im *pI* und Molekulargewicht unterscheiden. Darüber hinaus werden Proteine mit unterschiedlichen posttranslationalen Modifikationen in unterschiedlichen Spots abgebildet.

Ergänzend kann die Bindung von CFDA-Cisplatin an ein Protein die Menge an reaktivem Cisplatin in Tumorzellen begrenzen sowie eine Beeinträchtigung bzw. den Verlust der biologischen Aktivität des betreffenden Proteins bewirken. Daher kann die Bindung von CFDA-Cisplatin an ein Protein dessen Reaktivität in der Tumorzelle einschränken, veränderte Signalprozesse hervorrufen und demzufolge einen Einfluss auf das Überleben der Tumorzelle haben [99].

3.4 CFDA-CISPLATIN-BINDENDE PROTEINE

Einige der 14 CFDA-cisplatinhaltigen Proteinen werden im Zusammenhang mit der Tumorentstehung diskutiert [99, 100].

Die CFDA-cisplatinhaltigen Proteine PDIA1, PDIA3, PDIA6 und GRP78 sind molekulare Chaperone und im ER lokalisiert. Da die Proliferation der Tumorzellen eine erhöhte Proteinsynthese sowie die Akkumulation von ungefalteten Proteinen (ER-Stress) erzeugt, war die Identifizierung dieser Proteine vorhersehbar [119, 120]. „PDI und GRP78 besitzen am C-Terminus die spezifische ER-Retention-Aminosäuresequenz KDEL. Allerdings wurden signifikante Mengen von PDI und GRP78 auch auch außerhalb des ERs, im Zellkern, Zytosol und an der Zelloberfläche, nachgewiesen [120-124]. PDI und GRP78 zählen zu den zentralen Regulatoren der ungefalteten Proteinantwort (UPR), die durch Akkumulation von

ungefalteten Proteinen im ER sowie durch exogene und/oder endogene Stresssignale induziert werden [125-127]. Daher werden PDI und GRP78 auch mit der Cisplatinresistenz einiger Krebsarten in Verbindung gebracht [128-130].“[4] Wir zeigten, dass ein *Knockdown* von PDIA1 in der cisplatinresistenten OC-zelllinie A2780*cis* zu einer Erhöhung der Zytotoxizität von Cisplatin führt [101]. Des Weiteren bewirkte die Koinkubation von Tumorzellen mit Cisplatin und dem PDIA1 - Inhibitor PACMA 31 **(**N-(2,4-Dimethoxyphenyl)-N-(1-oxo-2-propyn-1-yl)-2-(2-thienyl)glycyl-glycine ethyl ester) eine Resensibilisierung für Cisplatin [101]. Für einen therapeutischen Ansatz ist die spezifische Inhibierung von PDIA1 durch PACMA 31 ein vielversprechendes Ziel. Zusätzlich konnten wir zeigen, dass ein *Knockdown* von PDIA3 die Zytotoxizität von Cisplatin in der Zelllinie A2780*cis* nicht beeinflusst [101]. Dagegen zeigte Tufo et *al.* keinen Hinweis von PDIA1 und PDIA3 zur Cisplatinresistenz beim NSCLC. Dafür eine Überexpression der Proteine PDIA4 und PDIA6, deren pharmakologische sowie genetische Inaktivierung eine cisplatininduzierte Apoptose über verschiedene zelluläre Signalwege zeigte. Die Inaktivierung von PDIA4 stellte die mitochondriale Apoptose wieder her, während die Inaktivierung von PDIA6 die nicht-kanonische Apoptose begünstigte [129]. Da PDIA6 auch CFDA-Cisplatin bindet, könnte es ein vielversprechendes Ziel für zukünftige Studien sein. Zudem lassen die Ergebnisse vermuten, dass die Proteindisulfid-Isomerasen Zelltyp-spezifisch wirken [101, 129]. Wie bei PDIA3 zeigte ein *Knockdown* von GRP78, dass die Zytotoxizität von Cisplatin in der OC-Zelllinie A2780*cis* nicht beeinflusst wird [102]. Dagegen führte ein *Knockdown* von GRP78 beim Nasopharynxkarzinom zu einer Erhöhung der Zytotoxizität von Cisplatin [131]. Da Tumorzellen eher heterogen sind, können verschiedene Tumore vermutlich mit verschiedener Signal- und Abwehrmechanismen Resistenzen gegen Cisplatin erwerben.

Die identifizierten CFDA-cisplatinhaltigen Proteine ENOA, GAPDH, und PKM sind am Glukosestoffwechsel beteiligt. Maligne, schnell wachsende Tumorzellen beziehen ihre Energie auch bei ausreichender Sauerstoffversorgung weitgehend aus der aeroben Glykolyse (Warburg-Effekt) [132, 133]. Die Stoffwechselumstellung in Tumorzellen kennzeichnet eine Überexpression von Genen des Glukosestoffwechsels, die mitochondriale Dysfunktionen

[4] Kotz 2015, S. 8

kompensieren sowie die Entstehung einer Resistenz gegenüber der Apoptose begünstigen [132, 134]. „ENOA spielt bei der Glykolyse, Hypoxietoleranz und Tumorinvasion eine Schlüsselrolle [135-137]. In der Glykolyse katalysiert ENOA die Umwandlung von 2-Phosphoglycerat zu Phosphoenolpyruvat, dem zweiten energiereichen Zwischenprodukt, welches Adenosintriphosphat (ATP) in der Glykolyse produziert [138]. ENOA ist auf der Oberfläche von Zellen exprimiert und bildet zusammen mit dem Urokinase-Rezeptor (uPAR), Integrinen und einigen Zytoskelettproteinen einen Multiprotein-Komplex, dem so genannten Metastasom, der für die Adhäsion, Migration und Proliferation von Ovarialtumorzellen verantwortlich ist [136]. Auf mRNA- und Proteinebene ist ENOA in mehreren Tumoren [78, 139-159] einschließlich dem OC [134, 160] hochreguliert. Die erhöhte Expression von ENOA kann den Therapieerfolg bei östrogenrezeptor-positiven Brusttumoren negativ beeinflussen, da ENOA die Resistenz gegen das Antiöstrogen Tamoxifen induziert [158].“ [5] Zudem konnte ENOA in einigen Tumoren einschließlich Pankreas [161], Leukämie [162, 163], Melanom [155, 164], Kopf und Hals [157, 165, 166], Brust [167, 168] und Lunge [142, 148, 168-173] gezeigt werden, dass ENOA die Bildung von Autoantikörpern induziert und bei diesen Tumorentitäten ein attraktives therapeutisches Ziel darstellt [174]. Der Organogold(III)-Komplex Aubipyc konnte in Studien eine bemerkenswerte Zytotoxizität gegenüber der humanen OC-Zelllinie A2780 zeigen. Dabei induziert Aubipyc den apoptotischen Zelltod und ist in der Lage die Resistenz gegenüber Cisplatin zu überwinden [175]. Zudem konnte gezeigt werden, dass die Glykolyse beim zytotoxischen Wirkmechanismus von Aubipyc eine Rolle spielt, da es glykolytische Enzyme wie ENOA und GAPDH beeinflusst [176, 177]. Innerhalb der Glykolyse katalysiert GAPDH die Umwandlung von Glycerinaldehyd-3-phosphat zu 1,3-Bisphosphoglycerat. Bei dieser Reaktion wird eine energiereiche Phosphat-Bindung aufgebaut, die auf Adenosindiphosphat (ADP) übertragen wird und ATP in der Glykolyse produziert. Kürzlich zeigten jedoch Studien, dass GAPDH zusätzlich an der Apoptose, dem Transfer-RNA(tRNA)-Transport sowie anderen Prozessen beteiligt ist [178], die GAPDH als potentielles Ziel für eine antitumorale Therapie limitieren [179, 180]. Das Enzym PKM katalysiert im finalen Schritt der Glykolyse die Umwandlung von Phosphoenolpyruvat und ADP zu

[5] Kotz 2018, S. 1495

Pyruvat und ATP. Die M2-Isoform der Pyruvatkinase (PKM2) wird in verschiedenen Tumorzellen exprimiert [181, 182] und trägt maßgeblich zum Warburg-Effekt, Tumorwachstum, Angiogenese, Zellteilung, Metastasierung und Apoptose bei [182-185]. Da PKM2 zum malignen Phänotyp vieler Krebsarten beiträgt, könnte der Regulator des Tumormetabolismus ein potentielles Ziel zur Bekämpfung des Ovarialkarzinoms sein [186].

„PHGDH, ein weiterer identifizierter intrazellulärer Bindungspartner vom CFDA-Cisplatin, fungiert als Schlüsselenzym bei der *de novo* Biosynthese von Serin. Zusammen wandeln PHGDH, Phosphoserin-Aminotransferase und Phosphoserin-Phosphatase das glykolytische Intermediat 3-Phosphoglycerat in L-Serin um [187]. L-Serin ist eine essentielle Aminosäure in der Proteinsynthese sowie in der Synthese von Sphingo- und Phospholipiden, die wichtige Komponenten der Zellmembranen sind [188, 189]. Zudem kann L-Serin durch die Serin-Hydroxy-Methyltransferase in Glycin umgewandelt werden, das zur *de novo* Synthese von Nucleinbasen benötigt wird [190]. Ein *Knockdown* von PHGDH in Mammakarzinom- und Melanomzelllinien führte zu einem Abbau der Serinsynthese sowie zur Beeinträchtigung der Proliferation [191-193], wobei zusätzliches Serin nicht immer die Funktion des PHGDHs ersetzen konnte [193]. Des Weiteren zeigte ein *Knockdown* von PHGDH in HeLa Zellen eine signifikante Hemmung der Proliferation sowie eine erhöhte Zytotoxizität gegenüber Cisplatin [194].“[6] In OC-Zelllinien (Caov-3, SKOV-3) konnte bisher gezeigt werden, dass PHGDH signifikant hochreguliert ist [195]. Für die Verwendung von PHGDH als potentielles Ziel für eine antitumorale Therapie muss ein signifikanter Unterschied zwischen der Aktivität des Enzyms in Tumorzellen zu normal proliferierenden Zellen gefunden werden, da die PHGDH-abhängige Biosynthese von Serin in allen Zellen wirksam ist [196]. Angeborene Mutationen in PHGDH können zu schweren neurologischen Symptomen führen. Neuronen sowie Gliazellen sind ausschließlich auf die *de novo* Biosynthese von Serin angewiesen, da Serin die Blut-Hirn-Schranke nicht passieren kann [197]. Dennoch bleibt die Hemmung des PHGDHs eine potentielle antitumorale Therapie, wenn der PHGDH-Inhibitor die Blut-Hirn-Schranke nicht passieren kann und Mangel an Serin durch exogenes

[6] Kotz 2018, S. 1495

Serin ergänzt wird, vorausgesetzt die Abhängigkeit der Tumore von PHGDH ist nicht mit dem Serin assoziiert [133, 197, 198].

„Ein weiteres identifiziertes CFDA-cisplatinhaltiges Protein war EF1A1, eine 50 kDa GTPase, die während der Proteintranslation die Bindung von Aminoacyl-tRNAs am Ribosom katalysiert [199, 200]. Frühere Studien zeigten, dass EF1A1 eine essentielle regulatorische Rolle beim Zellwachstum, der Tumorgenese und Apoptose spielt [200-204]. Zudem wurde EF1A1 als interagierendes Protein der Transkriptionsfaktoren p53 und p73 identifiziert, die eine wichtige Rolle bei der Tumorentstehung einschließlich Apoptose spielen [205]. Die Überexpression von EF1A1 hemmt die p53-, p73- und Chemotherapie-induzierte Apoptose, was zur Resistenz von Tumorzellen gegenüber der Chemotherapie führt. Blanch et *al*. konnten bei einem siRNA-induzierten *Knockdown* von EF1A1 zeigen, dass in Tumorzellen mit dem p53-Protein die Chemotherapie-induzierte Apoptose erhöht war, hingegen nicht in Tumorzellen ohne das p53-Protein [205]. Diese Ergebnisse legen nahe, dass EF1A1 als negativer Regulator auf das pro-apoptotisch wirkende p53 fungiert. Da EF1A1 anti-apoptotische Eigenschaften in der Signalgebung der p53-Familie hat, kann EF1A1 ein potentielles Ziel für eine antitumorale Therapie sein [205].“[7]

Die anderen identifizierten CFDA-cisplatinhaltigen Proteine β-Actin, Vimentin, Serpin H1, Heterogenous nuclear ribonucleoprotein (hnRNP) A/B und hnRNP H3 wurden bisher noch nicht im Zusammenhang mit der Chemoresistenz diskutiert.

ZUSAMMENFASSUNG UND AUSBLICK

Zur Identifizierung von intrazellulären cisplatinhaltigen Proteinen wurde eine analytische Methode, bestehend aus dem fluoreszierenden CFDA-Cisplatin, der 2D-Gelelektrophorese und Massenspektrometrie, etabliert. Mit dieser Methode wurde bestätigt, dass CFDA-Cisplatin innerhalb einer Zelle spezifisch an Proteine bindet und dadurch wurden neue Einblicke in die zelluläre Prozessierung von Cisplatin sowie in die erworbenen Resistenzmechanismen gegenüber Cisplatin gewonnen.

Zur Identifizierung CFDA-cisplatinhaltigen Proteine war die Optimierung einzelner Schritte der 2D-Gelelektrophorese notwendig, besonders für Proteine im alkalischen pH-Bereich (pH 6 - 10) [100]. Dies ermöglichte die Identifizierung von

[7] Kotz 2018, S. 1495

EF1A1 mit einem theoretischen p*I* von 9,10 als ein CFDA-cisplatinhaltiges Protein [100].

Die CFDA-cisplatinhaltigen Proteine PDIA1, PDIA3, PDIA6 und GRP78 sind molekulare Chaperone sowie zentrale Regulatoren der UPR und werden daher mit der erworbenen Cisplatinresistenz einiger Tumorarten in Verbindung gebracht. Wir zeigten, dass ein *Knockdown* von PDIA1 sowie die Koinkubation mit dem PDIA1-Inhibitor PACMA 31 eine Resensibilisierung von resistenten Tumorzellen gegenüber Cisplatin bewirkte [101]. Zudem zeigte ein *Knockdown* von PDIA3 und GRP78, dass die Zytotoxizität von Cisplatin nicht beeinflusst wird [101, 102]. Die spezifische Inhibierung von PDIA1 durch PACMA 31 und PDIA6, deren pharmakologische sowie genetische Inaktivierung die nicht-kanonische Apoptose begünstigte [129], sind potentielle antitumorale Therapieansätze. Zur Bestätigung der Wirksamkeit sind weitere pharmakologische Studien in anderen Entitäten sowie beim Wirksamkeitsnachweis eine Überprüfung in Tiermodellen nötig.

Ein Marker für eine schlechte Prognose sind die CFDA-cisplatinhaltigen Proteine GAPDH, ENOA, PKM und PHGDH und daher potentielle Ziele für eine antitumoralen Therapie [186, 206-208]. Maligne, schnell wachsende Tumorzellen stellen ihren Energiemetabolismus auf aerobe Glykolyse um, wodurch mitochondriale Dysfunktionen kompensiert und die Intermediate der Glykolyse verwendet werden können, um Nukleotide, Aminosäuren sowie Lipide zu synthetisieren. GAPDH, ENOA und PKM katalysieren in der Glykolyse Reaktionen, die ATP im Glykolyseweg produzieren. Dagegen wandelt PHGDH zusammen mit der Phosphoserin-Aminotransferase und Phosphoserin-Phosphatase das glykolytische Intermediat 3-Phosphoglycerat in L-Serin um. Bisher konnten wir noch nicht festzustellen, ob CFDA-Cisplatin durch direkte Hemmung der identifizierten glykolytischen Enzyme wirkt oder ob über die Verlangsamung der Glykolyse hinaus andere molekulare Mechanismen wirksam sind. Ein weiteres potentielles Ziel für eine antitumorale Therapie ist EF1A1. EF1A1 ist an der negativen Regulation des Tumorsuppressors p53 beteiligt und unterstützt somit die anhaltende Proliferation der Tumorzellen.

Für die Relevanz von PDIA6, EF1A1, PHGDH, ENOA und GAPDH hinsichtlich der erworbenen Resistenz von Ovarialtumorzellen gegenüber Cisplatin sind pharmakologische Studien nötig, wie sie für PDIA1, PDIA3 und GRP78 bereits durchgeführt wurden. Hierzu kann Bacitracin [129, 209] für die spezifische

Inhibierung von PDIA6 und Nannocystin A [210, 211], Didemnin B [212], Ternatin [213] und/oder Ansatrienin B [213] für die spezifische Inhibierung von EF1A1 verwendet werden. Der niedermolekulare Inhibitor von PHGDH CBR-5884 hemmt die *de novo* Biosynthese von Serin und wirkt selektiv in Tumorzellen mit erhöhter Biosyntheseaktivität von Serin. Daher ist CBR-5884 ein vielversprechender Ausgangspunkt für die Entwicklung von weiteren Wirkstoffmolekülen [214]. Zudem zeigte die Entwicklung von alpha-Enolase-Inhibitoren bisher vielversprechende Anhaltspunkte, den Tumor metabolisch zu bekämpfen [215]. Die Struktur sowie Regulation der Glykolyse legen nahe, dass dieser Mechanismus ein vielversprechender Ansatz für die Entwicklung neuer Strategien und antitumorale Wirkstoffe gegen glykolytische Enzyme ist. Kürzlich zeigte eine Studie, dass *Koningic acid* sowohl die Wirksamkeit als auch die Selektivität zur spezifischen Inhibierung von GAPDH in Tumorzellen besitzt [216]. Zur spezifischen Inhibierung von PKM kann Shikonin verwendet werden [186, 217]. Abschließend lassen die Ergebnisse der pharmakologischen Studien zu PDIA1, PDIA3 sowie GRP78 [101, 102] und die dazu detektierten Fluoreszenzsignale [99, 100] vermuten, dass die CFDA-Cisplatin-bindenden Proteine EF1A1 und PHGDH die aussichtsreichsten Kandidaten für weiterführende Studien sind.

Darüber hinaus sind Analysen erforderlich, die die Bindungsstellen von Cisplatin an den Proteinen identifizieren, um das Verständnis der Bindungsstabilität zu verbessern. „Cisplatin zeigt im Massenspektrum ein charakteristisches Isotopenmuster und modifiziert das Isotopenmuster eines Pt-haltigen Peptids. Die Bindungsstelle von Cisplatin erzeugt bei einem Peptid ein charakteristisch verändertes Isotopenmuster und ist mit der Massenspektrometrie nachweisbar [87]. Aufgrund der geringen Häufigkeit von platinierten Peptiden im Vergleich zu unplatinierten Peptiden ist der Nachweis von Cisplatin-Bindungsstellen innerhalb eines Peptids durch ESI(Elektrosprayionisation)-MS/MS(Tandem-Massenspektrometrie) jedoch schwierig. Daher kann eine Aufkonzentrierung von identifizierten CFDA-cisplatinhaltigen Proteinen hilfreich sein.“[8]

Zudem gehen durch die Verwendung der 2D-Gelelektrophorese in der analytischen Methode die nicht-kovalenten Wechselwirkungen zwischen CFDA-Cisplatin und Proteinen verloren. Die Verwendung einer *blue native PAGE,* die zur

[8] Kotz 2015, S. 8

Isolierung und nativen Auftrennung von Membranproteinen entwickelt wurde, ist auch zur Analyse löslicher Proteine sowie Proteinkomplexe geeignet und könnte weitere Einblicke in die zelluläre Prozessierung von Cisplatin sowie in die Resistenzmechanismen gegenüber Cisplatin liefern.

.

4 REFERENZEN

1. F. Prütz; P. Rattay; I. Schönfeld; A. Starker; A. Wienecke; U. Wolf, B.B.J.B.N.B.-S.J.F.S.J.K.K.H.N.E.N.C.P.-M.I., *Bericht zum Krebsgeschehen in Deutschland 2016*, in *Robert Koch Institut*2016. p. 1-274.
2. Kuchenbaecker, K.B., et al., *Risks of Breast, Ovarian, and Contralateral Breast Cancer for BRCA1 and BRCA2 Mutation Carriers.* JAMA, 2017. 317(23): p. 2402-2416.
3. Lynch, H.T., et al., *Genetics and ovarian carcinoma.* Semin Oncol, 1998. 25(3): p. 265-80.
4. Ramus, S.J., et al., *Germline Mutations in the BRIP1, BARD1, PALB2, and NBN Genes in Women With Ovarian Cancer.* J Natl Cancer Inst, 2015. 107(11).
5. Song, H., et al., *Contribution of Germline Mutations in the RAD51B, RAD51C, and RAD51D Genes to Ovarian Cancer in the Population.* J Clin Oncol, 2015. 33(26): p. 2901-7.
6. Hanahan, D. and R.A. Weinberg, *The hallmarks of cancer.* Cell, 2000. 100(1): p. 57-70.
7. Hanahan, D. and R.A. Weinberg, *Hallmarks of cancer: the next generation.* Cell, 2011. 144(5): p. 646-74.
8. Yap, T.A., C.P. Carden, and S.B. Kaye, *Beyond chemotherapy: targeted therapies in ovarian cancer.* Nat Rev Cancer, 2009. 9(3): p. 167-81.
9. Rosenberg, B., L. Vancamp, and T. Krigas, *INHIBITION OF CELL DIVISION IN ESCHERICHIA COLI BY ELECTROLYSIS PRODUCTS FROM A PLATINUM ELECTRODE.* Nature, 1965. 205: p. 698-9.
10. Hall, M.D., et al., *The role of cellular accumulation in determining sensitivity to platinum-based chemotherapy.* Annu Rev Pharmacol Toxicol, 2008. 48: p. 495-535.
11. Kishimoto, S., et al., *Role of Na+, K+-ATPase alpha1 subunit in the intracellular accumulation of cisplatin.* Cancer Chemother Pharmacol, 2006. 57(1): p. 84-90.
12. Klein, A.V. and T.W. Hambley, *Platinum drug distribution in cancer cells and tumors.* Chem Rev, 2009. 109(10): p. 4911-20.
13. Howell, S.B., et al., *Copper transporters and the cellular pharmacology of the platinum-containing cancer drugs.* Mol Pharmacol, 2010. 77(6): p. 887-94.
14. Safaei, R., *Role of copper transporters in the uptake and efflux of platinum containing drugs.* Cancer Lett, 2006. 234(1): p. 34-9.
15. Ciarimboli, G., et al., *Organic cation transporter 2 mediates cisplatin-induced oto- and nephrotoxicity and is a target for protective interventions.* Am J Pathol, 2010. 176(3): p. 1169-80.
16. Ciarimboli, G., et al., *Cisplatin nephrotoxicity is critically mediated via the human organic cation transporter 2.* Am J Pathol, 2005. 167(6): p. 1477-84.

17. Motohashi, H., et al., *Gene expression levels and immunolocalization of organic ion transporters in the human kidney.* J Am Soc Nephrol, 2002. 13(4): p. 866-74.

18. Kelland, L., *The resurgence of platinum-based cancer chemotherapy.* Nat Rev Cancer, 2007. 7(8): p. 573-84.

19. Fichtinger-Schepman, A.M., et al., *Adducts of the antitumor drug cis-diamminedichloroplatinum(II) with DNA: formation, identification, and quantitation.* Biochemistry, 1985. 24(3): p. 707-13.

20. Jamieson, E.R. and S.J. Lippard, *Structure, Recognition, and Processing of Cisplatin-DNA Adducts.* Chem Rev, 1999. 99(9): p. 2467-98.

21. Rebillard, A., D. Lagadic-Gossmann, and M.T. Dimanche-Boitrel, *Cisplatin cytotoxicity: DNA and plasma membrane targets.* Curr Med Chem, 2008. 15(26): p. 2656-63.

22. Kasherman, Y., S. Sturup, and D. Gibson, *Is glutathione the major cellular target of cisplatin? A study of the interactions of cisplatin with cancer cell extracts.* J Med Chem, 2009. 52(14): p. 4319-28.

23. Gonzalez, V.M., et al., *Is cisplatin-induced cell death always produced by apoptosis?* Mol Pharmacol, 2001. 59(4): p. 657-63.

24. Sancho-Martinez, S.M., et al., *Subcellular targets of cisplatin cytotoxicity: an integrated view.* Pharmacol Ther, 2012. 136(1): p. 35-55.

25. Rabik, C.A. and M.E. Dolan, *Molecular mechanisms of resistance and toxicity associated with platinating agents.* Cancer Treat Rev, 2007. 33(1): p. 9-23.

26. Kullmann, M., *Identifying intracellular cisplatin interaction partners and assessing their contribution to cisplatin resistance*, in *PhD thesis, University of Bonn, Bonn, 2013.*Bonn 2016.

27. Galanski, M., *Recent developments in the field of anticancer platinum complexes.* Recent Pat Anticancer Drug Discov, 2006. 1(2): p. 285-95.

28. Lebwohl, D. and R. Canetta, *Clinical development of platinum complexes in cancer therapy: an historical perspective and an update.* Eur J Cancer, 1998. 34(10): p. 1522-34.

29. Prestayko, A.W., et al., *Cisplatin (cis-diamminedichloroplatinum II).* Cancer Treat Rev, 1979. 6(1): p. 17-39.

30. Galluzzi, L., et al., *Molecular mechanisms of cisplatin resistance.* Oncogene, 2012. 31(15): p. 1869-83.

31. Galluzzi, L., et al., *Systems biology of cisplatin resistance: past, present and future.* Cell Death Dis, 2014. 5: p. e1257.

32. Agarwal, R. and S.B. Kaye, *Ovarian cancer: strategies for overcoming resistance to chemotherapy.* Nat Rev Cancer, 2003. 3(7): p. 502-16.

33. Davis, A., A.V. Tinker, and M. Friedlander, *"Platinum resistant" ovarian cancer: what is it, who to treat and how to measure benefit?* Gynecol Oncol, 2014. 133(3): p. 624-31.

34. Siddik, Z.H., *Cisplatin: mode of cytotoxic action and molecular basis of resistance.* Oncogene, 2003. 22(47): p. 7265-79.

35. Loh, S.Y., et al., *Reduced drug accumulation as a major mechanism of acquired resistance to cisplatin in a human ovarian carcinoma cell line: circumvention studies using novel platinum (II) and (IV) ammine/amine complexes.* Br J Cancer, 1992. 66(6): p. 1109-15.

36. Holzer, A.K., G.H. Manorek, and S.B. Howell, *Contribution of the major copper influx transporter CTR1 to the cellular accumulation of cisplatin, carboplatin, and oxaliplatin.* Mol Pharmacol, 2006. 70(4): p. 1390-4.

37. Ishida, S., et al., *Uptake of the anticancer drug cisplatin mediated by the copper transporter Ctr1 in yeast and mammals.* Proc Natl Acad Sci U S A, 2002. 99(22): p. 14298-302.

38. Ishida, S., et al., *Enhancing tumor-specific uptake of the anticancer drug cisplatin with a copper chelator.* Cancer Cell, 2010. 17(6): p. 574-83.

39. Katano, K., et al., *Acquisition of resistance to cisplatin is accompanied by changes in the cellular pharmacology of copper.* Cancer Res, 2002. 62(22): p. 6559-65.

40. More, S.S., et al., *Role of the copper transporter, CTR1, in platinum-induced ototoxicity.* J Neurosci, 2010. 30(28): p. 9500-9.

41. Cui, Y., et al., *Drug resistance and ATP-dependent conjugate transport mediated by the apical multidrug resistance protein, MRP2, permanently expressed in human and canine cells.* Mol Pharmacol, 1999. 55(5): p. 929-37.

42. Koike, K., et al., *A canalicular multispecific organic anion transporter (cMOAT) antisense cDNA enhances drug sensitivity in human hepatic cancer cells.* Cancer Res, 1997. 57(24): p. 5475-9.

43. Liedert, B., et al., *Overexpression of cMOAT (MRP2/ABCC2) is associated with decreased formation of platinum-DNA adducts and decreased G2-arrest in melanoma cells resistant to cisplatin.* J Invest Dermatol, 2003. 121(1): p. 172-6.

44. Komatsu, M., et al., *Copper-transporting P-type adenosine triphosphatase (ATP7B) is associated with cisplatin resistance.* Cancer Res, 2000. 60(5): p. 1312-6.

45. Korita, P.V., et al., *Multidrug resistance-associated protein 2 determines the efficacy of cisplatin in patients with hepatocellular carcinoma.* Oncol Rep, 2010. 23(4): p. 965-72.

46. Safaei, R., et al., *The role of copper transporters in the development of resistance to Pt drugs.* J Inorg Biochem, 2004. 98(10): p. 1607-13.

47. Yamasaki, M., et al., *Role of multidrug resistance protein 2 (MRP2) in chemoresistance and clinical outcome in oesophageal squamous cell carcinoma.* Br J Cancer, 2011. 104(4): p. 707-13.

48. Chen, H.H. and M.T. Kuo, *Role of glutathione in the regulation of Cisplatin resistance in cancer chemotherapy.* Met Based Drugs, 2010. 2010.

49. Kasahara, K., et al., *Metallothionein content correlates with the sensitivity of human small cell lung cancer cell lines to cisplatin.* Cancer Res, 1991. 51(12): p. 3237-42.

50. Kelley, S.L., et al., *Overexpression of metallothionein confers resistance to anticancer drugs.* Science, 1988. 241(4874): p. 1813-5.

51. Lewis, A.D., J.D. Hayes, and C.R. Wolf, *Glutathione and glutathione-dependent enzymes in ovarian adenocarcinoma cell lines derived from a patient before and after the onset of drug resistance: intrinsic differences and cell cycle effects.* Carcinogenesis, 1988. 9(7): p. 1283-7.

52. Ahmad, A., et al., *ERCC1-XPF endonuclease facilitates DNA double-strand break repair.* Mol Cell Biol, 2008. 28(16): p. 5082-92.

53. Shuck, S.C., E.A. Short, and J.J. Turchi, *Eukaryotic nucleotide excision repair: from understanding mechanisms to influencing biology.* Cell Res, 2008. 18(1): p. 64-72.

54. Shachar, S., et al., *Two-polymerase mechanisms dictate error-free and error-prone translesion DNA synthesis in mammals.* EMBO J, 2009. 28(4): p. 383-93.

55. Kunkel, T.A. and D.A. Erie, *DNA mismatch repair.* Annu Rev Biochem, 2005. 74: p. 681-710.

56. Vaisman, A., et al., *The role of hMLH1, hMSH3, and hMSH6 defects in cisplatin and oxaliplatin resistance: correlation with replicative bypass of platinum-DNA adducts.* Cancer Res, 1998. 58(16): p. 3579-85.

57. Aebi, S., et al., *Loss of DNA mismatch repair in acquired resistance to cisplatin.* Cancer Res, 1996. 56(13): p. 3087-90.

58. Brown, R., et al., *hMLH1 expression and cellular responses of ovarian tumour cells to treatment with cytotoxic anticancer agents.* Oncogene, 1997. 15(1): p. 45-52.

59. Massey, A., et al., *DNA mismatch repair and acquired cisplatin resistance in E. coli and human ovarian carcinoma cells.* DNA Repair (Amst), 2003. 2(1): p. 73-89.

60. Narod, S.A. and W.D. Foulkes, *BRCA1 and BRCA2: 1994 and beyond.* Nat Rev Cancer, 2004. 4(9): p. 665-76.

61. Smith, J., et al., *The ATM-Chk2 and ATR-Chk1 pathways in DNA damage signaling and cancer.* Adv Cancer Res, 2010. 108: p. 73-112.

62. Yang, Z., et al., *Cisplatin preferentially binds mitochondrial DNA and voltage-dependent anion channel protein in the mitochondrial membrane of head and neck squamous cell carcinoma: possible role in apoptosis.* Clin Cancer Res, 2006. 12(19): p. 5817-25.

63. Kroemer, G., L. Galluzzi, and C. Brenner, *Mitochondrial membrane permeabilization in cell death.* Physiol Rev, 2007. 87(1): p. 99-163.

64. Tajeddine, N., et al., *Hierarchical involvement of Bak, VDAC1 and Bax in cisplatin-induced cell death.* Oncogene, 2008. 27(30): p. 4221-32.

65. Vousden, K.H. and D.P. Lane, *p53 in health and disease.* Nat Rev Mol Cell Biol, 2007. 8(4): p. 275-83.

66. Branch, P., et al., *Spontaneous development of drug resistance: mismatch repair and p53 defects in resistance to cisplatin in human tumor cells.* Oncogene, 2000. 19(28): p. 3138-45.

67. Gadducci, A., et al., *Molecular mechanisms of apoptosis and chemosensitivity to platinum and paclitaxel in ovarian cancer: biological data and clinical implications.* Eur J Gynaecol Oncol, 2002. 23(5): p. 390-6.

68. Brozovic, A. and M. Osmak, *Activation of mitogen-activated protein kinases by cisplatin and their role in cisplatin-resistance.* Cancer Lett, 2007. 251(1): p. 1-16.

69. Erovic, B.M., et al., *Mcl-1, vascular endothelial growth factor-R2, and 14-3-3sigma expression might predict primary response against radiotherapy and chemotherapy in patients with locally advanced squamous cell carcinomas of the head and neck.* Clin Cancer Res, 2005. 11(24 Pt 1): p. 8632-6.

70. Han, J.Y., et al., *Death receptor 5 and Bcl-2 protein expression as predictors of tumor response to gemcitabine and cisplatin in patients with advanced non-small-cell lung cancer.* Med Oncol, 2003. 20(4): p. 355-62.

71. Michaud, W.A., et al., *Bcl-2 blocks cisplatin-induced apoptosis and predicts poor outcome following chemoradiation treatment in advanced oropharyngeal squamous cell carcinoma.* Clin Cancer Res, 2009. 15(5): p. 1645-54.

72. Ikeguchi, M. and N. Kaibara, *Changes in survivin messenger RNA level during cisplatin treatment in gastric cancer.* Int J Mol Med, 2001. 8(6): p. 661-6.

73. Janson, V., A. Johansson, and K. Grankvist, *Resistance to caspase-8 and -9 fragments in a malignant pleural mesothelioma cell line with acquired cisplatin-resistance.* Cell Death Dis, 2010. 1: p. e78.

74. Hengstler, J.G., et al., *Contribution of c-erbB-2 and topoisomerase IIalpha to chemoresistance in ovarian cancer.* Cancer Res, 1999. 59(13): p. 3206-14.

75. Slamon, D.J., et al., *Studies of the HER-2/neu proto-oncogene in human breast and ovarian cancer.* Science, 1989. 244(4905): p. 707-12.

76. Mitsuuchi, Y., et al., *The phosphatidylinositol 3-kinase/AKT signal transduction pathway plays a critical role in the expression of p21WAF1/CIP1/SDI1 induced by cisplatin and paclitaxel.* Cancer Res, 2000. 60(19): p. 5390-4.

77. Zhou, B.P., et al., *Cytoplasmic localization of p21Cip1/WAF1 by Akt-induced phosphorylation in HER-2/neu-overexpressing cells.* Nat Cell Biol, 2001. 3(3): p. 245-52.

78. Wang, J. and G.S. Wu, *Role of autophagy in cisplatin resistance in ovarian cancer cells.* J Biol Chem, 2014. 289(24): p. 17163-73.

79. Hagrman, D., et al., *Kinetic study on the reaction of cisplatin with metallothionein.* Drug Metab Dispos, 2003. 31(7): p. 916-23.

80. Hagrman, D., J. Goodisman, and A.K. Souid, *Kinetic study on the reactions of platinum drugs with glutathione.* J Pharmacol Exp Ther, 2004. 308(2): p. 658-66.

81. Ishikawa, T. and F. Ali-Osman, *Glutathione-associated cis-diamminedichloroplatinum(II) metabolism and ATP-dependent efflux from leukemia cells. Molecular characterization of glutathione-platinum complex and its biological significance.* J Biol Chem, 1993. 268(27): p. 20116-25.

82. Goto, S., et al., *Augmentation of transport for cisplatin-glutathione adduct in cisplatin-resistant cancer cells.* Cancer Res, 1995. 55(19): p. 4297-301.

83. Pinato, O., C. Musetti, and C. Sissi, *Pt-based drugs: the spotlight will be on proteins.* Metallomics, 2014. 6(3): p. 380-95.

84. Mena, M.L., et al., *OFFGEL isoelectric focusing and polyacrylamide gel electrophoresis separation of platinum-binding proteins.* J Chromatogr A, 2011. 1218(9): p. 1281-90.

85. Moraleja, I., et al., *A shotgun approach for the identification of platinum-protein complexes.* Anal Bioanal Chem, 2015. 407(9): p. 2393-403.

86. Moraleja, I., et al., *Combining TBP-based rOFFGEL-IEF with FASP and nLC-ESI-LTQ-MS/MS for the analysis of cisplatin-binding proteins in rat kidney.* Talanta, 2014. 120: p. 433-42.

87. Moreno-Gordaliza, E., et al., *Novel insights into the bottom-up mass spectrometry proteomics approach for the characterization of Pt-binding proteins: The insulin-cisplatin case study.* Analyst, 2010. 135(6): p. 1288-98.

88. Moreno-Gordaliza, E., et al., *Characterization of Pt-protein complexes by nHPLC-ESI-LTQ MS/MS using a gel-based bottom-up approach.* Talanta, 2012. 88: p. 599-608.

89. Will, J., W.S. Sheldrick, and D. Wolters, *Characterisation of cisplatin coordination sites in cellular Escherichia coli DNA-binding proteins by combined biphasic liquid chromatography and ESI tandem mass spectrometry.* J Biol Inorg Chem, 2008. 13(3): p. 421-34.

90. Eckstein, N., et al., *Hyperactivation of the insulin-like growth factor receptor I signaling pathway is an essential event for cisplatin resistance of ovarian cancer cells.* Cancer Res, 2009. 69(7): p. 2996-3003.

91. Zhang, N., et al., *Direct determination of the binding sites of cisplatin on insulin-like growth factor-1 by top-down mass spectrometry.* J Biol Inorg Chem, 2015. 20(1): p. 1-10.

92. Chappell, N.P., et al., *Mitochondrial proteomic analysis of cisplatin resistance in ovarian cancer.* J Proteome Res, 2012. 11(9): p. 4605-14.

93. Deng, J., et al., *Proteomics discovery of chemoresistant biomarkers for ovarian cancer therapy.* Expert Rev Proteomics, 2016: p. 1-11.

94. Li, S.L., et al., *Quantitative proteome analysis of multidrug resistance in human ovarian cancer cell line.* J Cell Biochem, 2010. 109(4): p. 625-33.

95. Pan, S., et al., *Quantitative proteomics analysis integrated with microarray data reveals that extracellular matrix proteins, catenins, and p53 binding protein 1 are important for chemotherapy response in ovarian cancers.* OMICS, 2009. 13(4): p. 345-54.

96. Stewart, D.J., *Mechanisms of resistance to cisplatin and carboplatin.* Crit Rev Oncol Hematol, 2007. 63(1): p. 12-31.

97. Yan, X.D., et al., *Identification of platinum-resistance associated proteins through proteomic analysis of human ovarian cancer cells and their platinum-resistant sublines.* J Proteome Res, 2007. 6(2): p. 772-80.

98. Molenaar, C., et al., *New insights in the cellular processing of platinum antitumor compounds, using fluorophore-labeled platinum complexes and digital fluorescence microscopy.* J Biol Inorg Chem, 2000. 5(5): p. 655-65.

99. Kotz, S., et al., *Combination of two-dimensional gel electrophoresis and a fluorescent carboxyfluorescein-diacetate-labeled cisplatin analogue allows the identification of intracellular cisplatin-protein adducts.* Electrophoresis, 2015. 36(21-22): p. 2811-2819.

100. Kotz, S., et al., *Optimized two-dimensional gel electrophoresis in an alkaline pH range improves the identification of intracellular CFDA-cisplatin-protein adducts in ovarian cancer cells.* Electrophoresis, 2018. 39(12): p. 1488-1496.

101. Kullmann, M., et al., *Assessing the contribution of the two protein disulfide isomerases PDIA1 and PDIA3 to cisplatin resistance.* J Inorg Biochem, 2015. 153: p. 247-52.

102. Kullmann, M., et al., *GRP78 knockdown does not affect cytotoxicity of cisplatin in ovarian cancer cells.* Int J Clin Pharmacol Ther, 2015. 53(12): p. 1038-40.

103. Kalayda, G.V., et al., *Altered localisation of the copper efflux transporters ATP7A and ATP7B associated with cisplatin resistance in human ovarian carcinoma cells.* BMC Cancer, 2008. 8: p. 175.

104. Ackermann, D., et al., *Comparative fluorescence two-dimensional gel electrophoresis using a gel strip sandwich assembly for the simultaneous on-gel generation of a reference protein spot grid.* Electrophoresis, 2012. 33(9-10): p. 1406-10.

105. Gorg, A., W. Postel, and S. Gunther, *The current state of two-dimensional electrophoresis with immobilized pH gradients.* Electrophoresis, 1988. 9(9): p. 531-46.

106. Hoving, S., et al., *Preparative two-dimensional gel electrophoresis at alkaline pH using narrow range immobilized pH gradients.* Proteomics, 2002. 2(2): p. 127-34.

107. Chevallet, M., et al., *New zwitterionic detergents improve the analysis of membrane proteins by two-dimensional electrophoresis.* Electrophoresis, 1998. 19(11): p. 1901-9.

108. Martins-de-Souza, D., et al., *The use of ASB-14 in combination with CHAPS is the best for solubilization of human brain proteins for two-*

dimensional gel electrophoresis. Brief Funct Genomic Proteomic, 2007. 6(1): p. 70-5.

109. Lamberti, C., et al., *Combined cup loading, bis(2-hydroxyethyl) disulfide, and protein precipitation protocols to improve the alkaline proteome of Lactobacillus hilgardii.* Electrophoresis, 2007. 28(10): p. 1633-8.

110. Pennington, K., et al., *Optimization of the first dimension for separation by two-dimensional gel electrophoresis of basic proteins from human brain tissue.* Proteomics, 2004. 4(1): p. 27-30.

111. Drews, O., et al., *Setting up standards and a reference map for the alkaline proteome of the Gram-positive bacterium Lactococcus lactis.* Proteomics, 2004. 4(5): p. 1293-304.

112. Gorg, A., et al., *2-DE with IPGs.* Electrophoresis, 2009. 30 Suppl 1: p. S122-32.

113. Wildgruber, R., et al., *Web-based two-dimensional database of Saccharomyces cerevisiae proteins using immobilized pH gradients from pH 6 to pH 12 and matrix-assisted laser desorption/ionization-time of flight mass spectrometry.* Proteomics, 2002. 2(6): p. 727-32.

114. McDonough, J. and E. Marban, *Optimization of IPG strip equilibration for the basic membrane protein mABC1.* Proteomics, 2005. 5(11): p. 2892-5.

115. Noiva, R., *Protein disulfide isomerase: the multifunctional redox chaperone of the endoplasmic reticulum.* Semin Cell Dev Biol, 1999. 10(5): p. 481-93.

116. Sobierajska, K., et al., *Protein disulfide isomerase directly interacts with beta-actin Cys374 and regulates cytoskeleton reorganization.* J Biol Chem, 2014. 289(9): p. 5758-73.

117. Dalle-Donne, I., et al., *Reversible S-glutathionylation of Cys 374 regulates actin filament formation by inducing structural changes in the actin molecule.* Free Radic Biol Med, 2003. 34(1): p. 23-32.

118. Kotz, S., et al., *Optimized two-dimensional gel electrophoresis in an alkaline pH range improving the identification of intracellular CFDA-cisplatin-protein adducts in ovarian cancer cells*, in *Manuskript*2018.

119. Ron, D. and P. Walter, *Signal integration in the endoplasmic reticulum unfolded protein response.* Nat Rev Mol Cell Biol, 2007. 8(7): p. 519-29.

120. Xu, S., S. Sankar, and N. Neamati, *Protein disulfide isomerase: a promising target for cancer therapy.* Drug Discov Today, 2014. 19(3): p. 222-40.

121. Ni, M., Y. Zhang, and A.S. Lee, *Beyond the endoplasmic reticulum: atypical GRP78 in cell viability, signalling and therapeutic targeting.* Biochem J, 2011. 434(2): p. 181-8.

122. Rigobello, M.P., et al., *Distribution of protein disulphide isomerase in rat liver mitochondria.* Biochem J, 2001. 356(Pt 2): p. 567-70.

123. Turano, C., et al., *Proteins of the PDI family: unpredicted non-ER locations and functions.* J Cell Physiol, 2002. 193(2): p. 154-63.

124. Yoshimori, T., et al., *Protein disulfide-isomerase in rat exocrine pancreatic cells is exported from the endoplasmic reticulum despite possessing the retention signal.* J Biol Chem, 1990. 265(26): p. 15984-90.

125. Hersey, P. and X.D. Zhang, *Adaptation to ER stress as a driver of malignancy and resistance to therapy in human melanoma.* Pigment Cell Melanoma Res, 2008. 21(3): p. 358-67.

126. Lovat, P.E., et al., *Increasing melanoma cell death using inhibitors of protein disulfide isomerases to abrogate survival responses to endoplasmic reticulum stress.* Cancer Res, 2008. 68(13): p. 5363-9.

127. Zhang, K. and R.J. Kaufman, *Signaling the unfolded protein response from the endoplasmic reticulum.* J Biol Chem, 2004. 279(25): p. 25935-8.

128. Li, J. and A.S. Lee, *Stress induction of GRP78/BiP and its role in cancer.* Curr Mol Med, 2006. 6(1): p. 45-54.

129. Tufo, G., et al., *The protein disulfide isomerases PDIA4 and PDIA6 mediate resistance to cisplatin-induced cell death in lung adenocarcinoma.* Cell Death Differ, 2014. 21(5): p. 685-95.

130. Xu, S., et al., *Discovery of an orally active small-molecule irreversible inhibitor of protein disulfide isomerase for ovarian cancer treatment.* Proc Natl Acad Sci U S A, 2012. 109(40): p. 16348-53.

131. Huang, Y.Y., et al., *Knockdown of GRP78 enhances cell death by cisplatin and radiotherapy in nasopharyngeal cells.* Anticancer Drugs, 2016. 27(8): p. 726-33.

132. Maccio, A. and C. Madeddu, *Cisplatin : an old drug with a newfound efficacy -- from mechanisms of action to cytotoxicity.* Expert Opin Pharmacother, 2013. 14(13): p. 1839-57.

133. Zogg, C.K., *Phosphoglycerate dehydrogenase: potential therapeutic target and putative metabolic oncogene.* J Oncol, 2014. 2014: p. 524101.

134. Altenberg, B. and K.O. Greulich, *Genes of glycolysis are ubiquitously overexpressed in 24 cancer classes.* Genomics, 2004. 84(6): p. 1014-20.

135. Diaz-Ramos, A., et al., *alpha-Enolase, a multifunctional protein: its role on pathophysiological situations.* J Biomed Biotechnol, 2012. 2012: p. 156795.

136. Saldanha, R.G., et al., *Proteomic identification of lynchpin urokinase plasminogen activator receptor protein interactions associated with epithelial cancer malignancy.* J Proteome Res, 2007. 6(3): p. 1016-28.

137. Subramanian, A. and D.M. Miller, *Structural analysis of alpha-enolase. Mapping the functional domains involved in down-regulation of the c-myc protooncogene.* J Biol Chem, 2000. 275(8): p. 5958-65.

138. Pancholi, V., *Multifunctional alpha-enolase: its role in diseases.* Cell Mol Life Sci, 2001. 58(7): p. 902-20.

139. Bae, S.M., et al., *Two-dimensional gel analysis of protein expression profile in squamous cervical cancer patients.* Gynecol Oncol, 2005. 99(1): p. 26-35.

140. Bae, S.M., et al., *Protein expression profile using two-dimensional gel analysis in squamous cervical cancer patients.* Cancer Res Treat, 2006. 38(2): p. 99-107.

141. Cappello, P., et al., *An integrated humoral and cellular response is elicited in pancreatic cancer by alpha-enolase, a novel pancreatic ductal adenocarcinoma-associated antigen.* Int J Cancer, 2009. 125(3): p. 639-48.

142. Chang, G.C., et al., *Identification of alpha-enolase as an autoantigen in lung cancer: its overexpression is associated with clinical outcomes.* Clin Cancer Res, 2006. 12(19): p. 5746-54.

143. Govekar, R.B., et al., *Proteomic profiling of cancer of the gingivo-buccal complex: Identification of new differentially expressed markers.* Proteomics Clin Appl, 2009. 3(12): p. 1451-62.

144. Hamaguchi, T., et al., *Glycolysis module activated by hypoxia-inducible factor 1alpha is related to the aggressive phenotype of hepatocellular carcinoma.* Int J Oncol, 2008. 33(4): p. 725-31.

145. Hennipman, A., et al., *Glycolytic enzyme activities in breast cancer metastases.* Tumour Biol, 1988. 9(5): p. 241-8.

146. Kabbage, M., et al., *Protein alterations in infiltrating ductal carcinomas of the breast as detected by nonequilibrium pH gradient electrophoresis and mass spectrometry.* J Biomed Biotechnol, 2008. 2008: p. 564127.

147. Katayama, M., et al., *Protein pattern difference in the colon cancer cell lines examined by two-dimensional differential in-gel electrophoresis and mass spectrometry.* Surg Today, 2006. 36(12): p. 1085-93.

148. Li, C., et al., *Proteome analysis of human lung squamous carcinoma.* Proteomics, 2006. 6(2): p. 547-58.

149. Li, L.S., et al., *Proteomic analysis distinguishes basaloid carcinoma as a distinct subtype of nonsmall cell lung carcinoma.* Proteomics, 2004. 4(11): p. 3394-400.

150. Malorni, L., et al., *Proteomic analysis of MCF-7 breast cancer cell line exposed to mitogenic concentration of 17beta-estradiol.* Proteomics, 2006. 6(22): p. 5973-82.

151. Qi, Y., et al., *Comparative proteomic analysis of esophageal squamous cell carcinoma.* Proteomics, 2005. 5(11): p. 2960-71.

152. Rubporn, A., et al., *Comparative proteomic analysis of lung cancer cell line and lung fibroblast cell line.* Cancer Genomics Proteomics, 2009. 6(4): p. 229-37.

153. Shen, J., et al., *Protein expression profiles in pancreatic adenocarcinoma compared with normal pancreatic tissue and tissue affected by pancreatitis as detected by two-dimensional gel electrophoresis and mass spectrometry.* Cancer Res, 2004. 64(24): p. 9018-26.

154. Somiari, R.I., et al., *High-throughput proteomic analysis of human infiltrating ductal carcinoma of the breast.* Proteomics, 2003. 3(10): p. 1863-73.

155. Suzuki, A., et al., *Identification of melanoma antigens using a Serological Proteome Approach (SERPA).* Cancer Genomics Proteomics, 2010. 7(1): p. 17-23.

156. Takashima, M., et al., *Overexpression of alpha enolase in hepatitis C virus-related hepatocellular carcinoma: association with tumor progression as determined by proteomic analysis.* Proteomics, 2005. 5(6): p. 1686-92.

157. Tsai, S.T., et al., *ENO1, a potential prognostic head and neck cancer marker, promotes transformation partly via chemokine CCL20 induction.* Eur J Cancer, 2010. 46(9): p. 1712-23.

158. Tu, S.H., et al., *Increased expression of enolase alpha in human breast cancer confers tamoxifen resistance in human breast cancer cells.* Breast Cancer Res Treat, 2010. 121(3): p. 539-53.

159. Zhao, J., et al., *Comparative proteomics analysis of Barrett metaplasia and esophageal adenocarcinoma using two-dimensional liquid mass mapping.* Mol Cell Proteomics, 2007. 6(6): p. 987-99.

160. Cao, L., et al., *Proteomic analysis of human ovarian cancer paclitaxel-resistant cell lines.* Zhong Nan Da Xue Xue Bao Yi Xue Ban, 2010. 35(4): p. 286-94.

161. Tomaino, B., et al., *Circulating autoantibodies to phosphorylated alpha-enolase are a hallmark of pancreatic cancer.* J Proteome Res, 2011. 10(1): p. 105-12.

162. Cui, J.W., et al., *Proteomics-based identification of human acute leukemia antigens that induce humoral immune response.* Mol Cell Proteomics, 2005. 4(11): p. 1718-24.

163. Zou, L., et al., *Identification of leukemia-associated antigens in chronic myeloid leukemia by proteomic analysis.* Leuk Res, 2005. 29(12): p. 1387-91.

164. Forgber, M., et al., *Proteome serological determination of tumor-associated antigens in melanoma.* PLoS One, 2009. 4(4): p. e5199.

165. Shukla, S., et al., *Tumor antigens eliciting autoantibody response in cancer of gingivo-buccal complex.* Proteomics Clin Appl, 2007. 1(12): p. 1592-604.

166. Shukla, S., et al., *Immunoproteomics reveals that cancer of the tongue and the gingivobuccal complex exhibit differential autoantibody response.* Cancer Biomark, 2009. 5(3): p. 127-35.

167. Ejma, M., et al., *Antibodies to 46-kDa retinal antigen in a patient with breast carcinoma and cancer-associated retinopathy.* Breast Cancer Res Treat, 2008. 110(2): p. 269-71.

168. Shih, N.Y., et al., *Anti-alpha-enolase autoantibodies are down-regulated in advanced cancer patients.* Jpn J Clin Oncol, 2010. 40(7): p. 663-9.

169. Dot, C., J. Guigay, and G. Adamus, *Anti-alpha-enolase antibodies in cancer-associated retinopathy with small cell carcinoma of the lung.* Am J Ophthalmol, 2005. 139(4): p. 746-7.

170. He, P., et al., *Proteomics-based identification of alpha-enolase as a tumor antigen in non-small lung cancer.* Cancer Sci, 2007. 98(8): p. 1234-40.

171. Jankowska, R., et al., *Serum antibodies to retinal antigens in lung cancer and sarcoidosis.* Pathobiology, 2004. 71(6): p. 323-8.

172. Nakanishi, T., et al., *Detection of eight antibodies in cancer patients' sera against proteins derived from the adenocarcinoma A549 cell line using proteomics-based analysis.* J Chromatogr B Analyt Technol Biomed Life Sci, 2006. 838(1): p. 15-20.

173. Ueda, K., *[Proteome analysis of autoantibodies in sera of patients with cancer].* Rinsho Byori, 2005. 53(5): p. 437-45.

174. Capello, M., et al., *alpha-Enolase: a promising therapeutic and diagnostic tumor target.* FEBS J, 2011. 278(7): p. 1064-74.

175. Marcon, G., et al., *Gold(III) complexes with bipyridyl ligands: solution chemistry, cytotoxicity, and DNA binding properties.* J Med Chem, 2002. 45(8): p. 1672-7.

176. Gamberi, T., et al., *Proteomic analysis of the cytotoxic effects induced by the organogold(III) complex Aubipyc in cisplatin-resistant A2780 ovarian cancer cells: further evidence for the glycolytic pathway implication.* Mol Biosyst, 2015. 11(6): p. 1653-67.

177. Gamberi, T., et al., *Proteomic analysis of A2780/S ovarian cancer cell response to the cytotoxic organogold(III) compound Aubipy(c).* J Proteomics, 2014. 103: p. 103-20.

178. Tristan, C., et al., *The diverse functions of GAPDH: views from different subcellular compartments.* Cell Signal, 2011. 23(2): p. 317-23.

179. Ganapathy-Kanniappan, S., *Evolution of GAPDH as a druggable target of tumor glycolysis?* Expert Opin Ther Targets, 2018. 22(4): p. 295-298.

180. Krasnov, G.S., et al., *Deregulation of glycolysis in cancer: glyceraldehyde-3-phosphate dehydrogenase as a therapeutic target.* Expert Opin Ther Targets, 2013. 17(6): p. 681-93.

181. Anastasiou, D., et al., *Pyruvate kinase M2 activators promote tetramer formation and suppress tumorigenesis.* Nat Chem Biol, 2012. 8(10): p. 839-47.

182. Christofk, H.R., et al., *The M2 splice isoform of pyruvate kinase is important for cancer metabolism and tumour growth.* Nature, 2008. 452(7184): p. 230-3.

183. He, X., et al., *PKM2 in carcinogenesis and oncotherapy.* Oncotarget, 2017. 8(66): p. 110656-110670.

184. Li, W., et al., *Sensitizing the therapeutic efficacy of taxol with shikonin in human breast cancer cells.* PLoS One, 2014. 9(4): p. e94079.

185. Lim, J.Y., et al., *Overexpression of the M2 isoform of pyruvate kinase is an adverse prognostic factor for signet ring cell gastric cancer.* World J Gastroenterol, 2012. 18(30): p. 4037-43.

186. Chao, T.K., et al., *Pyruvate kinase M2 is a poor prognostic marker of and a therapeutic target in ovarian cancer.* PLoS One, 2017. 12(7): p. e0182166.

187. Snell, K., *Enzymes of serine metabolism in normal, developing and neoplastic rat tissues.* Adv Enzyme Regul, 1984. 22: p. 325-400.

188. Futerman, A.H. and H. Riezman, *The ins and outs of sphingolipid synthesis.* Trends Cell Biol, 2005. 15(6): p. 312-8.

189. Kuge, O. and M. Nishijima, *Biosynthetic regulation and intracellular transport of phosphatidylserine in mammalian cells.* J Biochem, 2003. 133(4): p. 397-403.

190. de Koning, T.J., et al., *L-serine in disease and development.* Biochem J, 2003. 371(Pt 3): p. 653-61.

191. Chen, J., et al., *Phosphoglycerate dehydrogenase is dispensable for breast tumor maintenance and growth.* Oncotarget, 2013. 4(12): p. 2502-11.

192. Locasale, J.W., et al., *Phosphoglycerate dehydrogenase diverts glycolytic flux and contributes to oncogenesis.* Nat Genet, 2011. 43(9): p. 869-74.

193. Possemato, R., et al., *Functional genomics reveal that the serine synthesis pathway is essential in breast cancer.* Nature, 2011. 476(7360): p. 346-50.

194. Jing, Z., et al., *Downregulation of phosphoglycerate dehydrogenase inhibits proliferation and enhances cisplatin sensitivity in cervical adenocarcinoma cells by regulating Bcl-2 and caspase-3.* Cancer Biol Ther, 2015. 16(4): p. 541-8.

195. Zhang, X.Y., et al., *Proteomic alterations of fibroblasts induced by ovarian cancer cells reveal potential cancer targets.* Neoplasma, 2017.

196. Hamanaka, R.B. and N.S. Chandel, *Targeting glucose metabolism for cancer therapy.* J Exp Med, 2012. 209(2): p. 211-5.

197. de Koning, T.J., *Treatment with amino acids in serine deficiency disorders.* J Inherit Metab Dis, 2006. 29(2-3): p. 347-51.

198. Luo, J., *Cancer's sweet tooth for serine.* Breast Cancer Res, 2011. 13(6): p. 317.

199. Hershey, J.W., *Translational control in mammalian cells.* Annu Rev Biochem, 1991. 60: p. 717-55.

200. Thornton, S., et al., *Not just for housekeeping: protein initiation and elongation factors in cell growth and tumorigenesis.* J Mol Med (Berl), 2003. 81(9): p. 536-48.

201. Al-Maghrebi, M., J.T. Anim, and A.A. Olalu, *Up-regulation of eukaryotic elongation factor-1 subunits in breast carcinoma.* Anticancer Res, 2005. 25(3c): p. 2573-7.

202. Kato, M.V., et al., *Upregulation of the elongation factor-1alpha gene by p53 in association with death of an erythroleukemic cell line.* Blood, 1997. 90(4): p. 1373-8.

203. Lamberti, A., et al., *The translation elongation factor 1A in tumorigenesis, signal transduction and apoptosis: review article.* Amino Acids, 2004. 26(4): p. 443-8.

204. Tatsuka, M., et al., *Elongation factor-1 alpha gene determines susceptibility to transformation.* Nature, 1992. 359(6393): p. 333-6.

205. Blanch, A., et al., *Eukaryotic translation elongation factor 1-alpha 1 inhibits p53 and p73 dependent apoptosis and chemotherapy sensitivity.* PLoS One, 2013. 8(6): p. e66436.

206. Sirover, M.A., *Pleiotropic effects of moonlighting glyceraldehyde-3-phosphate dehydrogenase (GAPDH) in cancer progression, invasiveness, and metastases.* Cancer Metastasis Rev, 2018. 37(4): p. 665-676.

207. Song, Z., et al., *PHGDH is an independent prognosis marker and contributes cell proliferation, migration and invasion in human pancreatic cancer.* Gene, 2018. 642: p. 43-50.

208. Zhao, M., et al., *Enolase-1 is a therapeutic target in endometrial carcinoma.* Oncotarget, 2015. 6(17): p. 15610-27.

209. Roth, R.A., *Bacitracin: an inhibitor of the insulin degrading activity of glutathione-insulin transhydrogenase.* Biochem Biophys Res Commun, 1981. 98(2): p. 431-8.

210. Hoffmann, H., et al., *Discovery, Structure Elucidation, and Biological Characterization of Nannocystin A, a Macrocyclic Myxobacterial Metabolite with Potent Antiproliferative Properties.* Angew Chem Int Ed Engl, 2015. 54(35): p. 10145-8.

211. Krastel, P., et al., *Nannocystin A: an Elongation Factor 1 Inhibitor from Myxobacteria with Differential Anti-Cancer Properties.* Angew Chem Int Ed Engl, 2015. 54(35): p. 10149-54.

212. Ahuja, D., et al., *Inhibition of protein synthesis by didemnin B: how EF-1alpha mediates inhibition of translocation.* Biochemistry, 2000. 39(15): p. 4339-46.

213. Carelli, J.D., et al., *Ternatin and improved synthetic variants kill cancer cells by targeting the elongation factor-1A ternary complex.* Elife, 2015. 4.

214. Mullarky, E., et al., *Identification of a small molecule inhibitor of 3-phosphoglycerate dehydrogenase to target serine biosynthesis in cancers.* Proc Natl Acad Sci U S A, 2016. 113(7): p. 1778-83.

215. Lung, J., et al., *In silico-based identification of human alpha-enolase inhibitors to block cancer cell growth metabolically.* Drug Des Devel Ther, 2017. 11: p. 3281-3290.

216. Liberti, M.V., et al., *A Predictive Model for Selective Targeting of the Warburg Effect through GAPDH Inhibition with a Natural Product.* Cell Metab, 2017. 26(4): p. 648-659 e8.

217. Zhao, X., et al., *Shikonin Inhibits Tumor Growth in Mice by Suppressing Pyruvate Kinase M2-mediated Aerobic Glycolysis.* Sci Rep, 2018. 8(1): p. 14517.

5 ANHANG

5.1 LEBENSLAUF

Persönliche Daten:	
Geburtsdatum:	14.05.1982
Geburtsort:	Gronau (Westf.)
Familienstand:	ledig

Beruflicher Werdegang:	
Seit 04/2017	Fachreferentin Lungenkarzinom, Roche Pharma AG
09/2016 - 02/2017	Fachseminar: "Life Science Management" (ATV GmbH, Köln)
05/2014 - 11/2015	Wissenschaftliche Mitarbeiterin am Biozentrum der Universität zu Köln
09/2013 – 03/2017	Pharmazeutisch-technische-Assistentin (PTA), Vennhauser Allee Apotheke, Düsseldorf
04/2012 - 04/2014	Wissenschaftliche Mitarbeiterin am BMFZ der Heinrich-Heine-Universität Düsseldorf
01/2011	Studentische Hilfskraft an der WWU Münster, Kursbetreuung Laborbiologie - Blutgruppen und Membranen
05/2009 - 10/2009	Studentische Hilfskraft, Medizinische Fakultät der WWU Münster, Institut für Experimentelle Ophthalmologie
02/2002 - 10/2007	PTA, Hamaland - Apotheke, Ahaus
03/2001 - 01/2002	PTA, Anker - Apotheke, Steinfurt

	Studium:
Seit 04/2012	Promotionsstudium Heinrich-Heine-Universität Düsseldorf, BMFZ, Analytisches Zentrallabor Titel: „Identifizierung intrazellulärer Reaktionsprodukte zur Resistenzentwicklung gegen antitumorale Cisplatinkomplexe“
10/2009 - 04/2012	M. Sc. Biowissenschaften, Westfälische Wilhelms-Universität Münster (WWU Münster)
10/2006 - 09/2009	B. Sc. Biowissenschaften, WWU Münster

	Schul- und Berufsausbildung:
08/2002 - 07/2005	Hochschulreife (Abschlussnote: 2,5), Driland - Kolleg, Weiterbildungskolleg der Stadt Gronau
09/1998 - 03/2001	Ausbildung zur PTA (Abschlussnote: 2,5), Städt. PTA - Lehranstalt, Münster; PTA-Praktikum Marien-Apotheke, Vreden
08/1992 - 06/1998	Mittlere Reife, Walbert - Schule, Vreden

	Publikationen:
2018	Optimized two-dimensional Gel electrophoresis in an alkaline pH range improving the identification of intracellular CFDA-cisplatin-protein adducts in ovarian cancer cells **Kotz S.**, Kullmann M., Kalayda GV., Dyballa-Rukes N., Jaehde U, Metzger S., *Electrophoresis* 2018, 39, 1488 - 1496.
2015	GRP78 knockdown does not affect cytotoxicity of cisplatin in ovarian cancer cells

Kullmann M, **Kotz S**, Hellwig M. Kalayda GV, Hilger RA, Metzger S, Jaehde U., *Int J Clin Pharmacol Ther.* 2015, 53(12): 1038-40.

2015 Assessing the contribution of the two protein disulfide isomerases PDIA1 and PDIA3 to cisplatin resistance

Kullmann M, Kalayda GV, Hellwig M, **Kotz S**, Hilger RA, Metzger S, Jaehde U., *J. Inorg. Biochem.* 2015, 153: 247-252

2015 Combination of two-dimensional gel electro-phoresis and a fluorescent carboxyfluorescein-diacetate-labeled cisplatin analogue allows the identification of intracellular cisplatin-protein adducts

Kotz S., Kullmann M., Crone B., Kalayda GV., Jaehde U, Metzger S., *Electrophoresis* 2015, 00, 1–9

Posterpräsentationen:

2016 Identifizierung von intrazellulären Cisplatin-Proteinaddukten mithilfe des fluoreszierenden Cisplatin-Analogon CFDA-Cisplatin

Kotz S., Kullmann M., Crone B., Kalayda GV., Jaehde U, Metzger S.,

49. Jahrestagung DGMS in Hamburg

2015 Identifizierung von intrazellulären Cisplatin-Proteinaddukten mithilfe des fluoreszierenden Cisplatin-Analogon CFDA-Cisplatin

Kotz S., Kullmann M., Kalayda GV., Jaehde U, Metzger S

48. Jahrestagung Deutsche Gesellschaft für Massenspektrometrie (DGMS) in Wupptertal

2014	Identification of intracellular reaction products for development of resistance to cisplatin
	Kotz S., Kullmann M., Kalayda GV., Jaehde U, Metzger S
	20th International Mass Spectrometry Conference in Genf, Schweiz
2013	Identification of intracellular reaction products for development of resistance to cisplatin
	Kotz S., Kullmann M., Kalayda GV., Mohn C., Jaehde U, Metzger S
	Proteomic Forum, Berlin

5.2 DANKE!

Am Ende meiner Dissertation angelangt, möchte ich mich bei allen bedanken, die mich während dieser Zeit unterstützt haben:

Dr. Sabine Metzger - Für das spannende Projekt, deinen Zuspruch in dieser Zeit, den vielen interessanten Diskussionen, die notwendige Kritik sowie die vorgebrachten Verbesserungsvorschläge!

Prof. Dr. William F. Martin – Für die Betreuung meines Promotionsvorhabens als Erstgutachter an der Mathematisch-Naturwissenschaftlichen Fakultät.

Prof. Dr. Inge Bauer - Für die Betreuung meiner Promotion als Mentorin sowie den aufschlussreichen Diskussionen und Verbesserungsvorschlägen!

Prof. Dr. Ulrich Jaehde, Dr. Anya Kalayda, Dr. Maximillian Kullmann, Dr. Günther Weber und Dr. Robert Zabel - Für die gute Zusammenarbeit in allen Phasen des Projektes sowie den interessanten Diskussionen.

Dr. Nadine Dyballa-Rukes, Thorsten Strahl und Eva Bruns – Zu Beginn habt ihr mir wertvolle Hinweise für das Gelingen meiner Doktorarbeit gegeben sowie für ein Überleben im Laboralltag gesorgt.

Mareike Brocksieper, Katrin Brenig, Dr. Kathrin Schlücking und Dr. Christian Breuer – Für die vielen kleinen Pausen mit aufschlussreichen Diskussionen und Gesprächen abseits der Arbeit.

Dr. Anja Stefanski – Für die Durchführung einiger MS-Analysen.

Barbara Crone – Für die Durchführung der LA-ICP-MS-Analysen.

AG Haendeler (IUF) – Für die Aufnahme als Gastwissenschaftlerin, um einige MS-Analysen am Institut durchführen zu können.

Meinen Freund(inn)en Carola, Daniel, Stella, Sonja, Matthias und Gerrit für die erfordliche Abwechslung.

Zum Schluss möchte ich mich ganz besonders bei meiner Familie und meinem Freund Thomas bedanken! Sie waren immer für mich da, haben meine schlechte Laune geduldet sowie für meine innere Ausgeglichenheit gesorgt.